UTS UNIVERSITY OF TECHNOLOGY SYDNEY

Corrosion mechanisms of steel reinforcement in fly ash/slag based powder form of geopolymer concrete

by TRAN HUYEN VU

Thesis submitted in fulfilment of the requirements for the degree of

Doctor of Philosophy

under the supervision of Dr Nadarajah Gowripalan, Professor Vute Sirivivatnanon and Associate Professor Pre De Silva

University of Technology Sydney
Faculty of Engineering and Information Technology

September 2021

This page is intentionally left blank

CERTIFICATE OF ORIGINAL AUTHORSHIP

I, *Tran Huyen Vu,* declare that this thesis, is submitted in fulfilment of the requirements for the award of *Doctor of Philosophy*, in the *School of Civil and Environmental Engineering/Faculty of Engineering & Information Technology* at the University of Technology Sydney.

This thesis is wholly my own work unless otherwise referenced or acknowledged. In addition, I certify that all information sources and literature used are indicated in the thesis.

This research is supported by the Australian Government Research Training Program.

Signature:

Production Note:
Signature removed prior to publication.

Date: 28/09/2021

This page is intentionally left blank

ACKNOWLEDGEMENTS

Thank God for keeping me and my family healthy. I would like to dedicate this dissertation to my sons and my family for always loving me no matter what I treated them. I am enormously grateful to Dr Nadarajah Gowripalan, Professor Vute Sirivivatnanon and Associate Professor Pre De Silva, whose unfailing support and valuable advice, have encouraged and improved my work. Also, I would like to express my gratitude to Professor Tuan Van Nguyen who generously served as a mentor. Thank you, my friends who I have known and have not known for standing by my side in the worst times and forgiving my mistakes. Thank you, Sydney and Australia.

This study would not be able to be performed without the generous supports and involvements of Cement Australia and Australian Research Council Research Hub - Nanoscience Based Construction Materials Manufacturing.

I would love to express my sincere gratitude to Mulugheta Hailu, Rami Haddad, Peter Brown, Lam Dinh Nguyen, Habib Rasouli, Ann Yan and other staffs at Tech-lab for kindly supporting me when I was working there.

I should also mention my debt to Professor Arnaud Caste (School of Civil and Environmental Engineering- UTS), Dr. Quang Dieu Nguyen (School of Civil and Environmental Engineering- UTS), Dr. Md Abu Hasan Johir (Environmental Engineering Laboratories - UTS), Dr. Herbert Yuan (MAU-UTS), Dr. Mark Lockre (MAU-UTS), Dr. Katie McBean (MAU-UTS), Dr. Igor Shikhov (Research Associate, University of New South Wales), Dr. Duy Nguyen (Cement Concrete & Aggregates Australia), Dr. Amin Noushini (Rocla), Mr. Bede Harrington (Rocla) and Josephine Delacruz (Rocla) who generously helped and shared their knowledge and time to support my study.

I would love to acknowledge the help of people who I have forgotten mentioning here and request your forgiveness for my bad memory.

ABSTRACT

Investigation of the durability related aspects of geopolymer concrete has been increasingly conducted worldwide. The suitability of geopolymer concretes in structural applications, still, has not been well proven because of the lack of information on service history and durability performance. Further, the conventional production techniques of geopolymer binders requiring the handling of highly alkaline liquids that are dangerous. Therefore, one-part geopolymer, a new way of producing geopolymer, is introduced to deal with such a safety issue. However, one-part geopolymer invariably has an issue related to a short setting time. To promote the use of geopolymer materials in structure applications, this study aimed to investigate on carbonation and chloride resistance of one-part fly ash/slag geopolymer concretes, which have been deemed as the durability issues attributed to corrosion of steel reinforcement in geopolymer materials. Additionally, the possibility of using a sodium-based set retarder to address the issue of short setting time was included in the investigation.

The investigation of carbonation focused on changes of carbonation depth and pH under both accelerated and natural carbonation conditions. The influence of carbonation on porosity and pore size characteristics of one-part fly ash/slag geopolymer mortar was also investigated by using neutron tomography and mercury intrusion porosimetry (MIP). For assessing chloride resistance, accelerated chloride diffusion, rapid chloride permeability test (RCPT), and the movements of ions in RCPT were performed. A brief examination of chloride diffusion at seawater concentration was also carried out. To explore how the set retarder affects the setting time and other early age properties of one-part geopolymer concrete, changes of setting time, heat released, and compressive strength when different amounts of retarder

applied were thoroughly examined. Scanning electron microscopy (SEM) with energy dispersive X-ray spectrometry (EDS) was also performed in order to supplement the findings of the other tests.

The key findings indicated that using the set retarder mentioned above prolonged the setting time of one-part geopolymer binders and reduced the heat released by activation reactions. The compressive strength, however, was decreased when increasing the percentage of retarder. This problem could be avoided by using the retarder with an amount of 2-6%. The results obtained also showed that carbonation alone might not lead to steel corrosion in one-part geopolymer concrete investigated because the pH in carbonated parts was always higher than 10. For assessing chloride resistance of one-part fly ash/slag geopolymer concretes in an accelerated test in 16.5% NaCl solution, 40% fly ash/ 60% slag geopolymer concrete had a lower chloride resistance than OPC concretes, while chloride resistance of 60% fly ash/ 40% slag geopolymer concrete was worse. Due to the presence of both fly ash and slag in the precursor, chloride ions were physically and chemically bound when penetrating in the one-part geopolymer concretes. Regarding RCPT, using 60 voltage, advocated in ASTM C1202, caused the issue of overheating. RCPT performed at 30 voltage was highly suggested because it was well correlated with the accelerated chloride diffusion test. However, it was difficult to distinguish the ability of chloride resistance between different one-part geopolymer concretes based on the charge passed obtained in RCPT. It was because the charge passed was contributed by the movement of all ions present, not by only Cl^-.

CONTENTS

LIST OF TABLES

LIST OF FIGURES

PUBLICATIONS

Vu, T.H., Gowripalan, N., de Silva, P., Kidd, P. & Sirivivatnanon, V. 2020, „Investigating chloride resistance of one-part fly ash/slag geopolymer concrete"- About to submit to Cement and Concrete Research.

Vu, T.H., Gowripalan, N., de Silva, P., Kidd, P. & Sirivivatnanon, V. 2020, „Influence of set retarder on early age properties of one-part fly ash/ slag geopolymer pastes and mortars"- Under review of Construction and Building Materials.

Vu, T.H., Gowripalan, N., de Silva, P., Kidd, P. & Sirivivatnanon, V. 2020, „Assessing carbonation in one-part fly ash/slag geopolymer mortar: Change in pore characteristics using the state-of-the-art technique neutron tomography", Cement and Concrete Composites, 114:103759.

Vu, T.H., Gowripalan, N., de Silva, P., Kidd, P. & Sirivivatnanon, V. 2019, „Influence of curing and retarder on early-age properties of dry powder geopolymer concrete", Concrete in Australia 45(2):41-46.

Vu, T.H., Gowripalan, N., de Silva, P., Kidd, P. & Sirivivatnanon, V. 2019, „Assessing corrosion resistance of powder form of geopolymer concrete". Proceedings of Concrete 2019, Sydney, Australia, 9-12 September 2019.

Vu, T.H, Gowripalan, N. 2018, „Mechanism of heavy metal immobilisation using geopolymerization techniques – A review", Journal of Advanced Concrete Technology 16(3):124-135.

Vu, T.H., Gowripalan, N., de Silva, P., Kidd, P. & Sirivivatnanon, V. 2018, „Carbonation and Chloride Induced Steel Corrosion Related Aspects in Fly Ash/Slag Based Geopolymers - A Critical Review“. Proceedings of the 5th International fib Congress 2018, Melbourne, Australia, 7-11 October 2018.

Chapter 1: General Introduction

1.1 Introduction

Sustainable construction has become increasingly important to achieve lasting structures and to decrease the environmental impact of the construction industry. An important step to achieve sustainability in construction is using environmentally friendly construction materials. The production of Ordinary Portland Cement (OPC), a traditional binder, not only consumes a large quantity of natural resources and energy but also releases a significant amount of greenhouse gases into the atmosphere (Provis et al. 2014; Davidovits 1991). In Australia, in order to reduce greenhouse gas emissions, considerable efforts have been made by cement manufacturers through significant investments in new kiln technology, alternative fuels, raw materials, and energy efficiency (Australia Cement Industry Federation 2017). Industrial by-products and others wastes such as fly ash and slag have been used as supplementary cementitious materials for reducing gas emissions, apart from cost reduction and improvements in durability (Abdel-Gawwad, Mohamed & Mohammed 2019; Fernández-Jiménez et al. 2017; Torres-Carrasco & Puertas 2015). Despite these efforts, greenhouse gas emissions in cement production is still a major challenge. On the other hand, it is generally accepted that production of alkali activated material (AAM), a new binder compared to OPC, releases much lower CO_2 emissions (Provis 2014; Yang, Song & Song 2013; Zhuang et al. 2016). It is because the production of alkali activated materials (AAMs) predominantly uses fly ash and slag, and the selected alkali activators. High temperature kilns for manufacture are not required, and hence do not require significant levels of fuel energy and not release that much CO_2 as does OPC. More to this point, the production of the 50 grade concretes based on

geopolymer, a type of AAM, investigated in this study, can reduce 60% CO_2 emissions, compared with that of a 40 grade OPC concrete. To be more specific, a grade 40 OPC mix revealed 354kg of CO_2 emission equivalent (Turner & Collins 2013) as against 145kg of CO_2 emission equivalent for fly ash/slag geopolymer concrete mix (calculated in Table 1.1), currently being investigated. The environmental benefit of considerably reduced emission of geopolymer concrete, thus, is clearly revealed.

Table 1.1 CO_2 emissions per m^3 of one-part geopolymer concrete of 50 grade

Activities			CO_2 emissions (kg)	Reference
Placement			9	(Turner & Collins 2013)
Transport			9	
Curing (at ambient temperature)			<1	
Batching			3	
Materials	kg/m^3	kg CO_2 emissions/kg		Reference
Aggregate	1223.6	0.0408	49.9	(Collins 2010)
Sand	779.6	0.0139	10.9	
Fly ash	180.7	0.0270	4.9	
Slag	115.6	0.1430	16.6	
Sodium silicate (solid form)	28.9	1.1400	33.0	(Fawer, Concannon & Rieber 1999)
Sodium carbonate	28.9	0.2300	6.7	(IPCC Guidelines for National Greenhouse Gas Inventories 1996)
Admixture	7.3		<1	
Total CO_2 emissions (kg)			**145**	

Further, AAMs can be designed to have superior durability properties such as high resistance to alkali-silica reaction, freeze-thaw, acid attack and sulfate attack (Davidovits 1994; Pacheco-torgal et al. 2012; Zhuang et al. 2016). Therefore, attempts have been made to replace Portland cement-based concrete with AAM concrete in certain applications such as precast products.

AAMs are formed by the reactions between aluminosilicate precursors, or source materials and alkaline activators (Palomo et al. 2014; Provis & Bernal 2014). Aluminosilicate precursors are classified into three main groups:

(i) low calcium such as low calcium fly ash and meta-kaolin.

(ii) high calcium such as slag and

(iii) a blend of these two types such as a blend of fly ash and slag.

AAMs produced from a low calcium aluminosilicate precursor is deemed as geopolymer (Palomo et al. 2014; Provis & Bernal 2014). Those produced from a blend of low calcium precursors and high calcium ones (for example a blend of fly ash and slag), are also considered as geopolymer (Davidovits 2015). A blend of fly ash and slag is increasingly being investigated due to the benefits that can be derived from the presence of both types in the binder system (Ismail et al. 2013; Provis et al. 2012).

Despite these benefits mentioned above, the application of AAM in structure applications is still limited because available information on service history and durability performance of geopolymer concrete products is not sufficient to receive the public acceptance as a construction material. Another issue that AAM facing related with the way it was manufactured. Previously, the production of AAM required the use of a liquid activator which was highly alkaline, namely two-part geopolymer. Handling such liquid at construction site, especially in large quantities was quite dangerous. A new way of producing AAM, namely one-part geopolymer, therefore, was introduced

to deal with such safety issue. In one-part geopolymer technique, an activator in solid form was mixed with precursors such as fly ash and slag to produce a binder, akin to OPC. The use of one-part geopolymer binder, hence, is like that of OPC in the field applications. One-part geopolymer or AAM has been considered as safer and easier than two-part geopolymer (Vu et al. 2019). However, one-part geopolymer invariably has a short setting time, due to heat released from the dissolution of solid activators and from the reactions of precursors and activators, leading to an issue for casting concrete. This study aimed to cope with these two issues just mentioned. The outcomes of this research will help in promoting the applications of geopolymer or AAM in the field, thus, contribute to the environmental protection and sustainability.

1.2 Initial questions

The corrosion of steel reinforcement is the main cause of deterioration in more than 80% of the reinforced concrete structures (El-Reedy 2008). It has been recognized as a major durability issue of the reinforced concrete structures in many parts of the world (Portland Cement Association 2002). A major adverse effect of steel reinforcement corrosion on the structure is the strength loss of its members because of the reduction in the cross-sectional area of the steel bars and the concrete member (El-Reedy 2008). The process of reinforcing steel corrosion consists of two main stages: initiation and propagation (Tuutti 1982). Initiation is the first stage where depassivation of protective layer on the steel surface occurs, and the propagation stage is the result of corrosion reactions under the availability of oxygen, temperature, and moisture. The depassivation of the protective film takes place when the pH of the pore solution is reduced below 9 due to carbonation, or when there is a sufficient level of chloride ions in the pore solution, even at high pH levels (pH of 11.5 to 13.5), or by a

combination of these two aspects. Hence, carbonation and chloride induced corrosion are two major issues for steel corrosion in Portland cement-based concrete.

According to the Australian Standard AS 3600-2017, depending on the exposure environments, concrete structures and members must meet some specified requirements to guarantee the durability over the intended design life. For general concrete structures, the design life is about 50 years. For concrete pipes and culverts, their life expectation depends on their size and working conditions, as shown in Table 1.2.

Table 1.2 Requirement for durability of culvert headwalls, headwall extensions and cut-off walls

Type of structure	Pipe culvert diameter ≤ 800 mm Box culvert height ≤ 800 mm Soil cover ≤ 2.5 m	Pipe culvert diameter >800 mm Box Culvert height >800 mm All culvert sizes with soil cover > 2.5 m
Design life minimum	50 years	100 years
Minimum exposure classification	B1 to AS 3600-2017	B2 to AS 5100-2017
Minimum concrete strength	32MPa	40MPa

Pre-cast concrete pipes and culverts play an important role in every infrastructure system all-over the world. The ability of the pipes and culverts to maintain their design life expectation is a matter of concern to the manufacturers and users. The environmental loads caused by corrosive fluids these pipes and culverts carry

internally, and the aggressive ground water conditions can cause corrosion of steel reinforcement and damage to these structures (Roads and Traffic Authority 2010), especially for those that are partially buried or fully exposed to atmosphere. Geopolymer is a binder that is being developed rapidly over the past few decades, compared to Portland cement which has been around since 1824. Geopolymer is produced by the reaction between an aluminosilicate precursor, containing little or no calcium, and an alkaline activator (Palomo et al. 2014; Provis & Bernal 2014). The aluminosilicate precursors or source materials commonly used are metakaolin and/or fly ash. The blend of slag and fly ash was also used to produce fly ash/slag based geopolymer (Davidovits 2015). Geopolymer has been considered as a viable alternative material to traditional cement in concrete industry, for certain structures, due to its advantages over Portland cement with regard to environmental benefits (Davidovits 2002; Lloyd & Rangan 2009) and durability. The production process of geopolymer material does not involve the burning of lime, hence, consumes a much lower energy and reduces carbon dioxide emissions by 80-90%, compared to the manufacture of Portland cement. Additionally, the production of geopolymer can reuse a considerable number of by-products such as fly ash and slag, generated by industrial activities. These advantages on durability include high early strength, low shrinkage, high resistance to alkali-silica reaction, freeze-thaw, sulfate attack and reinforcement corrosion (Davidovits, 1994; Davidovits, 2002). Thus, geopolymer concrete may be an ideal material for producing pre-cast pipes and culverts.

However, the ability of geopolymer concretes to resist carbonation and chloride penetration, hence, to protect steel reinforcement was still a controversial topic and available information on this topic is limited. A thorough understanding of the real performance of geopolymer concrete in aggressive environments will be essential to

assess whether geopolymer concrete is a viable alternative to replace Portland cement-based concrete in the manufacture of the pre-cast pipes and culverts.

Further, the conventional production technology of the geopolymer binder requires the addition of high pH liquid activators that are highly corrosive and dangerous to use, whereas one-part fly ash/slag geopolymer introduces a new and safer method of production. However, one-part geopolymer has an issue of flash set, so using a suitable set retarder is essential for commercialisation and applications in construction industry. These aspects gave this study a clear focus and led to the following Research questions:

- Firstly, how can the issue of short setting time be extended by using a set-retarder, and how does such a retarder affect other properties of one-part geopolymer binder?
- Secondly, what are the curing conditions appropriate for producing concretes based on one-part geopolymer binder?
- Thirdly, what are the suitable methods of assessing carbonation and chloride resistance, the two main issues causing corrosion of steel reinforcement, in geopolymers or AAM concretes?

1.3. Research objectives

In order to address these questions mentioned above in section 1.2, this study aims to investigate the resistance to carbonation and chloride induced corrosion of one-part fly ash/slag geopolymer concrete. An investigation on the influence of set retarder on early-age properties of one-part geopolymer mortar, which is important to the production of mortar and concrete, is also carried out.

To evaluate the carbonation resistance in one-part geopolymer mortars, pH reduction and carbonation front depth indicated by two pH indicators are measured.

Due to carbonation, the change in porosity may happen, and hence, is included in the investigation. The effect of carbonation on compressive strength of one-part geopolymer concrete is also studied.

To access the resistance to chloride induced corrosion, apparent chloride diffusion coefficient determined by diffusion test up to 90 days in a 16.5% NaCl solution and charge passed determined by rapid chloride permeability test are performed. A correlation between chloride diffusion and charge passed in rapid chloride permeability test was investigated to find out the suitability of rapid chloride permeability test in evaluating chloride resistance of one-part geopolymer concrete.

The investigation on influence of a set retarder on early age properties of one-part geopolymer including setting time, heat evolution, workability and compressive strength development is examined in this study.

1.4 Significance of the study

To overcome the conventional production techniques of geopolymer binders requiring the handling of highly alkaline liquids that are dangerous, research on one-part geopolymer where water is used is essential. This will ensure the safety of the end users of geopolymers. This will also see an increased use of geopolymer in the field in the future.

The new findings of this study would promote a thorough understanding of resistance to carbonation and chloride penetration of one-part fly ash/slag geopolymer concretes, which is very useful to establish the durability design guidelines for structural/non-structural components using geopolymer concretes. Unless the issue of steel reinforcement corrosion in geopolymer concrete is well understood, widespread application of geopolymer in actual structures will be limited.

The results of this study would also be helpful in promoting the application and commercialisation of one-part geopolymer binder, a low carbon footprint material, which would protect and sustain the environment.

1.5. Organisation of the thesis

This thesis includes six chapters and each of the chapters is introduced as follows:

Chapter 1 presents the research background, current problems and research questions to guide the study. Significance and the objectives of the study is also presented.

Chapter 2 discusses about the available information in literature on carbonation and chloride penetration in geopolymer mortars and concretes. This chapter additionally shows a calculation of CO_2 release by producing geopolymer concretes investigated in this study.

Chapter 3 is devoted to the investigation on the influence of a set retarder on early age properties of fly ash/slag geopolymer pastes and mortars. Setting time and heat evolution and curing regimes of geopolymer mortars, which are important information for concrete production, are investigated with different amount of retarder.

Chapter 4 comprises an investigation in pH reduction and carbonation depth in one-part fly ash/slag mortars, under both natural and accelerated carbonation. Neutron tomography, an advanced technique in measuring pore size distribution and porosity in porous materials is applied to detect the change in porosity due to carbonation. A brief investigation on the influence of carbonation on compressive strength of one-part geopolymer is additionally included.

Chapter 5 deals with measurement and analysis of chloride diffusion by diffusion test and chloride permeability by rapid chloride permeability test. An analysis on correlation between the results of these two test methods is addressed.

Chapter 6 provides a summary of key outcomes of the study. Several limitations and future research suggestions are discussed.

CHAPTER 2: Literature Review

2.1 Introduction

This chapter presents a critical analysis of published sources on carbonation and chloride induced corrosion in geopolymer or alkali activated material (AAM). Basing on this, the research gaps is identified.

2.2 Steel reinforcement corrosion due to carbonation and chloride ions

Corrosion of steel reinforcement is a natural process because metals and alloys tend to convert into the more stable compounds having the lowest energy states (Hansson 2016). As for steel, these low energy compounds are commonly the metal oxides which are produced by the process of oxidation or corrosion. However, retarding the corrosion of steel reinforcement is possible (Buchler 2005; Polder 2005; Raupach & Robler 2005). This is vital to ensure the intended service life of concrete structures.

The corrosion of steel reinforcement in concrete is an electrochemical process (Hunkele 2005). This process comprises two half-cell reactions: anodic and cathodic. In steel reinforcement, some highly stressed regions or regions having a different electro-chemical potential on the surface can act as anode. At anodic site, electrons are produced, associated with the oxidation or dissolution of iron (see Equation 2.1). In contrast, electrons are consumed and hydroxyl ions are produced as a result of the reduction of oxygen at the cathodic site (see Equation 2).

$$Fe \rightarrow Fe^{2+} + 2e \quad (2.1)$$

$$2H_2O + \tfrac{1}{2} O_2 + 2e \rightarrow 2OH^- \quad (2.2)$$

Following that, iron cations react with hydroxyl ions, oxygen and water to produce rust products which have lager volume than the original steel that they replaced (Figure 2.1).

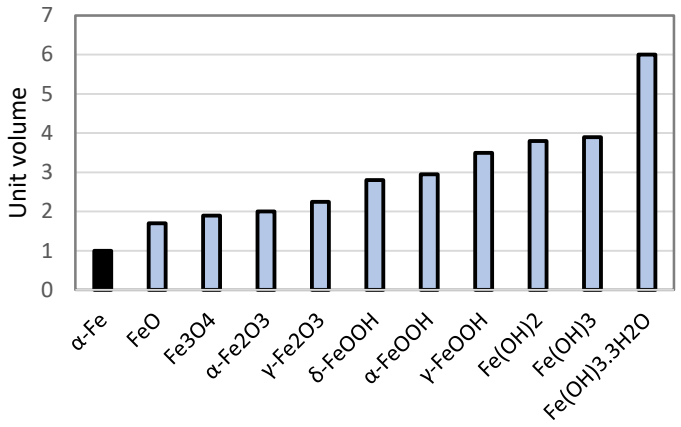

Figure 2.1 Volume of corrosion products relative to that of iron (modified from Poursaee 2016)

The reinforcing steel corrosion occurs when the protective films on the surface of embedded steel is partly or completely destroyed. These films are the dense iron oxide layers with thickness of about 5 nm, comprising crystalline layers of Fe_3O_4 with outer layers of γ -Fe_2O_3 (Chess 2014).

As mentioned previously, there are two main causes of the damage of the oxide protective films. One is carbonation and the other is the presence of chloride ions; chloride ion induced corrosion can be accelerated by the carbonation process (Papadakis, Vayenas & Fardis 1989). Carbonation causes a complete breakdown of the protective layer, whereas chloride induced corrosion just damages a relatively small area. While chloride attack is dominant in environments where the concrete surface comes into contact with chloride ions such as marine and coastal areas, carbonation

occurs in all other cases, especially in urban environments with high concentration of CO_2 in the atmosphere (Papadakis, Vayenas & Fardis 1989).

When CO_2 penetrates into Portland cement concrete, it reacts not only with $Ca(OH)_2$ available in the pore solution, but also with CSH and un-hydrated constituents (C_3S and C_2S), which are shown in Equations 2.3-2.6 (Papadakis, Vayenas & Fardis 1989).

$$Ca(OH)_2 + CO_2 \rightarrow CaCO_3 + H_2O \quad (2.3)$$

$$3CaO.2SiO_2.3H_2O + 3CO_2 \rightarrow 3CaCO_3.2SiO_2.3H_2O \quad (2.4)$$

$$3CaO.SiO_2 + 3CO_2 + nH_2O \rightarrow SiO_2.nH_2O + 3CaCO_3 \quad (2.5)$$

$$2CaO.SiO_2 + 2CO_2 + mH_2O \rightarrow SiO_2.mH_2O + 2CaCO_3 \quad (2.6)$$

In the hardened cement paste, water is always present, filling some of the pores. In water filled pores, CO_2 advances very slowly as compared with diffusion through unsaturated pores. Water plays a role as a medium for reactions of CO_2. The reduction of OH^- concentration in pore solution, caused by carbonation reactions, makes the pore solution pH decreased to below 9, resulting in the depassivation of the protective layer and then the emergence of a general corrosion if sufficient oxygen and water are present in the vicinity of the rebar (Zhou et al. 2015). Also, the total porosity of concrete is slightly reduced after carbonation because of the deposition of the formed $CaCO_3$ (García-González et al. 2006; Morandeau, Thiéry & Dangla 2014).

In contrast, the carbonation in geopolymer concrete produces potassium carbonate or sodium carbonate (Davidovits 2005), depending on the alkaline activator used. Additionally, under accelerated carbonation, there is an increase of the total porosity in carbonated geopolymer concrete due to the formation of alkali bicarbonate, a highly soluble substance (Badar et al. 2014).

On the other hand, chloride ions attack the protective layers in a different way. Chloride ions cause a localized corrosion, called “pitting corrosion”, if there is a sufficient amount of chloride ions, namely, chloride threshold, reaching the steel surface (Angst et al. 2011). In this process, chlorides act as catalysts to corrosion reactions, which are described in Equations 2.7 and 2.8 (Zhao & Jin 2016). To be more specific, chloride ions break down the passive layers and speed up the dissolution of iron. Thus, at anodic site, the corrosion rate is relatively high and this type of corrosion causes rapid loss of cross-section of steel rebar (Angst et al. 2011).

$$Fe^{2+} + 2Cl^- + 4H_2O \rightarrow FeCl_2.4H_2O \quad (2.7)$$

$$FeCl_2.4H_2O \rightarrow Fe(OH)_2 + 2Cl^- + 2H^+ + 2H_2O \quad (2.8)$$

Not all chloride ions penetrating into concrete can reach the steel. Some of them are captured or bound by hydration products. In Portland cement concrete, chloride ions can be bound chemically by the formation of Friedel‟s salt which is created by the reaction between chlorides and cement compounds such as C_3A and C_4AF (Delagrave et al. 1997). Also, chlorides can be physically held to the surface of hydration products C-S-H gel (Beaudoin, Ramachandran & Feldman 1990).

As for geopolymers, chlorides may be held in different ways, because there was no formation of the Friedel‟s salt even when geopolymers were immersed in NaCl solution for two years (Škvára, Jílek & Kopecký 2005). There might be other chloride-bearing substances in the geopolymer matrix. It is a fact that the geopolymerisation process of fly ash produces the main reaction product with a structure similar to zeolite precursor, a three dimensional framework (Fernández-Jiménez et al. 2006; Palomo, Alonso & Fernandez-jime 2004). Also, the secondary reaction product of this process is zeolite (Fernández-Jiménez, Palomo & Criado 2005; Palomo et al. 2014). It is well known that zeolite is a great absorbent of several ions and molecules. For

example, it has been used as an absorbent material for seawater desalination (Wajima et al. 2010; Wibowo et al. 2017). Hence, the ability of a geopolymer concrete to bind chloride ions might be associated with the absorption properties of reaction products of geopolymerisation process. Until now, the mechanisms of chloride ion binding of any geopolymer concrete is not well understood.

The corrosion of steel reinforcement in Portland cement concrete strongly depends on external and internal factors (Ahmad 2003; Bertolini et al. 2013). The former are the environmental factors such as humidity, temperature, concentration of aggressive agents, and availability of oxygen and moisture at rebar level. The later are factors related to the concrete, such as its alkalinity and permeability. For geopolymer concrete, factors affecting the corrosion rate of steel reinforcement are expected to be similar to those observed in Portland cement concrete. However, most of investigations on this aspect of geopolymer concrete focused on the internal factors, which are presented in Sections 5 and 6 below.

2.3 Comparison of carbonation induced corrosion in geopolymer and Portland cement concretes

2.3.1 Carbonation induced corrosion in fly ash geopolymer concrete

According to Davidovits (2005), pH of geopolymer is in the range of 11.5 to 12.5, depending on the formulation. If pH of geopolymer is higher than 12.5, it will be deleterious for the geopolymer and hence the formulation of geopolymer should be such that the pH is maintained between 11.5 and 12.5. Besides, the carbonation of geopolymer is significantly different from that of Portland Cement. Carbonation of Portland cement- based concretes yield calcium carbonate with a pH of 7-8, while carbonation of geopolymer concretes produce potassium carbonate or sodium

carbonate and pH will be decreased to a level of 10-10.5. This higher level of pH maintaining ability can be explained by the structure of geopolymers. In geopolymers, the alkali ions K^+ and Na^+ are strongly bound into the 3D framework and there is hardly any free alkalis available. Thus, carbonation does not significantly affect the pore solution pH of geopolymers. If pH is too high, then free alkali could be present outside the 3D framework and this may lead to carbonation.

This finding of Davidovits (2005) was in agreement with the results obtained by Law et al. (2015). The pH values of the pore water of low calcium fly ash geopolymer concrete were measured at different curing periods up to 28 days. All geopolymer mortar specimens had an initial pH of between 11.75 and 12, with compressive strength at 28 days of about 50 MPa. After exposing to accelerated carbonation tests (5 % CO_2 at a temperature of 20±1^oC and a relative humidity of 70 ± 1 %) for 28 days, all geopolymer specimens had a pH in the range of 10.46 - 11.23. They concluded that carbonation of low calcium fly ash geopolymer concrete may not be as potentially deleterious as carbonation of OPC and blended cement concretes, as the pH remains at a level that can provide protection to the reinforcing steel. This conclusion was supported by the findings of Pu et al. (2012). The initial pH values of pore solution of OPC and OPC/fly ash concretes were about 12.96 to 13.41 (Pu et al. 2012). When exposed to a similar accelerated carbonation test (5% CO_2 at a temperature of 20^oC and a relative humidity of 40%) for 28 days, the pH of pore solution of OPC and OPC/fly ash concrete was about 7.2. These samples were produced with water/cement ratios of 0.5 and 0.6, cement content of 400-600 kg/m^3, but no results on compressive strength or porosity were reported in this study.

Under natural carbonation conditions, the alkalinity of the low calcium fly ash based geopolymer concretes was found to be sufficient to maintain the passivation of

the steel reinforcement (Badar et al. 2014). These tests were carried out on cylinders of 70mm diameter and 150mm long with a central 6mm diameter deformed bar. These geopolymer specimens were cured at 80°C for 72 hours. Geopolymer samples were produced from three different types (named as OH, DH and MN) of fly ash having different calcium contents (5%, 1.97% and 12.93% CaO, respectively). The results were obtained using a corrosion potential method as per ASTM C876-15 over a period of 450 days. The half-cell potential results of OH and DH geopolymer concretes were more than -350 mV CSE, indicating a low risk of corrosion in accordance with ASTM C876-15. There are no results reported for these two geopolymer concretes, after 450 days. Only MN geopolymer with highest calcium content showed corrosion potential less than −350 mV CSE after 300 days, associated with 90 % probability of reinforcing steel corrosion. Similarly, under natural carbonation process over 1 year, the pore solution pH of geopolymer concretes was always higher than 10.5 (Pouhet & Cyr 2016).

2.3.2 Carbonation induced corrosion in fly ash/slag blended geopolymer concrete

Under real field exposure conditions, fly ash/slag (70% fly ash/30% slag) geopolymer concrete was tested after 8 years (Pasupathy et al. 2016). The geopolymer mix had a compressive strength of 53 MPa, and VPV of 14%, measured on cores obtained. The carbonation depth in this geopolymer concrete was 8-14 mm. These results were compared by Pasupathy el al (2016) with a 13 year old OPC concrete exposed elsewhere under similar conditions and reported by Castel, François & Arliguie (1999). In the latter case, the compressive strength of the OPC concrete was 56 MPa, obtained from cores, and the VPV was 15%. The carbonation depth in this OPC concrete was found to be 7-13 mm. Hence, Pasupathy et al. (2016) concluded

that the geopolymer concrete had performed as equally good as the OPC concrete with regard to carbonation.

In a study by Khan, Castel & Noushini (2016), on fly ash/slag (90% low calcium fly ash/10% slag) geopolymer concrete, having an average compressive strength 55.7 MPa at 28 days, specimens were subjected to natural carbonation process at temperature 23°C and relative humidity 55% for 18 months. In this case, fully carbonated region had a depth of 3mm. In another study (Rozière, Loukili & Cussigh 2009), a concrete produced from 30% fly ash blended Portland cement, having a similar compressive strength (above 52 MPa), was exposed to a natural carbonation process at 20^{o}C and 50% of relative humidity for 12 months. Its carbonation depth was found to vary between 2.1 and 9.5 mm, depending on the curing conditions (Rozière, Loukili & Cussigh 2009). Based on results of carbonation depth in fly ash/slag geopolymer in the above studies, it can be concluded that fly ash/ slag geopolymer concrete had better than or similar performance to blended Portland cement concrete, in the strength grade of 50MPa.

2.4 Comparison of chloride induced corrosion of steel reinforcement in geopolymer concrete and Portland cement-based concrete

When comparing the ability of geopolymer concrete and Portland cement concrete to resist chloride ion induced corrosion of reinforcement, the physical characteristics such as porosity, pore size and distribution and liquid/solid ratio (water/cement ratio for OPC concrete) should be taken into account. This is because concrete cover thickness plays a major role as a physical barrier between the external environment and steel reinforcement, and hence can significantly influence the penetration of chloride ions into concrete (Modena et al. 2014; Page & Treadaway

1982). Therefore, it is possible to produce a geopolymer concrete that has better resistance to chloride ion penetration than Portland cement concrete, by decreasing its pore size and porosity. The resulting geopolymer concrete may have a higher compressive strength.

2.4.1 Chloride induced corrosion of steel reinforcement in fly ash geopolymer concrete

Miranda et al. (2005) investigated the passivation of the steel reinfocement in the fly ash geopolymer mortar, in comparison to Portland cement mortar. The liquid/binder ratio of geopolymer mortar was 0.35 whereas the OPC mortar had a water/binder ratio of 0.55. The geopolymer specimens were cured at 85°C for 20 hours. The OPC mortar specimens were cured at 50°C and 95% relative humidity for 2 days. Although liquid to solid ratios and curing conditions were different for these two mortars, the compressive strength of geopolymer and OPC mortars were 38 amd 37 MPa (at 2 days of age), respectively. Therefore, the corrosion potentials of these two mixes were considered to be a valid comparison. For the mixes with no chloride addition, fly ash geopolymer mortars were found to passivate steel reinforcement as effectively as OPC mortars, as indicated by similar i_{corr} values. However, they reported that for mixes that had an addition of 2% chloride by weight of binder, the corrosion current density values i_{corr} were higher in fly ash geopolymer mortars than in OPC mortars, implying a higher corrosion rate in fly ash geopolymer mortars. This comparison is questionable as the fly ash geopolymer mortars had a higher binder content than OPC mortars and hence higher chlorides were added to the geopolymer mortars. It appears that on the basis of an equivalent strength of fly ash geopolymer and OPC mortars the rate of corrosion is similar. Results of Miranda et al. (2005) were also confirmed by a similar investigation by Bastidas et al. (2008).

A recent study on the severity of steel corrosion in a low calcium fly ash geopolymer concrete culvert, over 6 years of exposure in a saline lake environment was reported by (Pasupathy et al. 2017). Two culverts, one made of geopolymer concrete and the other made of OPC concrete (1200mm long, 1200mm wide and 600mm deep with the same cover to reinforcement) were studied. The compressive strengths of geopolymer and OPC concrete at 90 days of age were 39MPa and 43MPa, respectively. At the same age, the VPV values were 11.4% and 12.3%, respectively. After 6 years of exposure, they reported that the degree of corrosion of the steel reinforcement in geopolymer culvert was higher than that in OPC concrete culvert. The methods used to evaluate severity of corrosion were visual observation of the steel surface and SEM/EDX analysis of the steel/concrete interface. There was no direct corrosion measurement on the steel bars. Further studies on the corrosion severity of steel embedded in different geopolymer concretes, with different mix designs, in service is needed to establish the rate of corrosion in geopolymer concrete. Further the basis of comparison of geopolymer concretes and OPC concretes need to be clearly identified.

On the other hand, it was reported, by another researcher, that the fly ash geopolymer concrete had good resistance to chloride attack, with longer time to corrosion cracking compared to OPC concrete, under an accelerated condition (Reddy et al. 2011). However, the fly ash geopolymer concrete had a higher compressive strength of 40MPa at 28 days of age and OPC concretes examined had a lower compressive strength of 33MPa at the same age. Thus, the water/binder ratio in OPC and the liquid/solid ratio in geopolymer mixes might be different, leading to different levels of porosity.

Low calcium fly ash geopolymer concretes also exhibited much lower chloride diffusion coefficients than OPC concrete after exposed to a severe condition for 1 year (Kupwade-Patil & Allouche 2013). The severe condition consisted of 14 days of 7.5% NaCl solution exposure (wet cycle), followed by air exposure for 14 days (dry cycle). The results are compared in Fig. 2.2. When compared with their OPC counterparts, much lower levels of steel corrosion were seen in geopolymer samples that were produced from three different types (namely OH, DH and MN) of fly ash with different calcium contents (5%, 1.97% and 12.93% CaO, respectively).

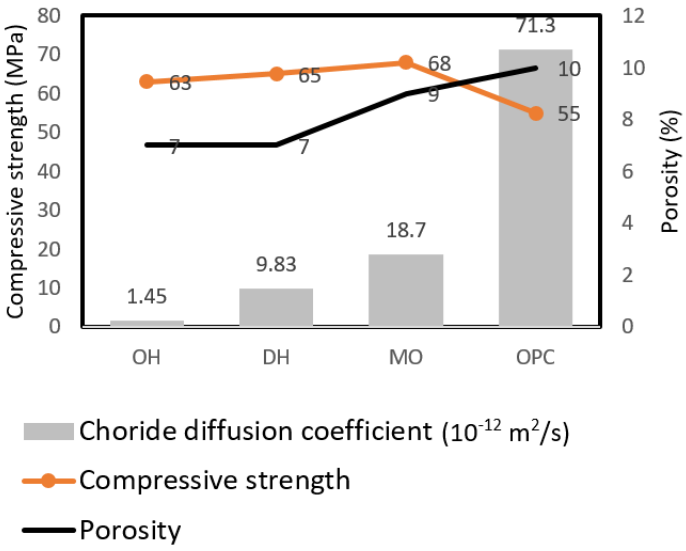

Figure 2.2 Chloride diffusion coefficients after 1 year of exposure, compressive strength at 28 days and porosity before exposure for fly ash geopolymer concretes and OPC concrete (Kupwade-Patil & Allouche 2013)

In a study by Olivia and Nikraz (2011), the time taken to reach active corrosion potentials (-350mV using half-cell potential method) and time to failure as indicated by crack initiation were measured under accelerated corrosion conditions. Steel mass loss was also measured. The results of half-cell potential measurements indicated that the corrosion level of steel reinforcement was higher in the fly ash geopolymer

concrete than in OPC concrete. Nonetheless, when corrosion rate of steel reinforcement was measured by measuring the steel mass loss, the fly ash geopolymer concrete had a much lower corrosion rate, approximately 48 to 97 times lower than that for OPC concrete, as shown in Fig. 2.3. Therefore, it is suggested that the interpretation of half-cell potential results to evaluate the corrosion severity of steel in geopolymer concrete needs further investigation. For example, a new criterion of half-cell potential threshold for steel reinforcement corrosion in geopolymer concrete needs to be established.

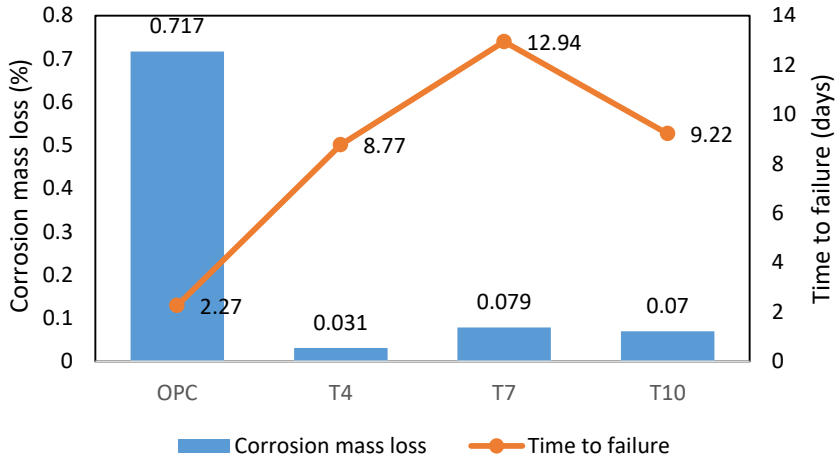

Figure 2.3 Corrosion rate and time to failure of steel reinforcement in OPC concrete and in geopolymer concrete T4, T7 and T10 (Olivia & Nikraz 2011)

The exposure conditions also have a significant influence on the chloride induced corrosion of steel reinforcement in fly ash geopolymer concrete as well as OPC concrete. Monticelli et al. (2016a) found that the corrosion behaviours of reinforcing bars in fly ash geopolymer (FA) mortars were worse than that in Portland cement mortar, under 11 weekly wet and dry cycles to 0.1M chloride solutions. The electrochemical tests, combined with an investigation of the mortar microstructures, were used to evaluate the corrosion level of steel. It was reported that 50% of steel

reinforcement in fly ash geopolymer concrete was affected by corrosion after 20 days, while steel in Portland concrete just suffered corrosion after 95 days.

However, it was noted that the 28-day compressive strengths of the fly ash geopolymer mortars (namely G-1, G-2 and G-3) were considerably lower than that of OPC mortar (REF) (see Table 2.1). Porosity levels were also different. Hence the basis of comparison is questionable. It would be more appropriate to compare geopolymer and OPC concretes having similar properties in terms of their strength and durability requirements.

Table 2.1 Porosity and compressive strength of mortars at 28 days (Monticelli et al. 2016a)

Sample	Total porosity, determined by specific intruded Hg volume (mm^3/g)	Compressive strength at 28 days (MPa)
Geopolymer G-1	57	34.2
Geopolyme G-2	60	27.0
Geopolyme G-3	85	22.5
OPC REF	50	47.0

Nevertheless, Monticelli et al. (2016b) also recorded a different performance of these fly ash geopolymer mortars when they were immersed in a 3.5% NaCl solution for 90 days, instead of wetting and drying cycles. Fly ash geopolymer (FA) mortars showed better protection capacity for steel reinforcement, although they had lower compressive strengths than OPC REF mortar. Two of three FA mortars showed a higher critical threshold chloride content for corrosion initiation (about 1–1.7% by weight of binder), than that of OPC mortar (around 0.5%). The chloride threshold

levels to initiate corrosion of steel reinforcement for geopolymer concretes need to be investigated further.

2.4.2 Chloride induced corrosion of fly ash/slag geopolymer concrete

The appropriate combination of fly ash and slag as source materials for producing geopolymer has advantage over using single fly ash or slag. It is ascertained that the main reaction product of alkaline activation of slag is CSH gel (Fernández-Jiménez et al. 2003; Huanhai et al. 1993; Richardson et al. 1994), while that of fly ash is geopolymer gel such as N-A-S-H and K-A-S-H. The coexistence of these two gels can make the resultant matrix denser because the formation of C-S-H and N-A-S-H gels may help to bridge the gaps between the different hydrated phases and unreacted particles (S. A. Bernal et al. 2013; Saha & Rajasekaran 2017; Yip, Lukey & van Deventer 2005). It is well known that the lower the porosity of the concrete is, the more difficult for chlorides to reach steel surface. Thus, fly ash/slag geopolymer concrete is expected to have a better level of durability.

A comparison of chloride permeability in the fly ash/slag geopolymer concretes and OPC concrete was carried out by Ismail et al.(2013). Although the compressive strength and volume of permeable voids of the 50% slag/50% fly ash geopolymer concrete seems similar to that of OPC concrete, it showed better resistance against chloride ingress regarding penetration depth and diffusion coefficient when tested as per the accelerated test NT Build 492 and the ponding test ASTM C1543.

In another study, the corrosion of the reinforcement in 50%fly ash/50%slag geopolymer concrete and OPC concrete was compared (Tennakoon et al. 2017). Fly ash/slag geopolymer concrete had compressive strengths about 50MPa at the age of 28 days and the OPC concrete was a 40 grade mix with w/c ratio of 0.46 and cement content of 400 kg (geopolymer mix also had a binder content of 400 kg and w/c ratio

of 0.43). Also, 2% NaCl by mass of binder was added in geopolymer and OPC mixes to assess the corrosion behaviour of steel reinforcement in contaminated concretes. All reinforced samples (95mm× 95mm× 300mm), with a thickness of concrete cover 40 mm, were then partially immersed in water. From 0 to 150 days, half-cell potential of steel embedded in geopolymer concrete was in the range of -500 to -550 mV, more negative than that of steel embedded in OPC concrete (from -350 to -400mV). This indicated a higher corrosion degree of embedded steel in geopolymer concrete. However, results obtained by visual inspection showed different trend. The steel embedded in OPC concrete showed a high level of corrosion after 150 days, while the steel embedded in geopolymer concrete does not show any pitting corrosion products. It was concluded that half-cell potential results seemed to misunderstand the corrosion state of steel reinforcement in contaminated fly ash/slag geopolymer concrete.

Better performance (in terms of chloride penetration) of the 50% fly ash/50% slag geopolymer concrete than OPC concrete was also recorded in a study by Lee & Lee (2016). The compressive strength and VPV at 28 days of OPC concrete examined in this work were 61 MPa and 28%, respectively. For 50% fly ash/50% slag geopolymer concrete these values were 81 MPa and 23%, respectively. The bottom 10mm of cubes of 50 mm size was immersed in 10% NaCl solution for 91 days. Chloride penetration depth, measured by spraying Silver Nitrate solution, of geopolymer concrete (about 7.7 mm) was half of that of OPC concrete (approximately 14,4 mm). The total chloride concentrations at a height of 30mm from the bottom surface of specimens were measured. In geopolymer concrete it was 0.0632 (mg/g), much lower than that of OPC concrete where it was 0.6666 (mg/g). Hence a fly ash/slag geopolymer shows a lower depth of penetration of concentrated salt solution. It is probably because geopolymer has the higher compressive strength (81 MPa) and

lower VPV (23%) than its OPC counterpart, thus, it is more difficult for salt to penetrate in geoplymer specimens.

2.5 Factors affecting carbonation induce corrosion in geopolymer concrete

The main factors affecting carbonation in geopolymer concrete are identified as the synthesis condition (such as composition of raw materials and alkaline activator**,** and curing regime) and the carbonation condition. These factors are discussed in details below:

2.5.1 Synthesis condition

It was reported that geopolymer concrete prepared with fly ash bearing a small calcium content is more suitable for the production of durable concrete for structures exposed to carbonating environments (Badar et al. 2014). The relationship of CaO/SiO_2 ratio of fly ash and porosity of resulting geopolymer concrete at the rebar/ concrete interface was shown in Fig. 2.4. This indicated that the geopolymer concrete prepared with fly ashes (DH, OH) having a small calcium content exhibit a denser structure than that with fly ash (MN) having high calcium content (Badar et al. 2014). This dense microstructure was useful in preventing the ingress of CO_2, and so to mitigate the pH reduction induced by carbonation. As a result, corrosion level of the reinforcement embedded in the DH and OH geopolymer concretes were thus smaller than that in MN geopolymer concrete, which was observed by results of half-cell potential (E_{corr}) and scanning electron microscopy with energy dispersive X-ray (SEM/EDX).

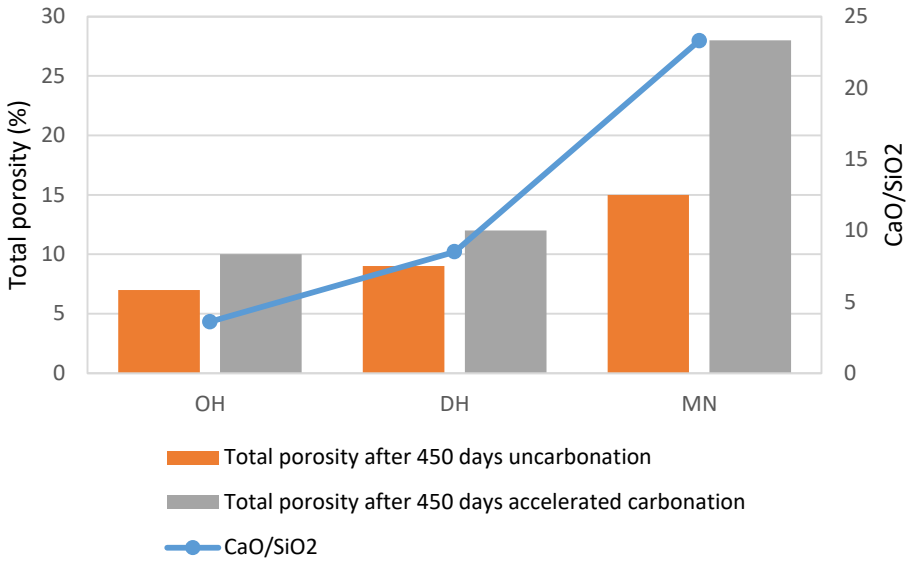

Figure 2.4 The relationship of CaO/SiO_2 of fly ash and porosity of resulting geopolymer concrete. Data from a study of Badar et al. (2014).

Slag having higher MgO content can reduce the susceptibility to carbonation of alkali activated binder (Bernal et al. 2014). It was explained that the activation of high content MgO slag produced the main secondary product, hydrotalcite, which acts as an internal CO_2 sorbent and favours the formation of stable carbonation product. Hence, carbonation in fly ash/slag geopolymer may be reduced if slag bearing a high content of MgO is used. Further, alkali-activated fly ash/slag pastes, prepared with more than 50% slag in the blend, showed good carbonation resistance (Nedeljkovic et al. 2017).

In a recent report, the addition of nano-TiO_2 particles into fly ash geopolymer paste was found to improve the carbonation resistance and reduce the drying shrinkage of this paste (Duan et al. 2016). This is mainly because the incorporation of nano-TiO_2 particles made microstructure denser and less cracks, which was proved by quantitative results on the pore structure of geopolymer with and without nano-TiO_2.

Composition of alkali activator was reported to affect the carbonation in geopolymer (Pasupathy et al. 2016). After 8 year exposure to outdoor field conditions,

fly ash/slag geopolymer concrete prepared with activator containing Na_2SiO_3 showed higher carbonation rate (8.3-9.8 mm/year$^{1/2}$) than fly ash/slag geopolymer produced with activator containing no Na_2SiO_3 (2.8 -5 mm/year$^{1/2}$).

The curing regime also has an influence on the carbonation in geopolymer. If the curing conditions are appropriate, a quick carbonation process can be avoidable (Criado, Palomo & Fernández-Jiménez 2005). These authors also recommended a high relative humidity as a suitable curing condition for geopolymer.

2.5.2 Carbonation condition

When geopolymer are exposed to different concentration of CO_2, different products of carbonation reaction are produced. In the atmosphere where concentration of CO_2 is low (0.03–0.04%), carbonation in geopolymer leads to the formation of alkali carbonate (S. A. Bernal et al. 2013; Cyr & Pouhet 2016). By contrast, if concentration of CO_2 is higher, the formation of alkali bicarbonate is favoured. It is well known that alkali bicarbonate is a less stable product, or soluble salt, which can make the pore solution pH of geopolymer concrete decreased rapidly. Thus, accelerated carbonation test, which is often used to faster carbonation and so to shorten testing time, seems to underestimate the carbonation resistance of geopolymer materials (S. A. Bernal et al. 2013; Cyr & Pouhet 2016).

2.5.3 Factors affecting chloride induced corrosion of steel reinforcement in geopolymer concrete

The presence of calcium in source materials was believed to be extremely important to reduce the alkali loss which decreases the pore solution pH, and so causes depassivation of protective film on embedded steel‟s surface (Lloyd et al., 2010).

Thus, Lloyd et al. (2010) suggested that the presence of calcium in the source material seems necessary for manufacturing a durable geopolymer concrete. Considering the fact that an increase in pore solution pH will enhance the passivation of protective films on steel surface, this suggestion is reasonable. However, in terms of the microstructure of the geopolymer concrete, it might not be fair. It is because geopolymer concrete that is produced from fly ash with high calcium content showed higher porosity than that is produced from fly ash having low calcium content (Badar et al. 2014).

The substitution of 20–40% fly ash by slag in the fly ash/slag geopolymer concrete mix at the constant liquid/solid of 0.7 does not change the porosity too much but reduces the sizes of pores and also increases the tortuosity, resulting in a reduced porosity and an increased tortuosity (Zhu *et al.*, 2014). As a result of this, the chloride penetration rate is decreased.

The variation of slag content in the mix design of fly ash/slag geopolymer concrete affected the chloride-binding capacity and the resistance to chloride penetration in different way. Increasing the slag content up to 50% in the mixes resulted in an increase of C-(A)-S-H gel, leading to the denser geopolymer concretes. Thus, the chloride penetration depth was greatly decreased (Lee & Lee 2016). However, the authors pointed out that the chloride-binding capacity increased with the number of N-A-S-H gels. As a result of this, when the slag content was increased, the chloride binding capacity was decreased.

When fly ash geopolymer concrete was prepared from an alkaline activator having a high NaOH concentration, the quantity of free and total chloride ions penetration was decreased. This led to a decrease of chloride diffusion coefficient and

steel corrosion in this geopolymer concrete, after 3 year exposure in a marine environment (Chindaprasirt & Chalee, 2014).

2.5.4 Conclusions

From the information presented above the following main conclusions can be reached:

The incorporation of fly ash and slag, with appropriate ratios with NaOH with no or minimum activator $NaSiO_3$ dosage, seems helpful in producing a geopolymer binder that has better carbonation resistance than a comparable OPC binder. After carbonation, the pH levels of low calcium fly ash based geopolymers can be maintained above 10.5 offering protection to steel reinforcement against carbonation induced corrosion.

The results of studies on corrosion of steel reinforcement in geopolymer concrete can be affected significantly by the type of measurements used. These measurements have been mainly established and developed for Portland cement-based concretes, not for geopolymer concretes. Until new methods for testing steel rebar corrosion in geopolymer concretes are set up, a combination of several methods are strongly recommended.

The rate of corrosion as measured by steel weight loss clearly indicate the superior performance of geopolymers of equal strength grades to OPC concrete. The half-cell potential level to initiate corrosion in geopolymers is very different to OPC concrete. This aspect needs further investigation.

The chloride threshold levels to initiate corrosion in geopolymers concrete need further investigation.

The performance of geopolymer concretes should be compared with that OPC or blended cement-based concretes that have similar initial properties and pore characteristic, in order to obtain useful findings.

Fly ash/slag blended geopolymer concrete with appropriate mix design could serve as an effective substitute for OPC in reinforced concrete structures. However, more work on the chloride induced corrosion of steel reinforcement in fly ash/slag blended geopolymer concrete should be performed.

CHAPTER 3: Influence of Set Retarder on Early Age Properties of Fly ash/Slag Geopolymer Pastes and Mortars

3.1 Introduction

In the conventional way to produce geopolymer, the activator was in a liquid form. However, handling this highly corrosive liquid at site, in large quantities, is a challenge for production of geopolymer concrete in construction industry. One-part mix is a new way to produce geopolymer. In this technique, solid alkaline activator is mixed with precursors, resulting in geopolymer binder. This method is safe method to produce geopolymer concrete, because only water is added to activate the binder and handling highly alkaline activator at site is eliminated. Thus, one-part mix geopolymer binder can be similarly used as Portland cement in field applications.

However, one-part mix geopolymer has a limitation of flash setting due to the heat released by the dissolution of solid activators and the geopolymerisation reactions. This chapter investigated the effect of a sodium borate based retarder on setting time, heat release, workability and compressive strength development of dry powder fly ash/slag geopolymer pastes and mortars. The influence of retarder on setting time also was investigated by X-ray and scanning electron microscopy (SEM) with energy dispersive X-ray spectrometry (EDS). The findings confirmed the suitability of the retarder in prolonging setting time of one-part mix geopolymer, making such binder more appropriate for precast work.

3.2 Experimental program

3.2.1 Materials and mix proportions

In this study, low calcium fly ash and ground granulated blast furnace slag were used as precursors to produce two types of one-part geopolymer binders, named Geo 1 and Geo 2. The chemical compositions of these precursors are shown in Table 3.1 and their Thermogravimetry and Derivative Thermogravimetry (TG/DTG) results are depicted in Figure 3.1. Ground granulated blast furnace slag tested contains inherent reduced species such as iron and sulfate and manganese, which gain mass on heating or oxidizing. As a result, often slag gives nearly zero or a slightly negative LOI as recorded in this case.

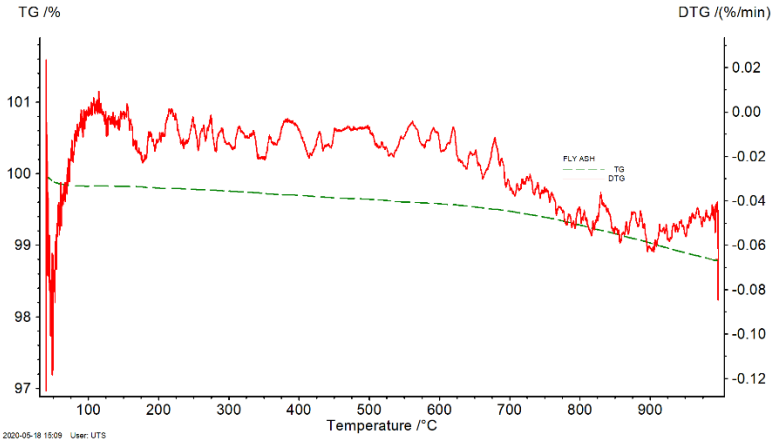

(a)

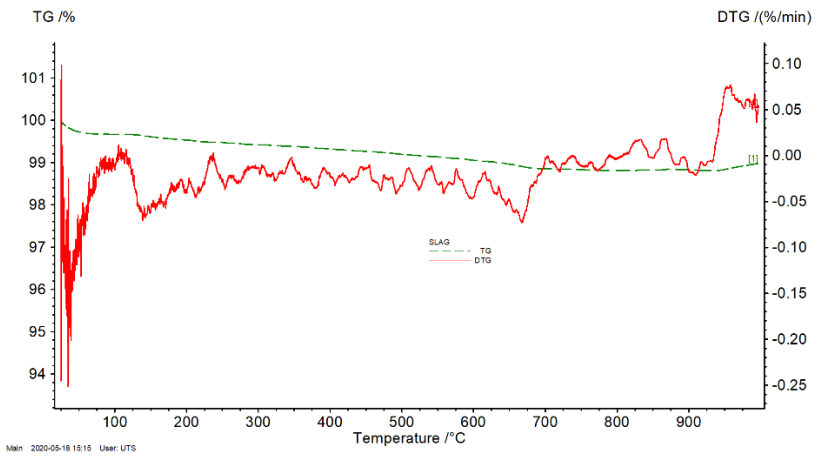

(b)

Figure 3.1 TG/DTG curves of (a) fly ash and (b) ground granulated blast slag

A solid alkali activator, at the dosage of 16%, was mixed with fly ash and ground granulated blast furnace slag to produce Geo 1 and Geo 2 binders. This alkali activator contained solid anhydrous sodium meta-silicate and a carbonate mineral that imparts hydroxide anions (OH^-) on hydration. The ratios of fly ash to slag in Geo 1 and Geo 2 binders are 0.4 and 0.6, respectively (see Table 3. 2).

Table 3.1 Chemical compositions of fly ash and ground granulated blast furnace slag

	Oxide compositions wt.%										
	SiO_2	Al_2O_3	CaO	MgO	Fe_2O_3	TiO_2	SO_3	K_2O	Na_2O	Other	LOI
Fly ash	58.15	22.29	5.39	1.28	6.95	1.03	0.15	1.39	0.47	1.81	1.09
Slag	33.89	14.14	40.46	6.84	0.45	0.58	1.59	0.28	0.32	1.56	-0.11

Table 3.2 Mix proportions (by weight) of Geo 1 and Geo 2 binders

	Slag/(Fly ash + Slag)	SiO_2/Al_2O_3 in binder	Sodium activator powder (%)
Geo 1	0.4	2.6	16
Geo 2	0.6	2.4	16

The particle size distribution of Geo 1 and Geo 2 binders was measured by a Malvern Mastersizer instrument using a dispersing agent Isopropyl alcohol, shown in Figure 3.2.

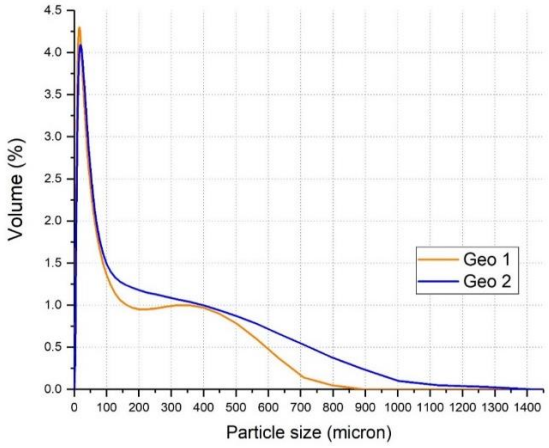

Figure 3.2 Particle size distribution of Geo 1 and Geo 2 binders

Sand, used to prepare mortar specimens, was Sydney sand (dune sand) with specific gravity of 2.6 kg/l and fineness modulus of 2.5. Sand to geopolymer powder ratio used was kept as 2.5 for all specimens.

3.2.2 Experimental procedure

The Geo 1 and Geo 2 pastes and mortars were produced in a Hobart mixer (see Figure 3.3a) as per ASTM C305-14 (American Society for Testing and Materials 2014). For producing pastes, water was first added to the mixing bowl and then the dry power Geo 1 or Geo 2 was added. The mixing process started at low speed ((140 ± 5 r/min) for 30 seconds, then stopped for 15 s to scrape down into the batch any paste that may have collected on sides of the bowl, then finishing by 60 seconds at medium speed (285 ± 10 r/min). Regarding producing mortars, water was first placed in the bowl, then the dry power Geo 1 or Geo 2 was added. The mixer was started at the slow speed (140 ± 5 r/min) for 30 s. Sand was introduced and mixed for further 30 seconds at low speed and 30 seconds at medium speed. After that, the mixer was stopped for 90 s to let the mortar stand. Finally, the mixing was then started for 60 s at medium speed.

(a) (b)

Figure 3.3 (a) Hobart mixer and (b) Mortar flow test

The workability of mortars was measured immediately upon completion of mixing, by mortar flow test (see Figure 3.3b) per ASTM C1437 (American Society for Testing and Materials 2015). Two 25 mm layers of mortar were placed in the mould and tamped 20 times each layer with the tamper. Using the straightedge or the edge of the trowel with a sawing motion across the top of the mould to make the top surface flat. The mould was then lifted away from the mortar, and the table was 25 times in 15 s. Following that, the diameter of the mortar along the four lines scribed in the table top was measured by using the calliper. The flow (nearest 1%) is the result of the dividing average of such four readings by the original base diameter.

Immediately after completion of the flow test, the mortar was returned to the mixing bowl and remixed for 30 s at medium speed. Cube specimens were cast in the 50x50x50 mm steel moulds. All the specimens were cured at a temperature of 23^{o}C and a relative humidity of 90% in a moisture cabinet. After 1 day, all the specimens were removed from their moulds and cured under three different curing conditions. The first is sealed curing where specimens are wrapped in plastic film and placed in the laboratory air. The second is sealed and heat curing, in which specimens are

wrapped in plastic film and kept in an oven at 60^{o}C for 6 hours, then placed in laboratory air. The third is heat curing that specimens are heated at 60^{o}C for 24 hours, then placed in the laboratory air.

The compressive strength test of these 50 mm cubic mortar specimens was performed following ASTM C109/C109M-16a (American Society for Testing and Materials 2016). The load was applied to specimen faces that were in contact with the true plane surfaces of the mould, with a load rate of 1400 N/s. The compressive strength of each specimen was the result of dividing the total maximum load (N) by the area of loaded surface (mm^2). The maximum permissible range between specimens from the same mortar batch, at the same test age, is 8.7 % of the average when three cubes represent a test age and 7.6 % when two cubes represent a test age.

Initial and final setting times of dry powder geopolymer Geo 1 and Geo 2 were measured using Vicat apparatus as per to ASTM C191-19 (American Society for Testing and Materials 2019). The test started by mixing the dry powder geopolymer binder with water required to produce the paste as per ASTM C305-14 (American Society for Testing and Materials 2014), then filling the conical ring with the resulting paste, cutting and smoothing the top surface of the test specimen. Following that, determining the penetration of the 1 mm needle every 15 minutes was performed until a penetration of 25 mm or less obtained. The elapsed time between the initial contact of cement and water and the penetration of 25 mm was the initial setting time. After that, determining the first penetration measurement when the endpoint of the needle did not mark the specimen surface with a complete circular impression. The elapsed time between the initial contact of cement and water and the time mentioned above is the final setting time.

The progress of reactions of the pastes, from 5 minutes after mixing to 1 day, were investigated by X-ray diffraction (XRD). XRD patterns were obtained by a Bruker D8 Discover X-ray diffractometer operating at 40mA and 40 kV with Cu-Kα radiation. The data were collected from 10° to 80° 2θ for 32 minutes, at a step size of 0.02°. Scanning electron microscopy (SEM) with energy dispersive X-ray spectrometry (EDS) were also performed in this study, to supplement the findings of XRD.

Heat evolution was measured by isothermal calorimetry using I-Cal 4000 HPC Isothermal Calorimeter. The dry powder geopolymer binders Geo 1 and Geo 2 were mixed with water for 2 min with water/powder (W/P) of 0.3 to achieve a homogeneous paste. Fifty grams of each paste was then poured into small plastic ampoules. The measurement was done at 25°C, and the data was recorded for a period of 48 hours.

To verify the influence of the retarder on setting time, heat evolution, workability and compressive strength development of geopolymer mortars, different quantities of a sodium-based retarder were added to the mixes.

3.3 Results and discussion

3.3.1 Influence of set retarder on setting time of Geo 1 and Geo 2 pastes

As shown in Tables 3.3 and 3. 4, the amount of set retarder prolonged both initial and final times of setting. For Geo 1, more than 2% retarder is required to give reasonable change in initial and final setting times. Regarding Geo 2, however, a minimum of 4% is required.

Table 3.3 Setting time of Geo 1 pastes with different amounts of retarder

Water/Powder	Retarder (%)	Geo 1	
		Initial setting time (min)	Final setting time (min)
0.2	1	80	100
	2	88	120
	4	218	-
	6	> 300	-
0.3	1	95	155
	2	110	269
	4	239	388
	6	> 330	-

Table 3.4 Setting time of Geo 2 pastes with different amounts of retarder

Water/ Powder	Retarder (%)	Geo 2	
		Initial setting time (min)	Final setting time (min)
0.2	2	14	29
	4	53	117
	6	181	316
	8	274	-
0.3	2	37	78
	4	75	203
	6	218	425
	8	-	-

3.3.2 Influence of set retarder on geopolymerisation process, investigated by XRD and SEM/EDX

The changes of geopolymerisation process after being mixing to one month

Changing in geopolymerisation reaction up to one month, detected by using X-ray powder diffraction (XRD), were clearly shown in Figures 3.4 and 3.5 for Geo 1 paste with 2% retarder and Geo 2 paste with 4% retarder. XRD pattern of fly ash contain mineral phases like quartz (Q), magnetite (Mg), mullite (M), hematite (H), and other minor minerals. Amorphous content in the fly ash was recorded at halo from

20.0-35.0^0 2θ. Figure 3.5 also show that the crystalline products present in the GBFS are akermanite (Ak) and quartz (Q).

The reactions of source materials and alkaline activator results in amorphous phases, which are N-A-S-H or/and C-(N)-A-S-H gels, to partially crystalline phases like zeolite crystals (Palomo et al. 2014; Provis & Bernal 2014). In Figures 3.4 and 3.5, peaks (X) at 2θ = 13.5^0 and 27.5^0, assigned to NaX-type zeolite crystal (Muriithi, Petrik & Doucet 2020), happened after initial setting time. The hierarchical structure of NaX-type zeolite, which was plate-like structures arranged in ball-like clusters, observed by scanning electron microscopy (SEM) with energy dispersive X-ray spectrometry (EDS), was shown in Figures 3.7 and 3.8. Two above-mentioned peaks were not observed in the 10 minutes- XRD pattern, while their intensity increased and then became high peaks after 1 day. The intensities of peaks X increased gradually over time, indicating the formation and development of crystals of NaX-type zeolite, and thus, the developments of geopolymer reactions.

The peaks (S) at 17.00, 29.50, 35.00 and 38.00 2θ are assigned to a silicate mineral in sodium activator powder, as shown in Figure 3.6. In Figures 3.4 and 3.5, these peaks were observed at 10 minutes and mostly disappear after 1 day for Geo 1 paste and after final setting time for Geo 2 paste. This implied the process which silicate ions in solid activator were gradually dissolved and participated in the formation of amorphous geopolymer gels when the geopolymerisation proceeded. From now on, the observation of X and S peaks was used to trace the progress of geopolymer reactions.

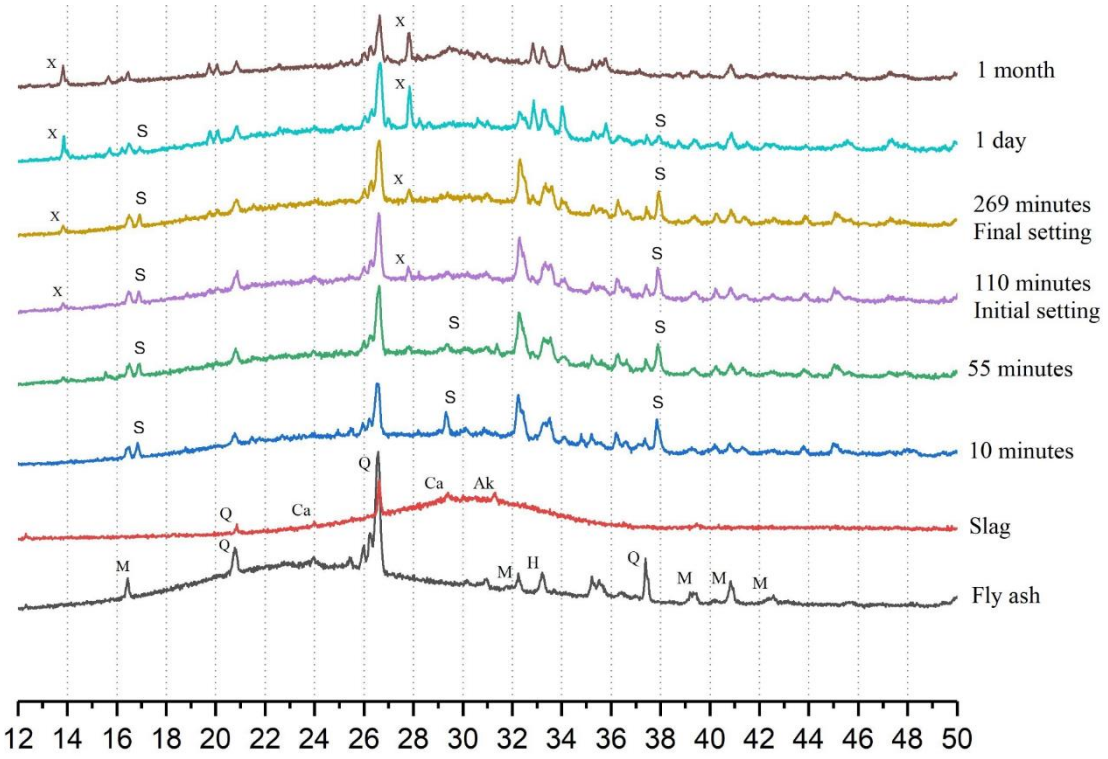

Figure 3.4 XRD results of Geo 1 with 2% retarder

Further, a diffuse halo peak from 28^0 to 32^0 2θ, a feature of amorphous alumina-silicate in geopolymers (Davidovits 1991), was not seen at 1 day of age, but observed clearly at 1 month in both Geo 1 and Geo 2 (see Figures 3.4 and 3.5). The emergence of such halo peak implied the significant development of geopolymerisation process and compressive strength as well.

The geopolymers, investigated in this study, use high slag contents, thus, the C-(N)-A-S-H gel was primary reaction product. The presence of C-(N)-A-S-H gel in the Geo 1 and Geo 2 systems at 1 month was shown in Figures 3.9 and 3.10, obtained by using SEM/EDS.

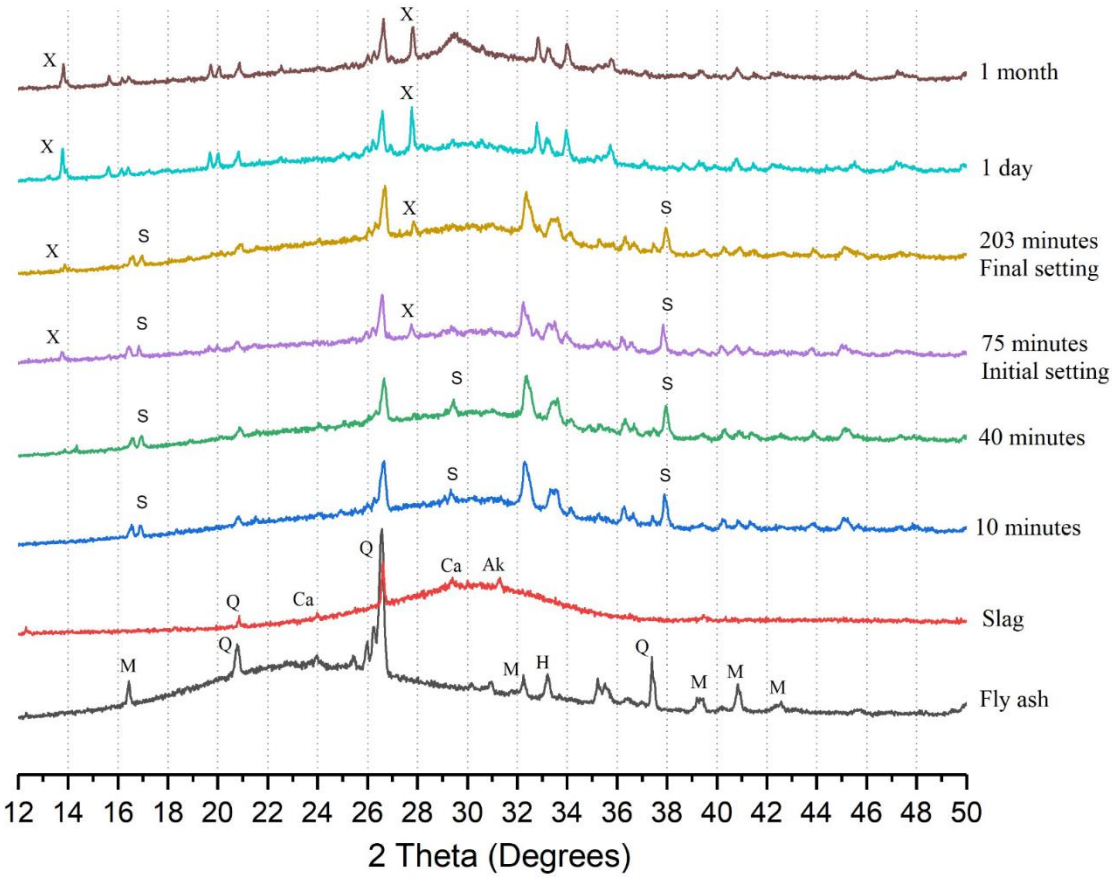

Figure 3.5 XRD results of Geo 2 with 4% retarder

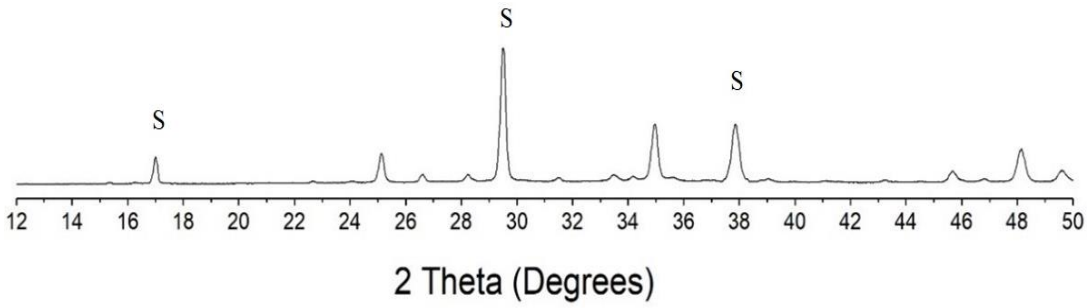

Figure 3.6 XRD results of silicate mineral in activator

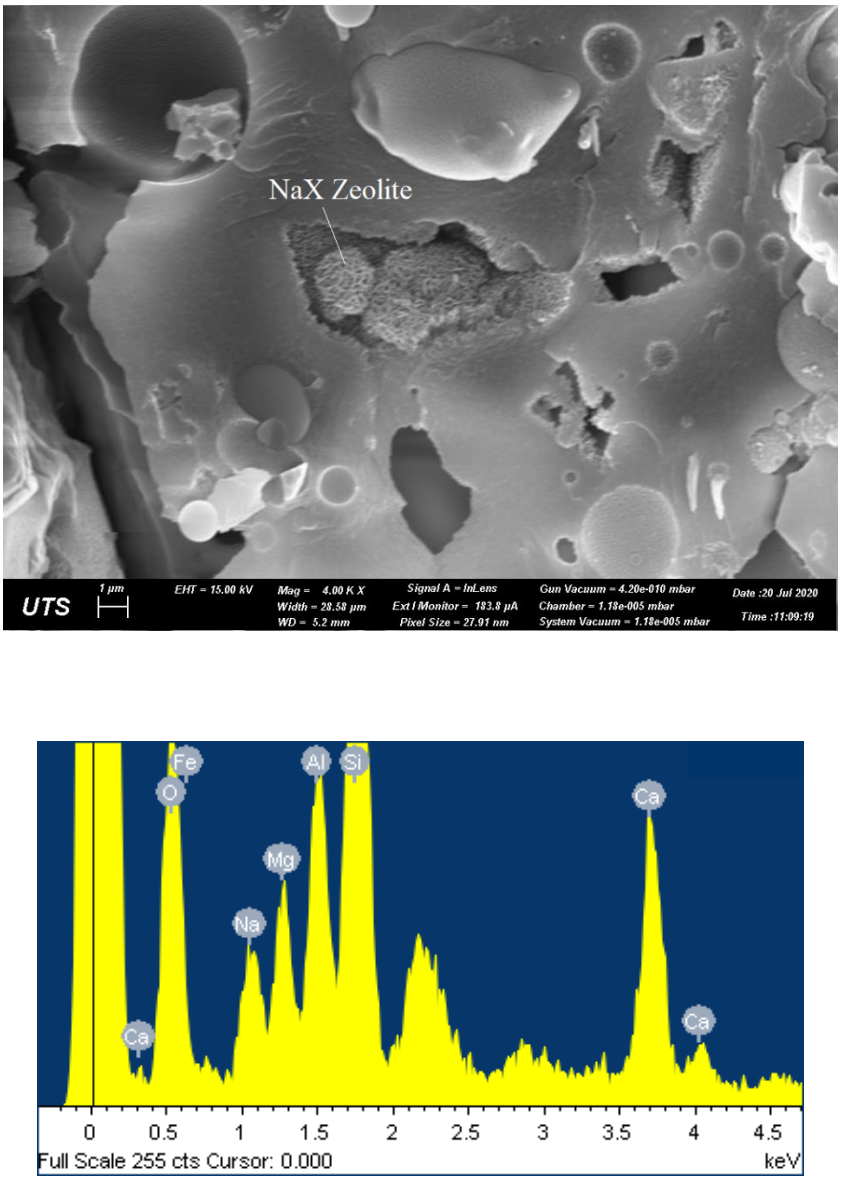

Figure 3.7 SEM/EDS results of NaX-type zeolite in Geo 1 paste

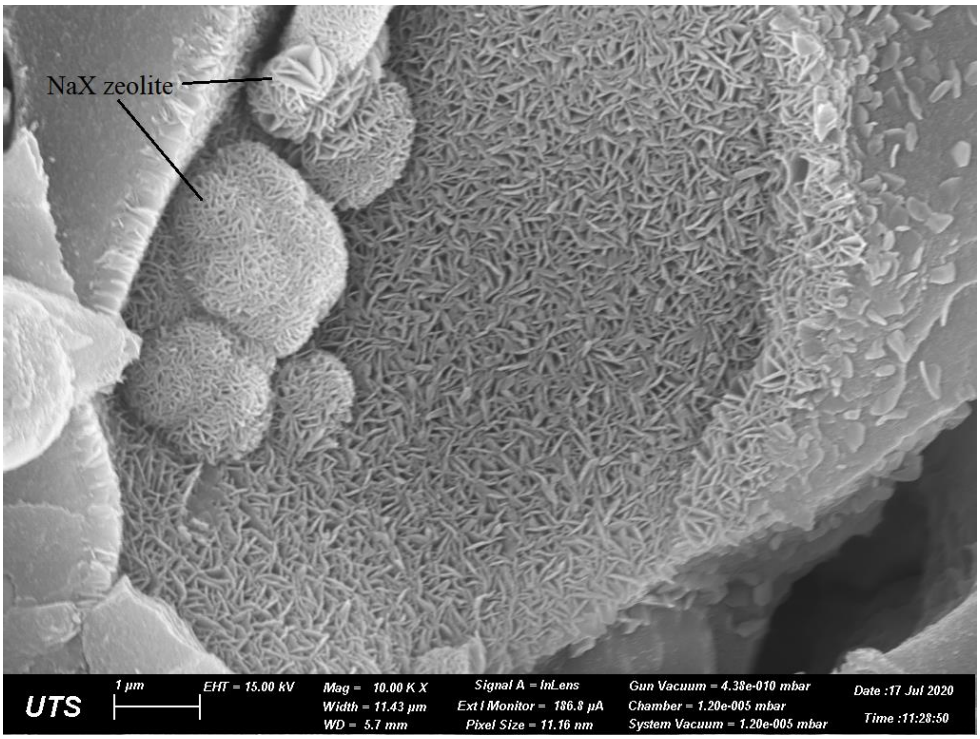

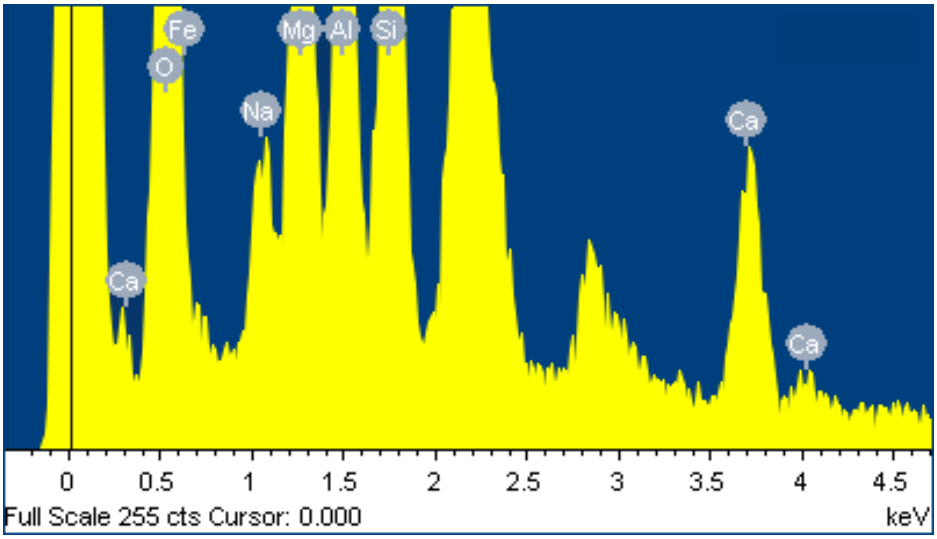

Figure 3.8 SEM/EDS results of NaX-type zeolite in Geo 2 paste

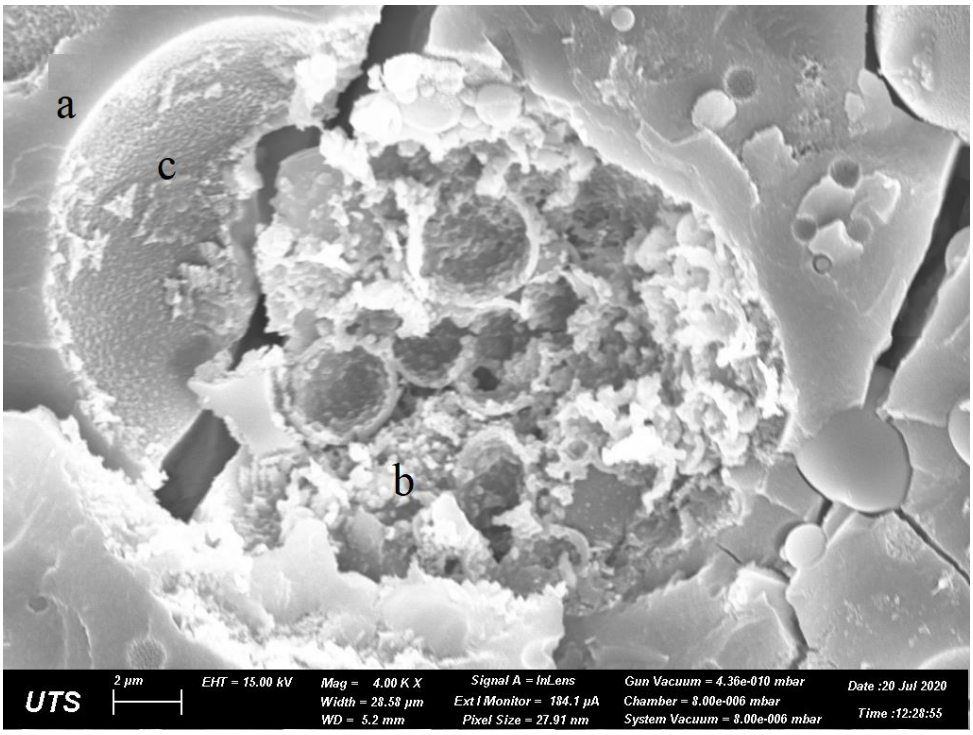

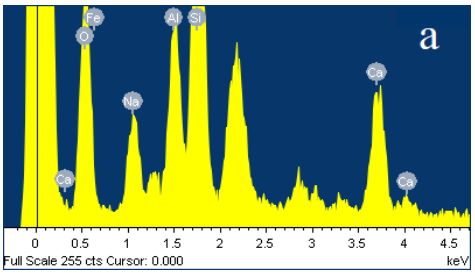

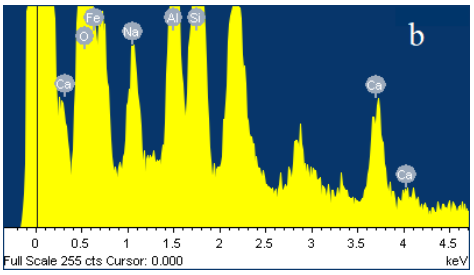

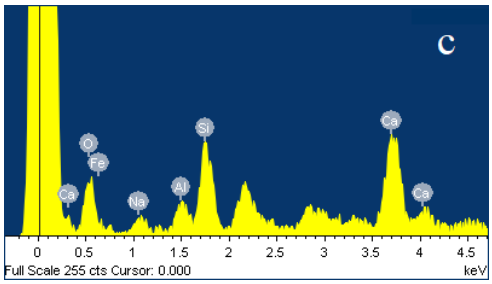

Figure 3.9 SEM/EDS results of N-(C)-A-S-H gels in Geo 1 paste

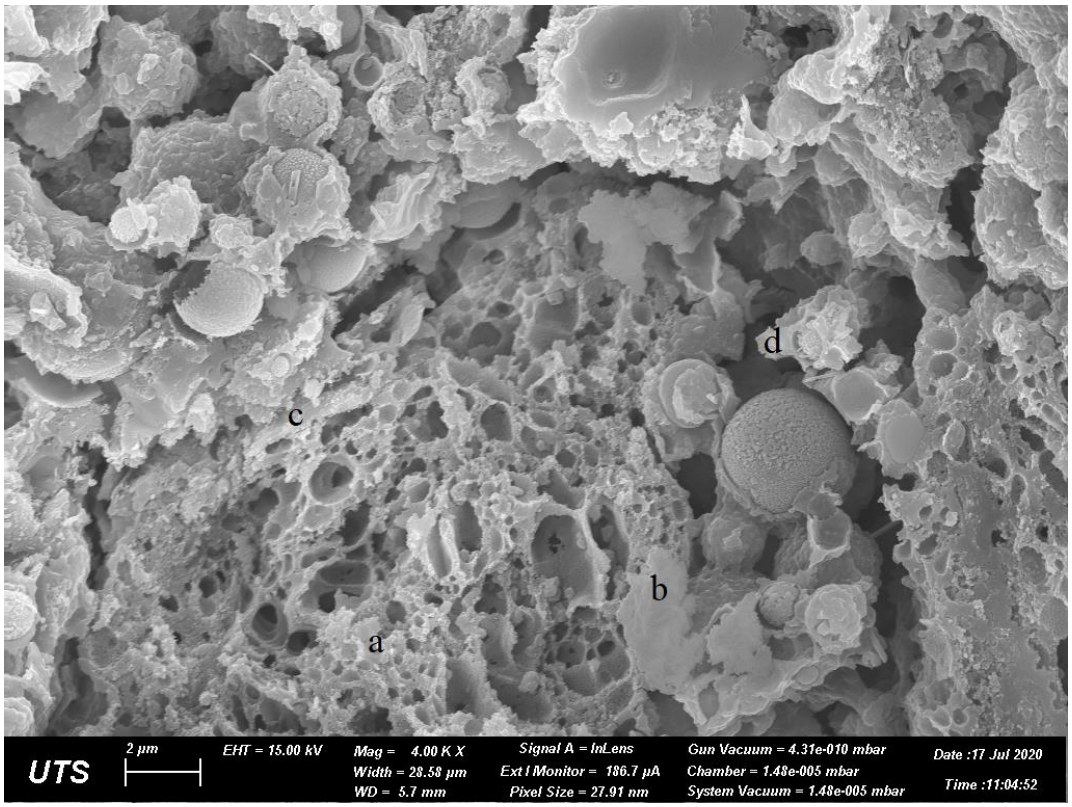

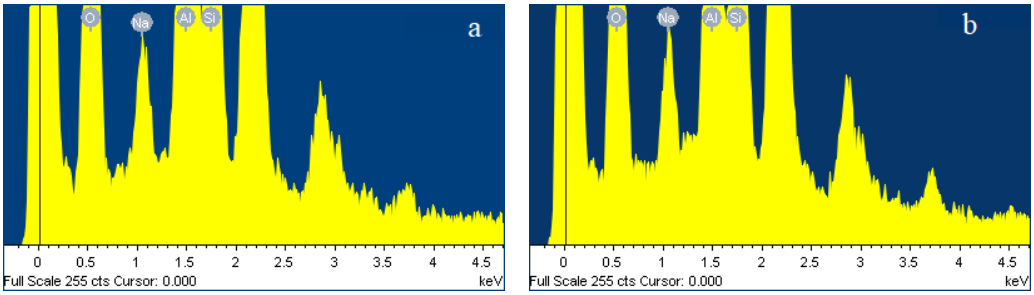

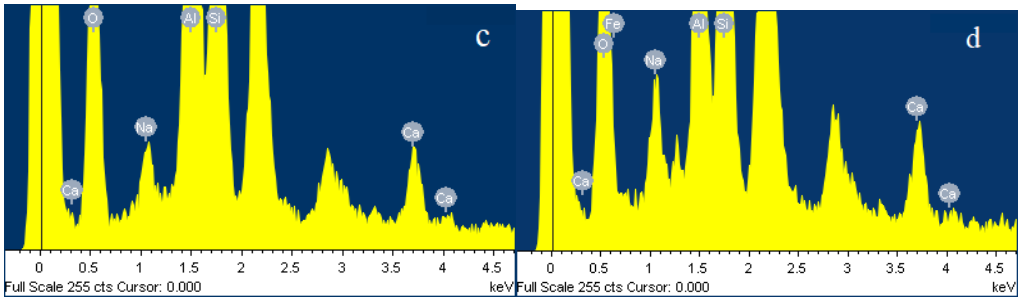

Figure 3.10 SEM/EDS results of N-(C)-A-S-H gels in Geo 2 paste

The changes of geopolymerisation process due to retarder

Changes of geopolymerisation process due to retarder, investigated by XRD, were carried out for Geo 2 with 0% and 8% retarder. The emergence of NaX-type zeolite, detected by peaks at 2θ = 13.5^0 and 27.5, was seen at 40 minutes in XRD pattern of 0% retarder Geo 2 (see Figure 3.11), while at 75 minutes in XRD results of 8% retarder Geo 2 (see Figure 3. 12). At 203 minutes, the intensity of these two peaks were very high for 0% retarder Geo 2 while still low for 8% retarder Geo 2.

In the meantime, peaks at 17.0^0, $29.5^{0,}$ 35.0^0 and 38.0^0 2θ, linked with silicate mineral, disappeared after 75 minutes for 0% retarder Geo 2 paste. In contrast, such peaked merely vanished after 203 minutes for 8% retarder Geo 2 paste.

The observation obtained by XRD results above evinced the effectiveness of such set retarder in extending the setting time for Geo 1 and 2 binder.

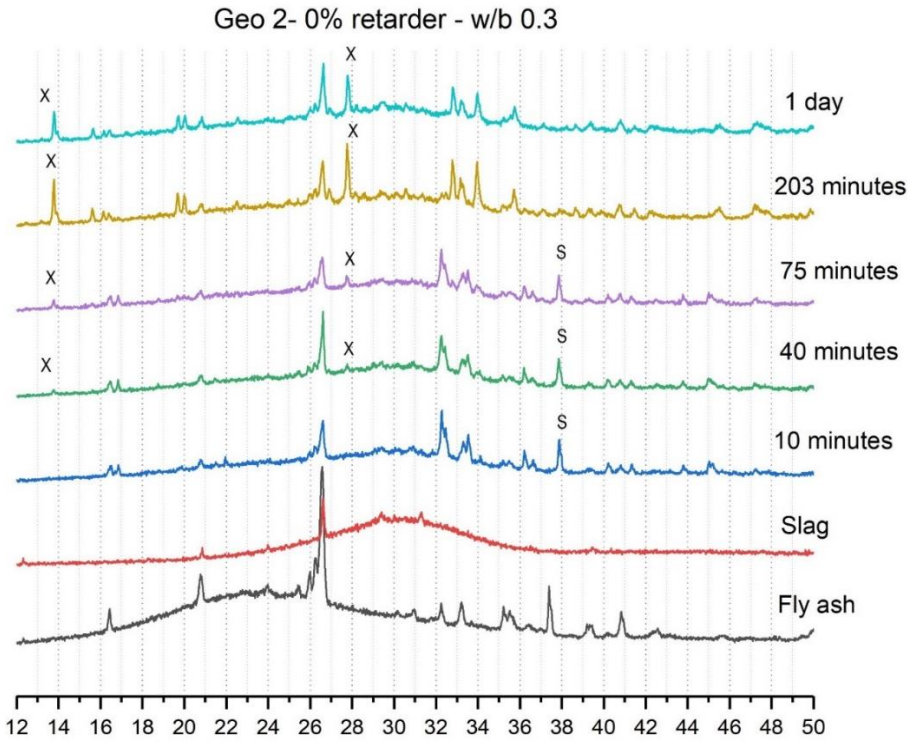

Figure 3.11 XRD results of Geo 2 with 0% retarder

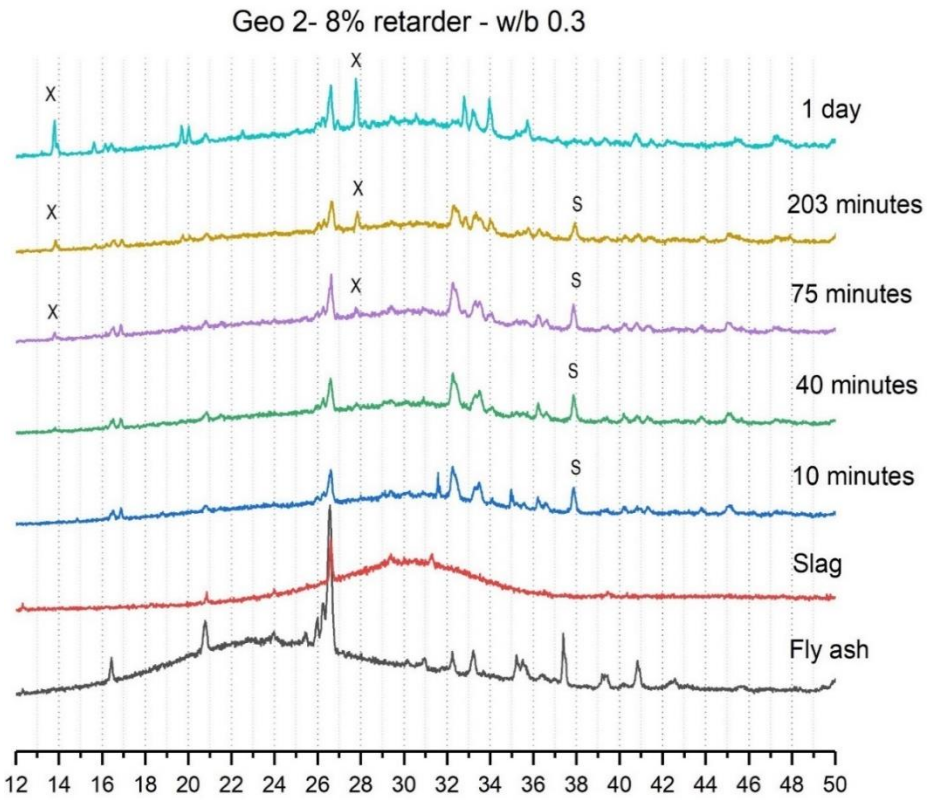

Figure 3.12 XRD results of Geo 2 with 8% retarder

3.3.3 Influence of set retarder on heat evolution of Geo 1 and Geo 2 pastes

The heat evolution of Geo 1 and Geo 2 with the percentage of set retarder in the range of 0 to 8% was depicted in Figure 3.13. The first peak of heat evolution appeared shortly after mixing powder with water due to the dissolution of solid activators and retarder. The second peak of heat appeared due to dissolution and geopolymerization reactions. Increasing the percentage of retarder led to the reduction in heat release and thus, a substantial increase in setting time was achieved. Additionally, the peaks of heat released by Geo 2 pastes happened sooner and their intensities were higher than those of Geo 1 with the same amount of retarder. These results explained well why Geo 2 pastes have shorter initial and final setting times than Geo 1 pastes.

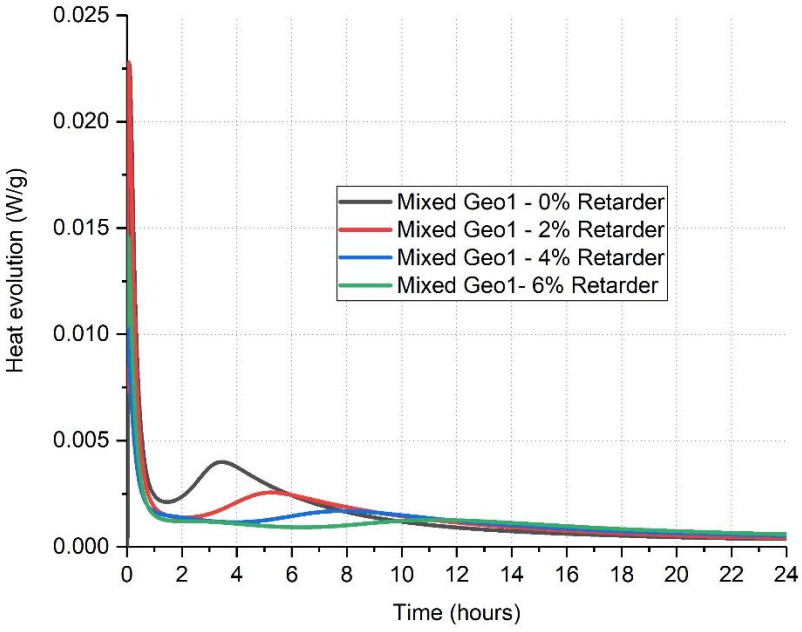

(a)

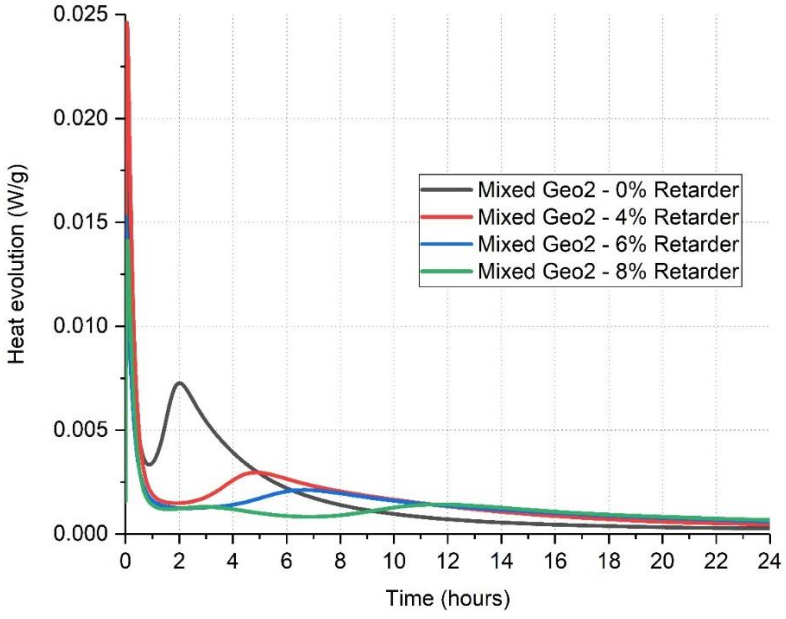

(b)

Figure 3.13 Heat evolution of (a) Geo 1 and (b) Geo 2 paste with increasing percentages of set retarder

3.3.4 Influence of set retarder on workability of Geo 1 and Geo 2 mortars

The flow of Geo 1 and Geo 2 mortars varied with the percentages of set retarder and water to powder ratios. As shown in Fig. 14, Geo 1 and Geo 2 mortars with a W/P ratio of 0.3 exhibited virtually no flow and the mixes were very dry. Mixes with W/P ratio of 0.4 gave flow values of workable range mortar mixes. Mixes with W/P ratio of 0.4 also showed a considerable increase in flow with increasing retarder content. Considering the practicality of casting, retarder percentages of 2-4% and 4-6% are sufficient for Geo 1 and Geo2 mixes, respectively with W/P ratio of 0.4. This will be verified with concrete mixes later.

Further, at the same water to powder (W/P) ratios, Geo 1 mortars had higher flow values than those of Geo 2 mortars, with sand/powder ratio 2.5. This is because Geo 1 binder contained 60% fly ash, higher than that in while Geo 2 binder with 40% fly ash.

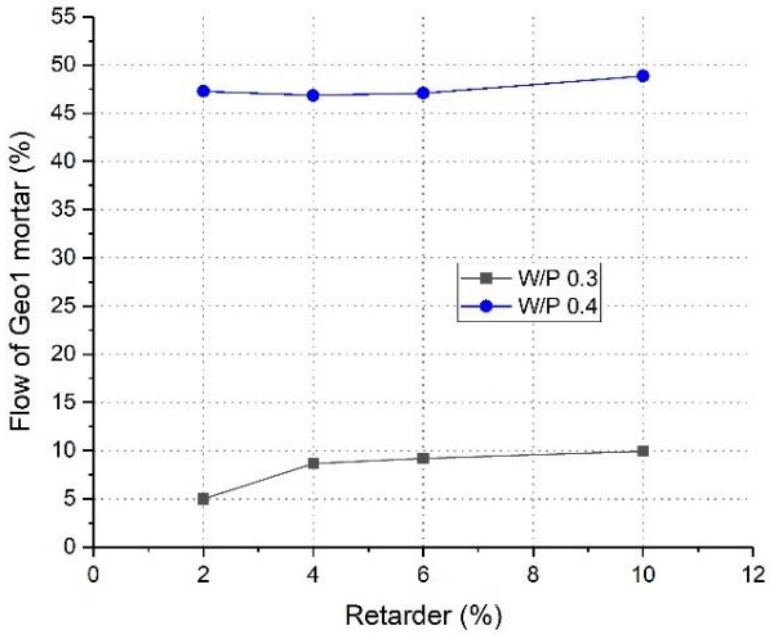

(a)

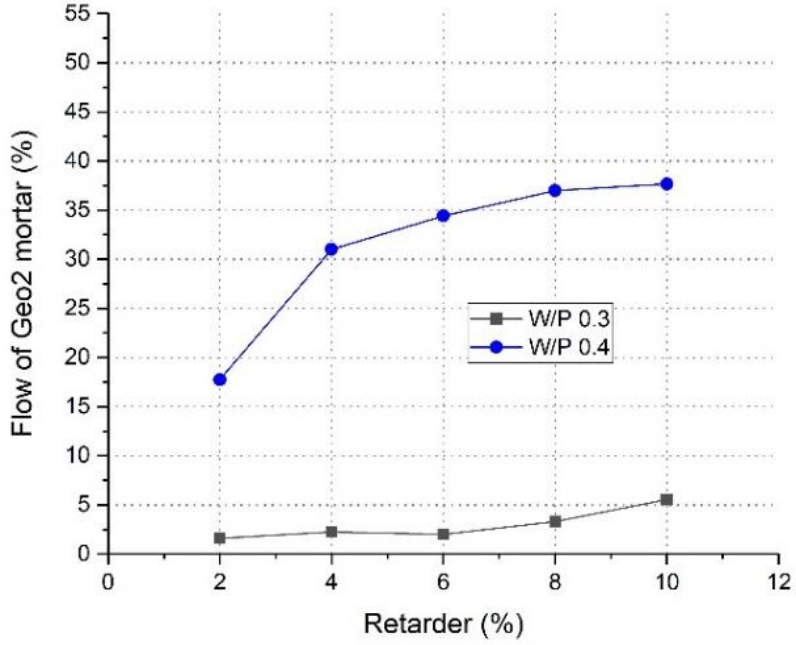

(b)

Figure 3.14 Flow of (a) Geo 1 and (b) Geo 2 mortars with increasing amounts of set retarder

3.3.5 Influence of set retarder content and curing conditions on compressive strength development of one-part mix geopolymer mortars

Three different curing conditions were applied to investigate the influence of set retarder on compressive strength of one part mix geopolymer mortars. The first was sealed curing in which specimens were wrapped in plastic film. The second was sealed and heat cured curing, in which specimens were wrapped in plastic films and put in oven at 60^{o}C for 6 hours, then exposed to the air. The third, heat curing, where specimens were heated at 60^{o}C for 24 hours. The development of compressive strength of Geo 1 mortars and Geo 2 mortars were depicted in Figures 3.15 and 3.16. As can be seen in these Figure 3.15, heat curing, was by far less effective curing condition, while sealed curing was the most appropriate to geopolymer mortars investigated. For example, with sealed curing a 2% retarder Geo 1 mortar had compressive strength of

64.2 MPa (Figure 3.15a), while with heat curing it only had 33.2 MPa (Figure 3.15b). Regarding producing precast concrete, the sealed and heat curing was the most appropriate regime because it gave high early age compressive strength. At 3 days, 2% retarder Geo 1 mortar under sealed and heat curing gave a compressive strength of 41.3 MPa, while under sealed curing it only had a compressive strength of 22.2 MPa.

Increasing the amount of retarder generally reduced the compressive strength of Geo 1 and 2 mortars at any age day and under any curing conditions. The optimum amount of retarder for strength development of Geo 1 is 2- 4% by weight of the powder, while that of for Geo 2 is 2- 6% by weight of the powder. The resulting compressive strength was in the range from 45 to 70 MPa at 28 days. At 3 days of age, a significant difference between the compressive strengths of mortars with retarder percentage from 2 to 6% was seen, which was about more than 50%. However, this gap was narrowed at 28 days, implying that the retarder considerably slowed down the geopolymerisation reactions, and hence compressive strength of Geo 1 and 2 mortars at early days. Additionally, the amount of such retarder should not be more than 6%, otherwise compressive strength would be severely decreased.

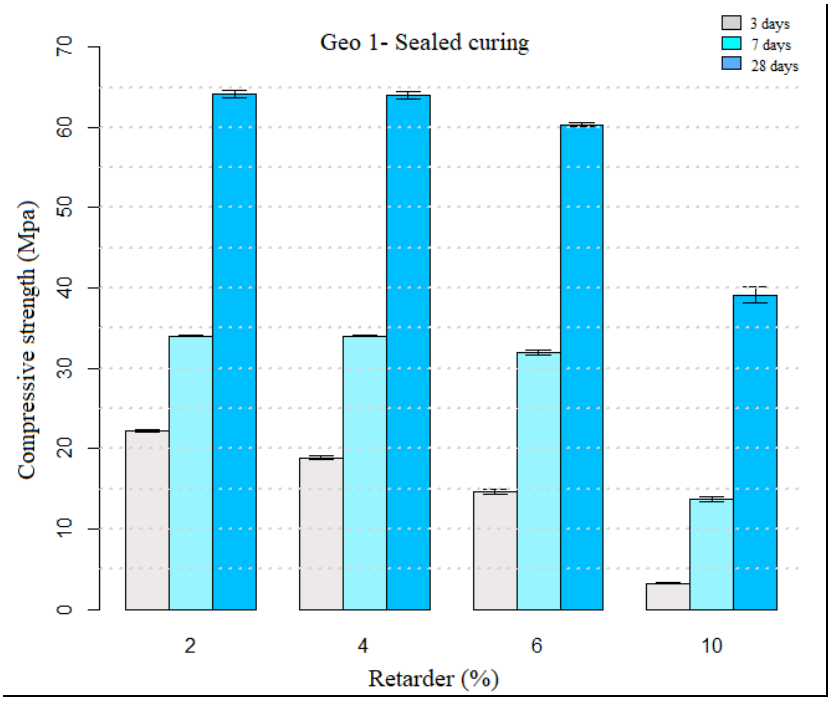
Geo 1- Sealed curing
3 days
7 days
28 days
Compressive strength (Mpa)
0
10
20
30
40
50
60
70
2
4
6
10
Retarder (%)

(a)

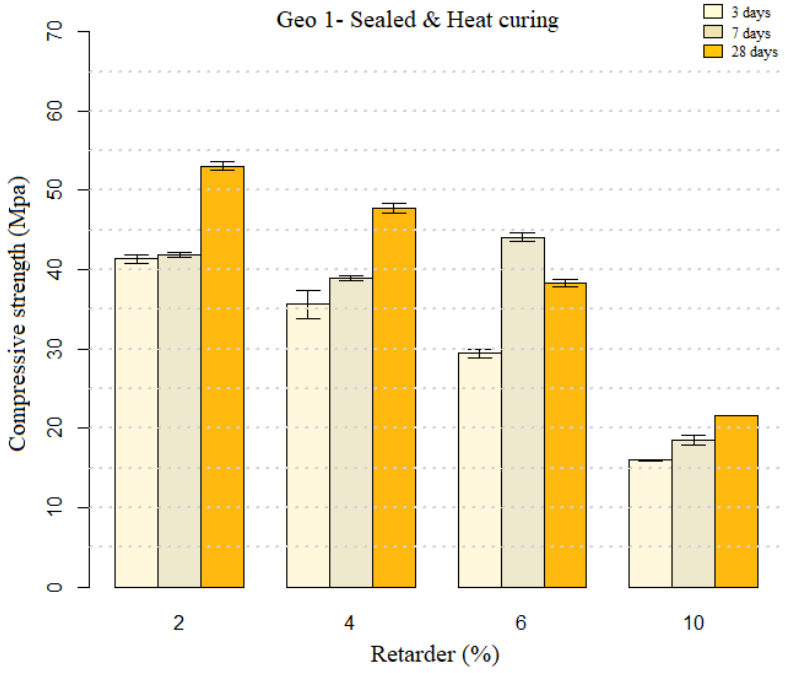
Geo 1- Sealed & Heat curing
3 days
7 days
28 days
Compressive strength (Mpa)
0
10
20
30
40
50
60
70
2
4
6
10
Retarder (%)

(b)

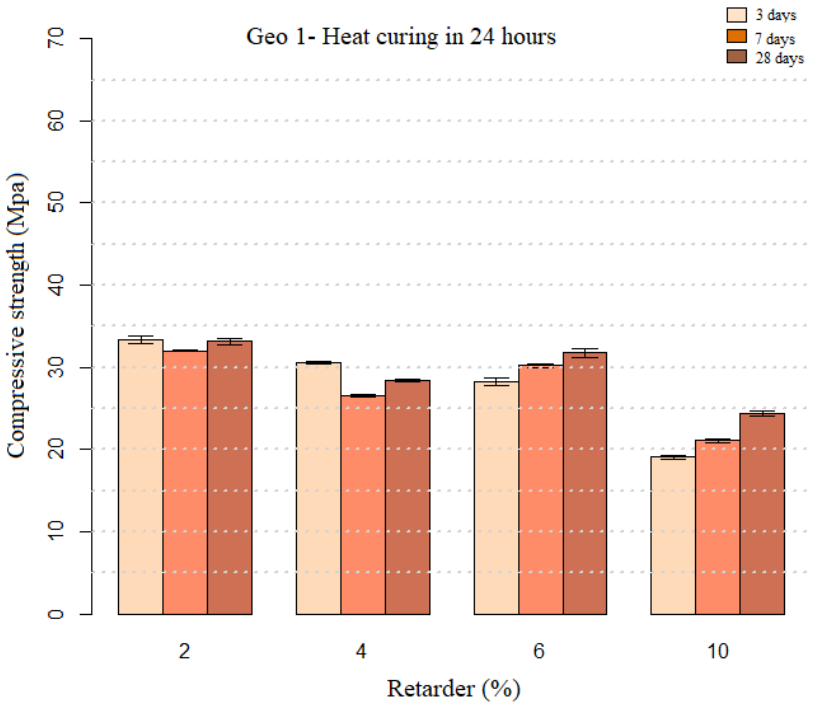

(c)

Figure 3.15 Compressive strength development of Geo 1 mortar under (a) sealed curing and (b) sealed & heat curing

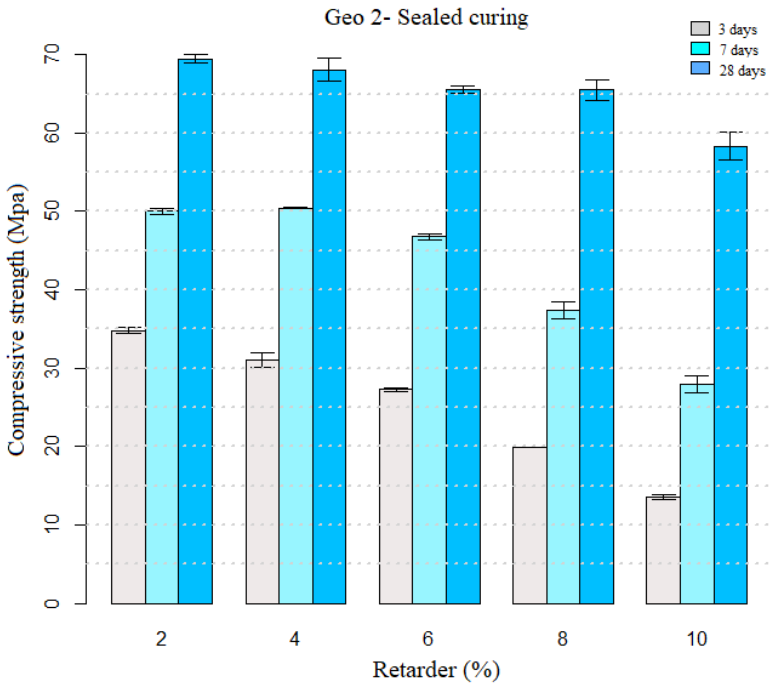

(a)

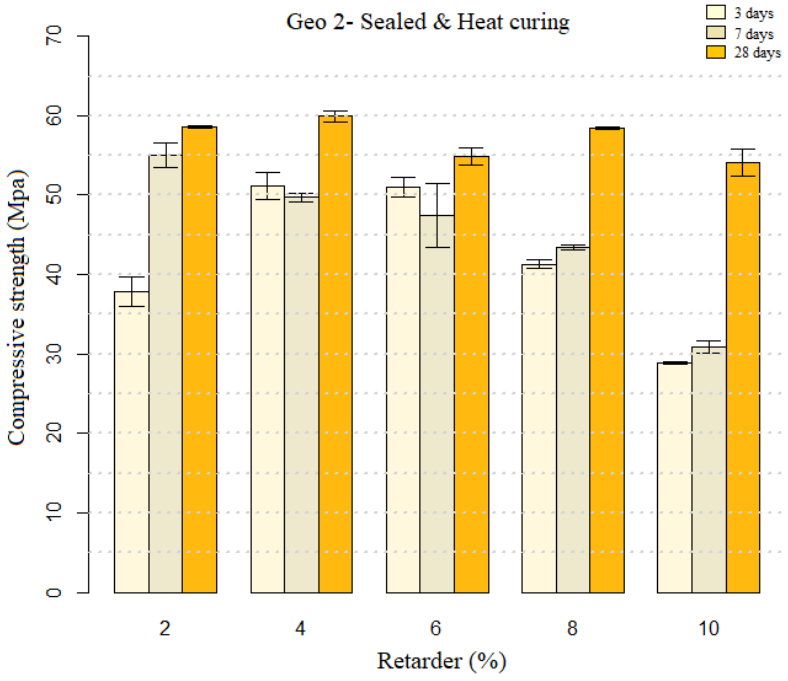

(b)

Figure 3.16 Compressive strength development of Geo 2 mortar under (a) sealed curing and (b) sealed & heat curing

3.4 Conclusions

For one-part mix geopolymer produced from fly ash and slag, the set retarder investigated can be used successfully to control the setting time to desired levels. Not only did this retarder prolong the setting time of dry powder geopolymers, but also it reduced the heat released as a result of the dissolution and geopolymerisation reactions. Using this retarder can reduce the compressive strength of geopolymer mortars if the retarder content is over 8%. However, using less than 8% retarder, the reduction in compressive strength is inconsiderable. An appropriate amount of retarder is 2-6 % in terms of setting time, workability and compressive strength. Among three curing conditions investigated, seal curing, where specimens were wrapped in plastic films and placed in the ambient temperature, gave the highest compressive strength regardless of the retarder content. The sealed and heat curing, in which specimens were wrapped in plastic films, put in the oven at 60^{o}C for 6 hours, then exposed to the air, can be applied for precast concrete production with an adjustment.

CHAPTER 4: Carbonation in Fly Ash/Slag Geopolymer Mortar and Concrete

4.1 Introduction

Carbonation has long been recognised as a durability issue attributed to corrosion of steel reinforcement in geopolymer materials. The currently available information, however, is not sufficient to gain a deep understanding of this issue. Several studies showed that the pH of carbonation regions in fly ash geopolymer (Badar et al. 2014; Davidovits 2005; Law et al. 2015; Pu et al. 2012) and slag geopolymer materials (Nedeljković et al. 2018) were higher than 10 and sufficient to provide the protection for steel. Additionally, the performance of protecting steel reinforcement of fly ash/slag blended geopolymer concrete was similar to OPC and 30% fly ash blended OPC concretes (Khan, Castel & Noushini 2016; Pasupathy et al. 2016; Rozière, Loukili & Cussigh 2009). However, all these studies were carried out on two-part geopolymer materials or performed on fly ash/slag geopolymer materials with high percentage of fly ash. This chapter is focused on investigating carbonation in one-part fly ash/slag geopolymer concretes using high percentage of slag (40% and 60% slag). Firstly, carbonation front depth and pH profile in carbonated geopolymer mortars under accelerated and natural carbonation conditions were assessed. The influence of carbonation on porosity and pore size characteristics of one-part fly ash/slag geopolymer mortar were also investigated by using neutron tomography and mercury intrusion porosimetry (MIP). Elemental mapping by scanning electron microscopy (SEM) with energy dispersive X-ray spectrometry (EDS) was also performed in this study, in order to supplement the findings of neutron tomography

and MIP. The change of compressive strength and carbonation depth of one-part fly ash/slag geopolymer concrete were also included in this investigation.

4.2 Experimental program

4.2.1 Material and mix proportions

The experimental investigation on carbonation were carried out on one-part geopolymer mortars and concretes. Mortar and concrete specimens were produced from two binders Geo 1 and Geo 2 that were described in chapter 3, section 3.2.1. Sand, used to prepare specimens, was Sydney sand (dune sand) with specific gravity of 2.6 kg/l and fineness modulus of 2.5. All coarse aggregates are crushed aggregates having a maximum size of 20mm and bulk density of 1.4 kg/l. For mortar specimens, sand: powder ratio used was kept as 2.5 for all specimens. For concrete specimens, the mix proportion is shown in Table 4.1. All four types of concrete have the same amount of binder, sand and aggregate, but different water to binder ratios. The curing conditions of Geo 1 and Geo 2 concretes were heat and sealed curing where concrete specimens were wrapped in plastic films and heat at 60^{o}C for 6 hours. For OPC and OPC+25% fly ash, specimens after being demoulded were put in the lime water until the testing day. The compressive strength of all concrete was about 50 MPa at 28 days.

Table 4.1 Mix proportion of concretes

Binder type	Binder mass (kg/m^3)	Sand (kg/m^3)	10 mm aggregate (kg/m^3)	20 mm aggregate (kg/m^3)	W/B	Compressive strength at 28 days (MPa)
Geo1	411	833	523	788	0.33	52.9
Geo 2	411	833	523	788	0.35	52.1
OPC	411	833	523	788	0.5	52.5
OPC+25% Fly ash	411	833	523	788	0.47	46.5

4.2.2 Preparation of specimens

The procedure of preparing mortar specimens were described carefully in chapter 3, section 3.2.2. For concrete specimen production, binder, sand and aggregate were mixed in 2 minutes in a drum mixer, then water was added and continually mixed in 2 minutes. After stopped for 2 minutes, the mixing process continued for 4 minutes. When mixing process finished, 100 mm cube concrete specimens were cast and removed from the moulds after 1 day. The sealed and heat curing (where specimens are wrapped in plastic film and kept in an oven at 60^oC for 6 hours, then placed in laboratory air) were applied for curing mortar and concrete specimens.

4.2.3 Carbonation testing for mortar and concrete

When reaching 28 days, 50 mm cube mortar and 100 mm cube concrete specimens were exposed to natural and accelerated carbonation conditions. For the accelerated carbonation test, specimens were placed in a carbonation chamber where CO_2 concentration was maintained at 1%. The accelerated carbonation test using 1%

of CO_2 was found to be suited to assess carbonation in geopolymer materials in an reasonably short time (Gluth et al. 2020) because it stimulated well to the natural carbonation condition. The relative humidity (RH) of the carbonation chamber was controlled at 60% and the temperature was 23^{o}C. Regarding natural carbonation, specimens were subjected to normal atmosphere within the indoor lab where the temperature was about 23±2^{o}C and RH was 50± 5%.

4.2.4 Measurement of compressive strength of mortar and concrete

The compressive strength test of the 50 mm cube mortar and 100 mm cube concrete specimens were performed at 28 days in accordance with ASTM C109/C109M and AS 1012.9: 2014.

4.2.5 Measurement of carbonation depth of carbonated mortar and concrete

For carbonation depth, specimens were split-opened and sprayed either a phenolphthalein solution (1%) or an alizarin yellow R solution (0.5%) on the fracture surfaces. Alizarin yellow R changes colour from yellow to red when pH is above 11 (at higher pH levels, the colour is red), whereas phenolphthalein changes from colourless to pink when pH is above 9 (at higher pH levels, the colour is pink). The depths of carbonation front were measured by a digital caliper with a resolution of 0.01 mm.

4.2.6 Measurement of pH profile of mortar specimens

To measure pH, a method already proposed by Rasanen & Penttala (Räsänen & Penttala 2004) was applied in this study, with a slight modification. The mortar powders, which were sampled every 1mm against 25 mm depth of Geo 1 and Geo 2 specimens, were mixed with distilled water. The ratio of powder: water was 1:10 and

the stirring time was 3 minutes. The pH value of each suspension was measured using a calibrated pH probe.

4.2.7 Porosity analysis and visualisation in noncarbonated and carbonated mortar

The exploration of porosity and pore size distribution were carried out using neutron tomography acquired by the instrument DINGO at ANSTO and MIP. DINGO is a neutron radiography and tomography instrument which is fed by a thermal neutron beam at the Open Pool Australian Lightwater (OPAL) reactor. The specification of such instrument was carefully elaborated in a study of Garbe et al. (2015) (Garbe et al. 2015). In this study, the specimens were wrapped in aluminium foil and placed in an aluminium holder. Each specimen (25mm x 25mm) was scanned with 1895 projections and 0.19degree steps. The overall beam time per sample was 12 hours with a resulting pixel size of 30μm. The calculation of a porosity analysis was then performed with VGStudio Max (Volume Graphics 2014). Specimens used for the experiment were 25mm cube mortars, which were placed in accelerated carbonation conditions for 3 months, then some of them were split and measured carbonation depths. Following that the neutron tomography experiment was performed on the remaining cubes.

To study the influence of carbonation on pore characteristics of geopolymer mortars, the porosity analyses were separately carried out on noncarbonated and carbonated portions in the same specimen. Additionally, the analyses were also performed on the different portions within one specimen, which contained both noncarbonated and carbonated parts.

MIP experiment was performed by a Quantachrome PoreMaster PM33-17 porosimeter, using the procedure described in a study of Shikhov and Arns (Shikhov & Arns 2015). Data were acquired by assuming a surface tension value of 480 dynes/cm^2

and a contact angle of 140^{o}. The samples used in MIP were fragments, with dimension of 8mm x 8mm x 15mm, collected from the same specimens used in tomography measurements mentioned above.

4.3. Results and discussion

4.3.1 Carbonation depth of one-part fly ash/slag geopolymer mortars over time

Carbonation depths of Geo 1 and Geo 2 mortars over time, determined by using two indicators phenolphthalein solution (1%) and alizarin yellow R solution (0.5%), were shown in Table 4.2. The carbonation front depths indicated by alizarin yellow R were slightly greater and more clearly defined than those shown by phenolphthalein. However, the difference in carbonation depths indicated by phenolphthalein and alizarin yellow R was insignificant. Additionally, under the accelerated and natural carbonation conditions, the carbonation depths of mortars produced from Geo 1 binder (60% fly ash and 40% slag) were always greater than those of mortars from Geo 2 binder (bearing 40% fly ash and 60% slag), as shown in Figure 4.1. After 18 months in the atmosphere, two types of geopolymer mortars were fully carbonated, depicted in Figure 4.2.

Table 4.2 Carbonation depth – under accelerated & natural carbonation conditions

Type	Geo1 mortar – 53 MPa		Geo 2 mortar – 60 MPa	
	Carbonation depth (mm) - **Accelerated** carbonation			
Exposure time (months)	Phenolphthalein	Alizarin Yellow R	Phenolphthalein	Alizarin Yellow R
1	1.5	1.8	1.2	1.6
2	5.1	6.8	3.7	3.9
3	7.9	8.5	5.2	6.3
8	-	-	7.5	7.8
	Carbonation depth (mm) - **Natural** carbonation			
Exposure time (months)	Phenolphthalein	Alizarin Yellow R	Phenolphthalein	Alizarin Yellow R
8	15.3	15.5	10.6	11.2
18	Fully carbonated	Fully carbonated	Fully carbonated	Fully carbonated

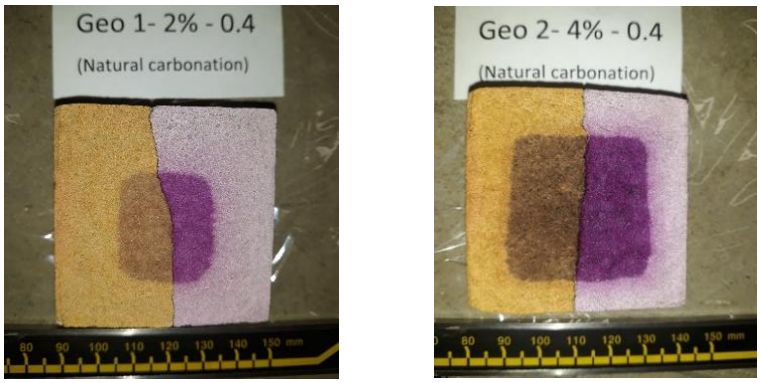

(a) (b)

Figure 4.1 Carbonation depth of (a) Geo 1 and (b) Geo 2 mortars after 8 months in atmosphere

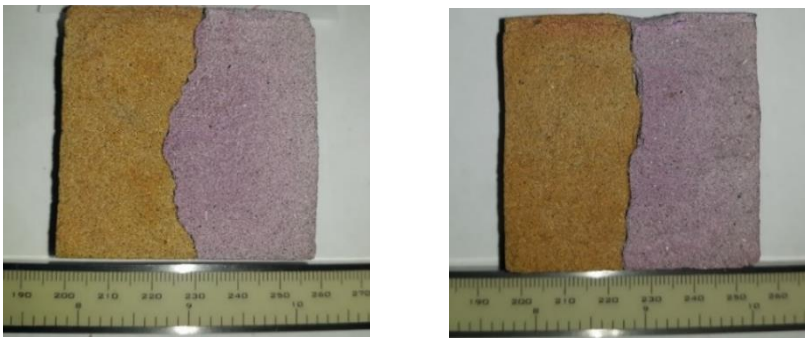

(a) (b)

Figure 4.2 Carbonation depth of (a) Geo 1 and (b) Geo 2 mortars after 18 months in atmosphere

4.3.2 Change in pH due to carbonation of one-part geopolymer mortars

The variation in pH against the depth of surfaces of Geo 2 mortars, which were exposed to accelerated and natural carbonation up to 8 months are presented in Figure 4.3 and Figure 4.4, respectively. Under both of the accelerated and natural carbonation conditions in 8 months, the pH dropped from around 11.8 to roughly 11.0 for both Geo 1 and Geo 2 mortars, despite the fact that carbonation front depths were always greater than 7 mm under accelerated carbonation tests or than 15 mm under natural CO_2 exposure. The findings suggested that using phenolphthalein as an indicator for carbonation front depths in carbonated geopolymer mortars appeared not appropriate. Phenolphthalein solution generally changes from pink to colourless (indicated by white areas on a sample surface) when the pH of the carbonated surface drops to around 9 (Villain, Thiery & Platret 2007), while alizarin yellow R changes colour from red to yellow in colour when pH of the carbonated surface reduces to below 11 (Martín-Del-Río et al. 2013). Based on the results of pH profiles presented in Figure 4.3 and Figure 4.4, the carbonation front depths estimated by alizarin yellow R seem correlated well with the measurements of pH profiles.

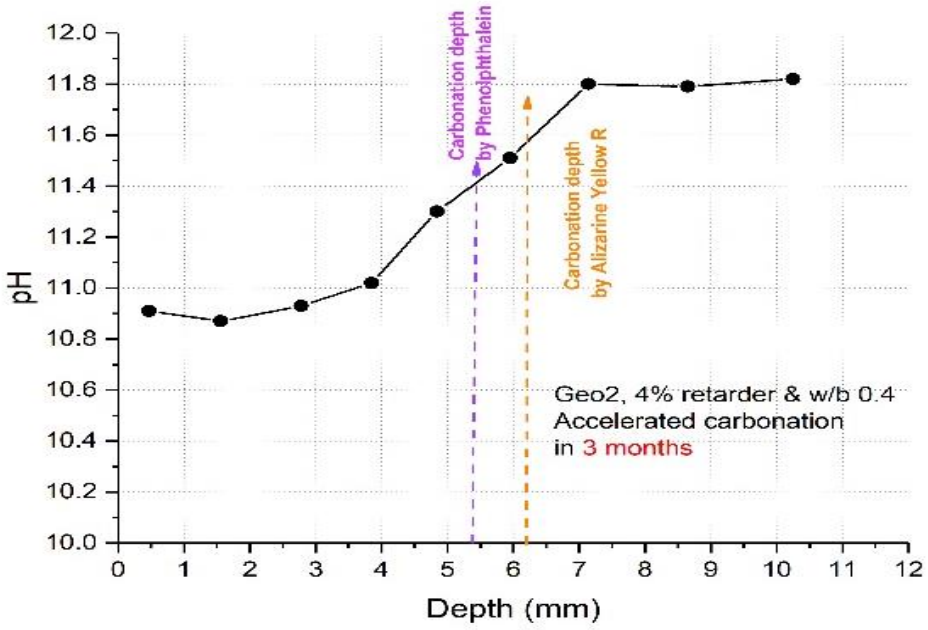

(a)

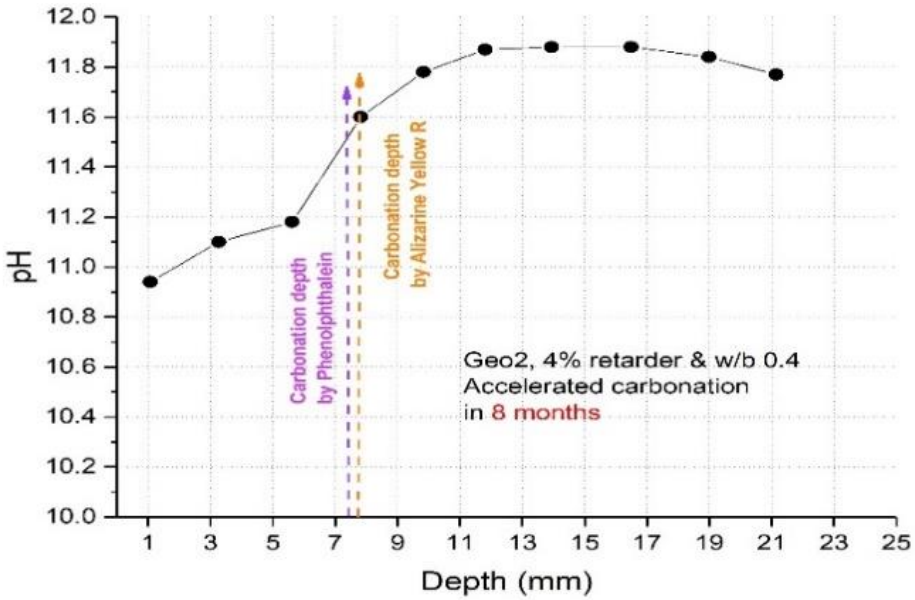

(b)

Figure 4.3 pH change of Geo 2 mortar after 3 months (a) and 8 months (b) under accelerated carbonation

Nonetheless, the colour of carbonated surfaces after being sprayed with phenolphthalein was not completely in a white colour, yet in a light pink colour, as portrayed in Figure 4.1. Phenolphthalein, thus, provided the appropriate values of

carbonation depths in geopolymer mortars. However, the difference between a light pink and white colours is probably difficult to be able to be detected by naked eyes, especially if the reading light is not of sufficiently good.

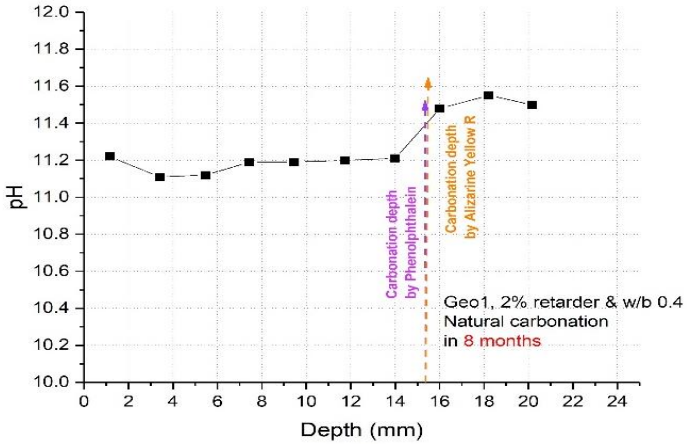

(a) Geo 1

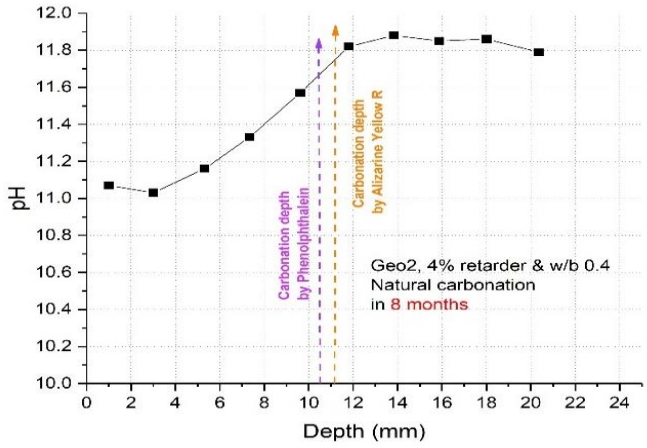

(b) Geo 2

Figure 4.4 Change in pH of Geo1 (a) and Geo 2 (b) mortars after 8 months under natural carbonation

More to this point, the pH at the surface of the carbonated mortar specimens remained close to 11. This is probably due to main carbonation products are Na_2CO_3 or $NaCO_3 \cdot 10H_2O$ (natron) (Susan A. Bernal et al. 2013). The pH values of Na_2CO_3

solutions of 0.1 N concentration was found to be 11.6. This is a major reason why accelerated carbonation tests are carried out at 1% CO_2 and not at higher concentrations. At higher CO_2 concentration, the product formed are mainly $NaHCO_3$ (nahcolite) which the pH at concentration of 0.1 N is 8.4. Hence if steel corrosion tests are performed at high CO_2 concentration, it will enormously mislead, indicating higher rate of steel corrosion due to the low pH of about 8.4. Hence, it is essential to carry out any corrosion of steel reinforcement studies in geopolymer concrete at CO_2 concentration levels of less than 1%.

The result in Figure 4.4 also suggested that the risk of steel reinforcement corrosion due to carbonation in reinforced geopolymer materials would be low. Over 6 months under accelerated carbonation, there was no sign of steel corrosion in Geo 1 and Geo 2 concretes (see Figures 4.5a and 4.6a). Steel reinforcements were still in the purple area when phenolphthalein was used as indicator (Figures 4.5b and 4.67b) and in the brown area when alizarin yellow R was utilized as indicator (Figures 4.5c and 4.6c).

The findings was also seen in a study of Babaee et al. (2018) (Babaee, Khan & Castel 2018), in which no sign of steel corrosion in the reinforced geopolymer concrete specimens was observed after 500 days being exposed to 1% of CO_2.

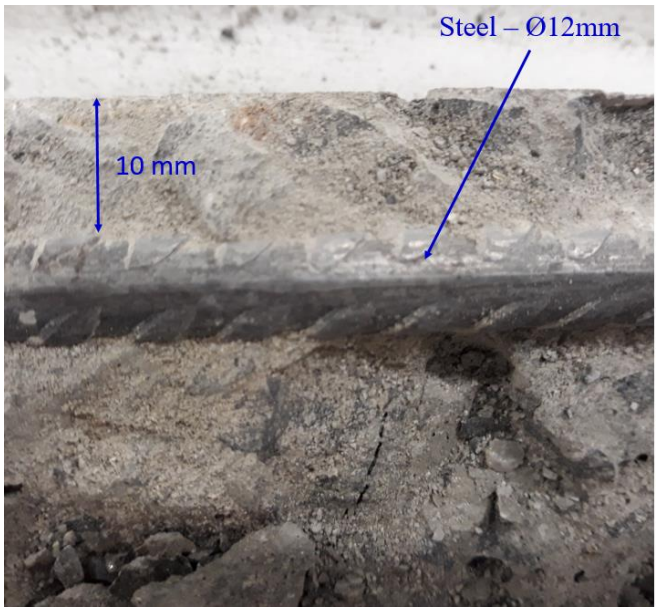

(a)

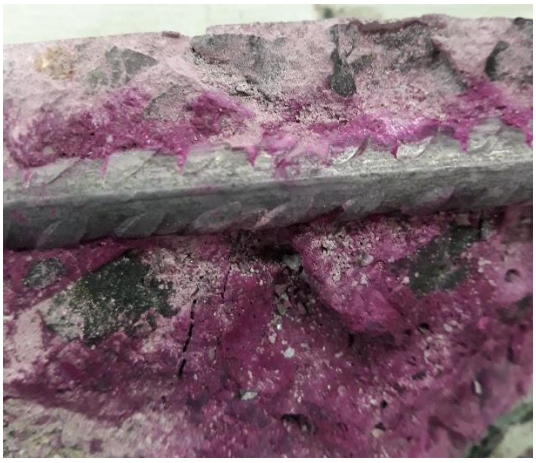

(b) (c)

Figure 4.5. Steel reinforcement in Geo 1 concrete after 6 months under accelerated carbonation

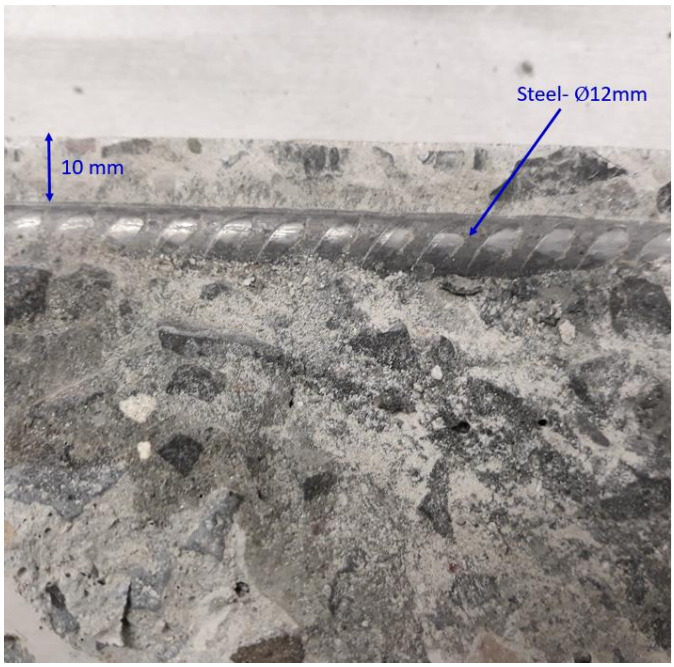

(a)

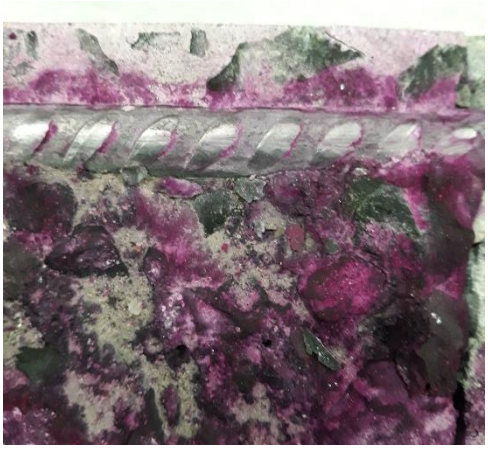

(b) (c)

Figure 4.6 Steel reinforcement in Geo 2 concrete after 6 months under accelerated carbonation

4.3.3 Carbonation front depth of one-part fly ash/ slag geopolymer concrete

Carbonation depth of Geo 1 and Geo 2 concretes over 6 months, were depicted in Figures 4.7 and 4.8, respectively. Under both natural and accelerated carbonation conditions, the carbonation front depths, indicated by Phenolphthalein and Alizarine Yellow R were from 8 to 10 mm. For OPC and OPC+25% fly ash, the depths of carbonation, shown in Table 4.3, were from 2 to 3 mm, lower than those in Geo 1 and Geo 2 concretes. However, it did not mean that carbonation resistance of Geo 1 and Geo 2 concretes was worse than that of OPC and OPC+25% fly ash concretes. As presented in section 4.3.2, the pH values at the surface depths of Geo 1 and Geo 2 mortars were around 11, hence, carbonation only is probably not a main cause of steel corrosion.

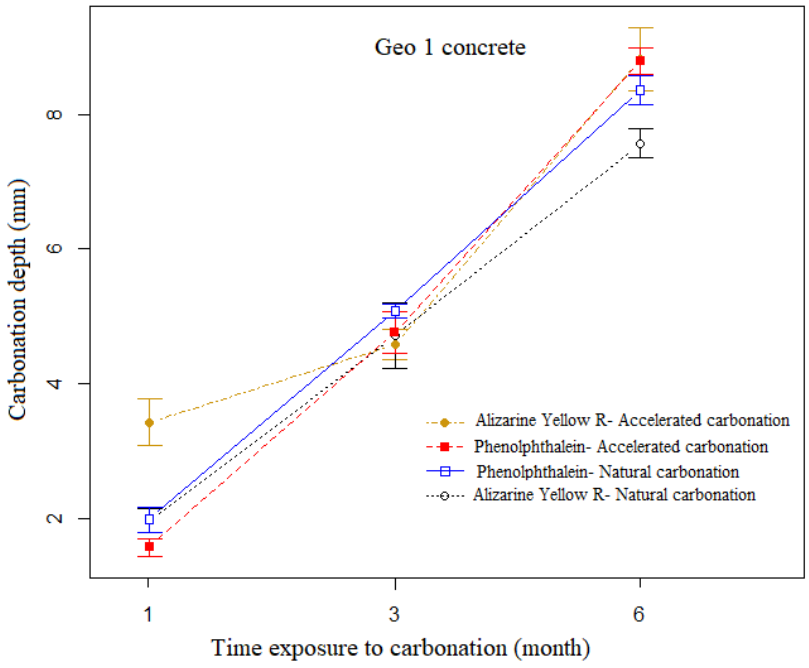

Figure 4.7 Carbonation depth of Geo 1 concrete, indicated by Phenolphthalein and Alizarine Yellow R

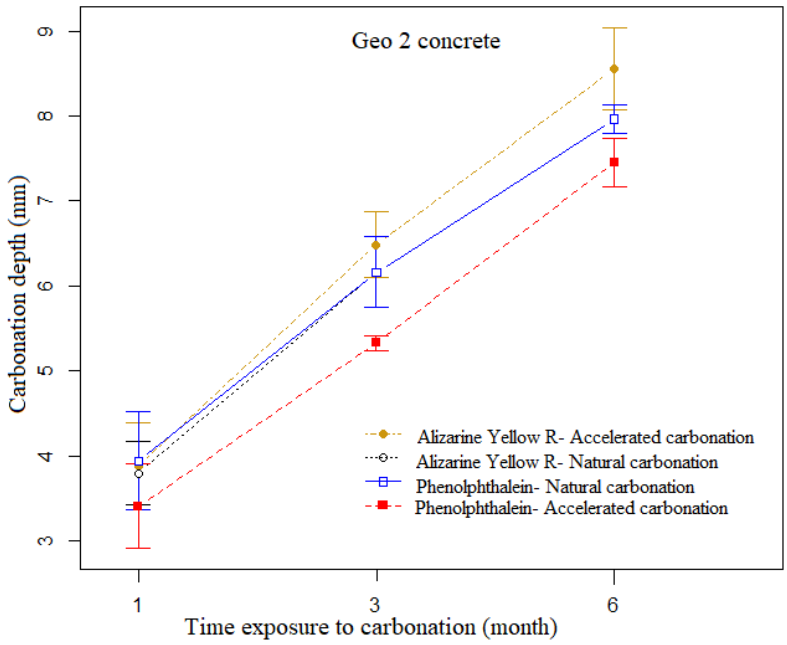

Figure 4.8 Carbonation depth of Geo 2 concrete, indicated by Phenolphthalein and Alizarine Yellow R

Table 4.3 Carbonation depth in concrete after 6 month- exposure to carbonation

Carbonation depth (mm) - Mean (SD)		
Natural carbonation		
Concrete type	Phenolphthalein	Alizarine Yellow R
Geo 1	8.3 (0.7)	7.6 (0.8)
Geo 2	7.8 (0.6)	7.5 (0.9)
OPC	2.6 (1.2)	2.2 (0.7)
OPC+25% Fly ash	2.9 (0.7)	3.2 (0.6)
Accelerated carbonation		
Geo 1	8.8 (0.8)	8.8 (1.8)
Geo 2	7.5 (0.9)	8.6 (1.5)
OPC	1.6 (0.5)	2.1 (1.0)
OPC+25% Fly ash	3.2 (0.6)	2.9 (0.6)

4.3.4 Influence of carbonation on compressive strength of one-part fly ash/ slag geopolymer concrete

The compressive strength of four different types of concretes under natural and accelerated carbonation conditions were shown in Figures 4.9 and 4.10. The compressive strength of Geo 1 concrete before being exposed to carbonation conditions (at 28 days) was 65.5MPa (see Figure 4.9). After 6 months under natural carbonation, compressive strength of carbonated Geo 1 concretes was 66.1 MPa. For Geo 2 concrete, the values of compressive strength before and after 6 months exposure to natural carbonation conditions were around 65.0 MPa. Regarding OPC concrete and OPC+25% fly ash concrete, their compressive strengths increased about 15% after being exposed to carbonation conditions because of the development of hydration reactions, then reduced slightly due to the effect of carbonation. For Geo 1 and Geo 2 concretes, the development due to geopolymerisation reactions was not significant probably because they were heated in curing process, thus the compressive strength rapidly developed in the early days, but then slowly. Meanwhile, the curing condition of OPC and OPC+25% fly ash concrete specimens was lime water curing, thus a significant development in compressive strength after 1 month was seen. After 6 months exposure to natural carbonation, the change in the compressive strength of all specimens was insignificant.

A similar trend was seen in the change of compressive strength of four types of concrete under accelerated carbonation conditions, depicted in Figure 4.10. After 6 months exposure to accelerated carbonation, the compressive strength of Geo 1, Geo 2, OPC and OPC+25% fly ash concretes were 65.3, 65.0, 58.2 and 55.3 MPa, not much different from their compressive strength before exposed to CO_2, although there were increases in compressive strength in between.

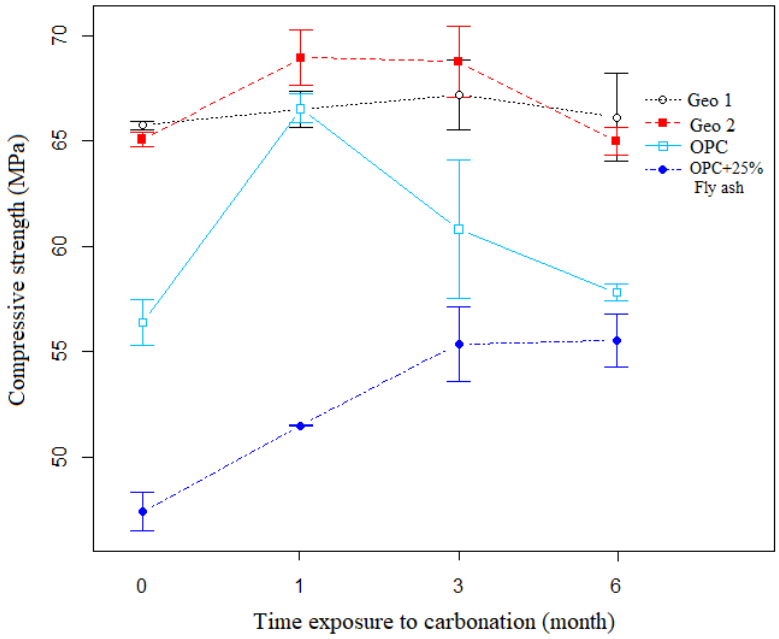

Figure 4.9 Change in compressive strength of concretes over 6 months exposure to natural carbonation conditions

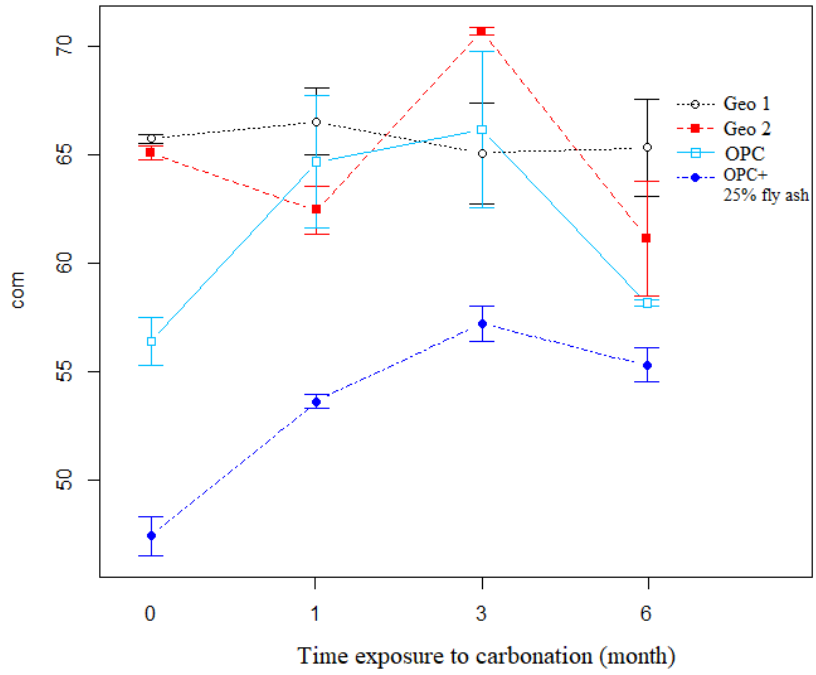

Figure 4.10 Change in compressive strength of concretes over 6 months exposure to accelerated carbonation conditions

4.3.5 Influence of carbonation on porosity and pore size distribution in one-part fly ash/ slag geopolymer mortars

a. Porosity analysis of the whole specimen using neutron tomography

Carbonation depths Geo 1 and Geo 2 mortar specimens, in the shape of 25 mm cubes, after 3 month exposure under accelearated carbonation indicated by both indicators mentioned above were about 9 mm and 6 mm, respectively (see Figure 4.11)

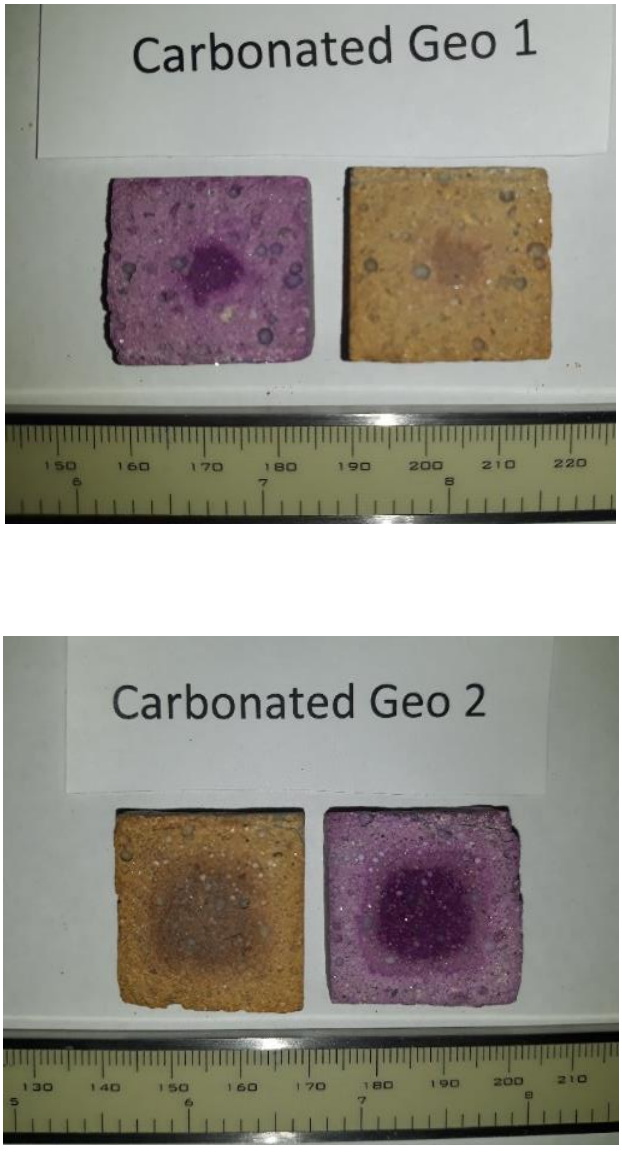

Figure 4.11 Specimens of carbonated Geo 1 and carbonated Geo 2 mortars used for neutron tomography experiments

The tomographic reconstruction provided 3D images of carbonated Geo 1 (Figure 4.12a) and carbonated Geo 2 (Figure 4.13a) cubes. Volumetric reconstruction (Figure 4.12b and Figure 4.13b) also highlighted the distribution of pores inside the 25 mm cubes. The pore size characteristics, calculated by VGStudio Max, are shown in Figure 4.14, in which the total porosity of carbonated Geo 1 mortars (3.27%) was lower than that of Geo 2 mortars (5.51%). As can be seen in Figure 4.14 the higher porosity of Geo 2 belonged to all the pore size ranges.

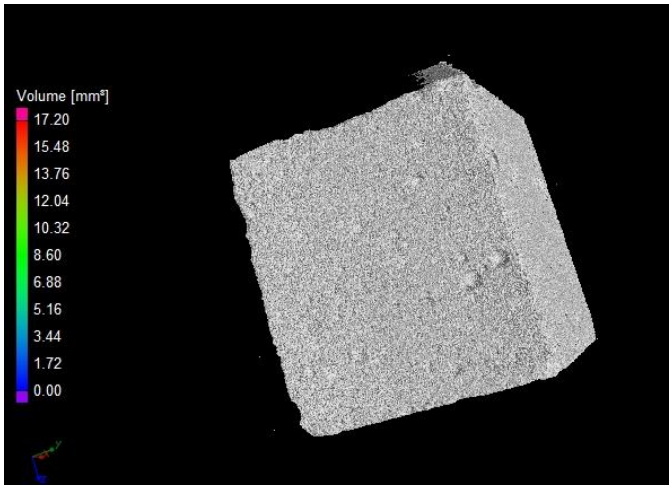

(a)

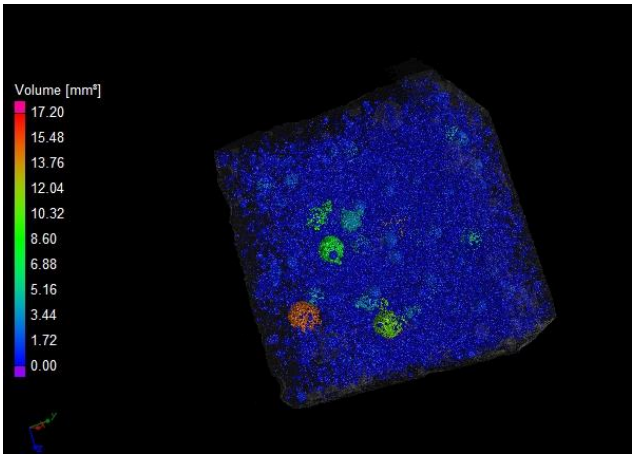

(b)

Figure 4.12 Tomographic reconstruction of carbonated Geo 1 mortar in the shape of a 25 mm cube

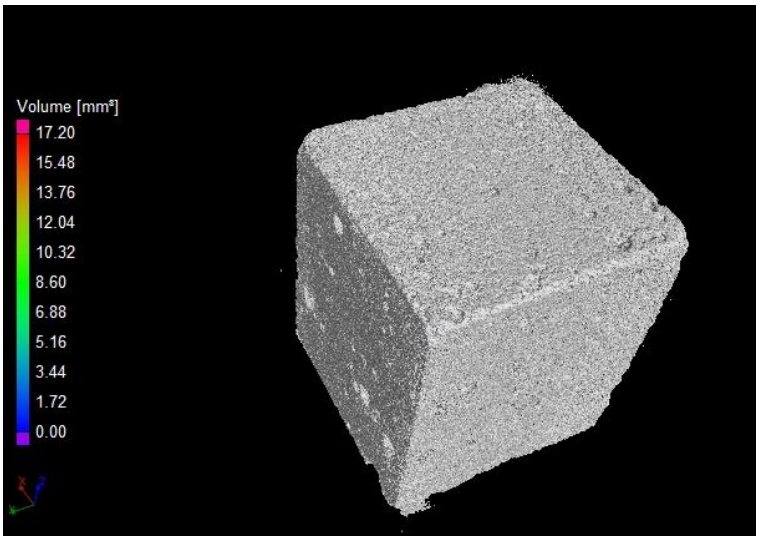

(a)

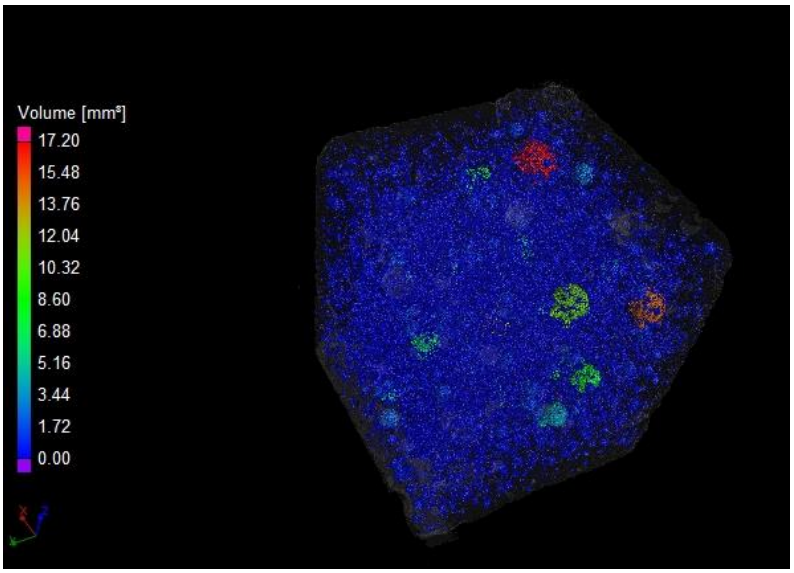

(b)

Figure 4.13 Tomographic reconstruction of carbonated Geo 2 mortar in the shape of a 25 mm cube

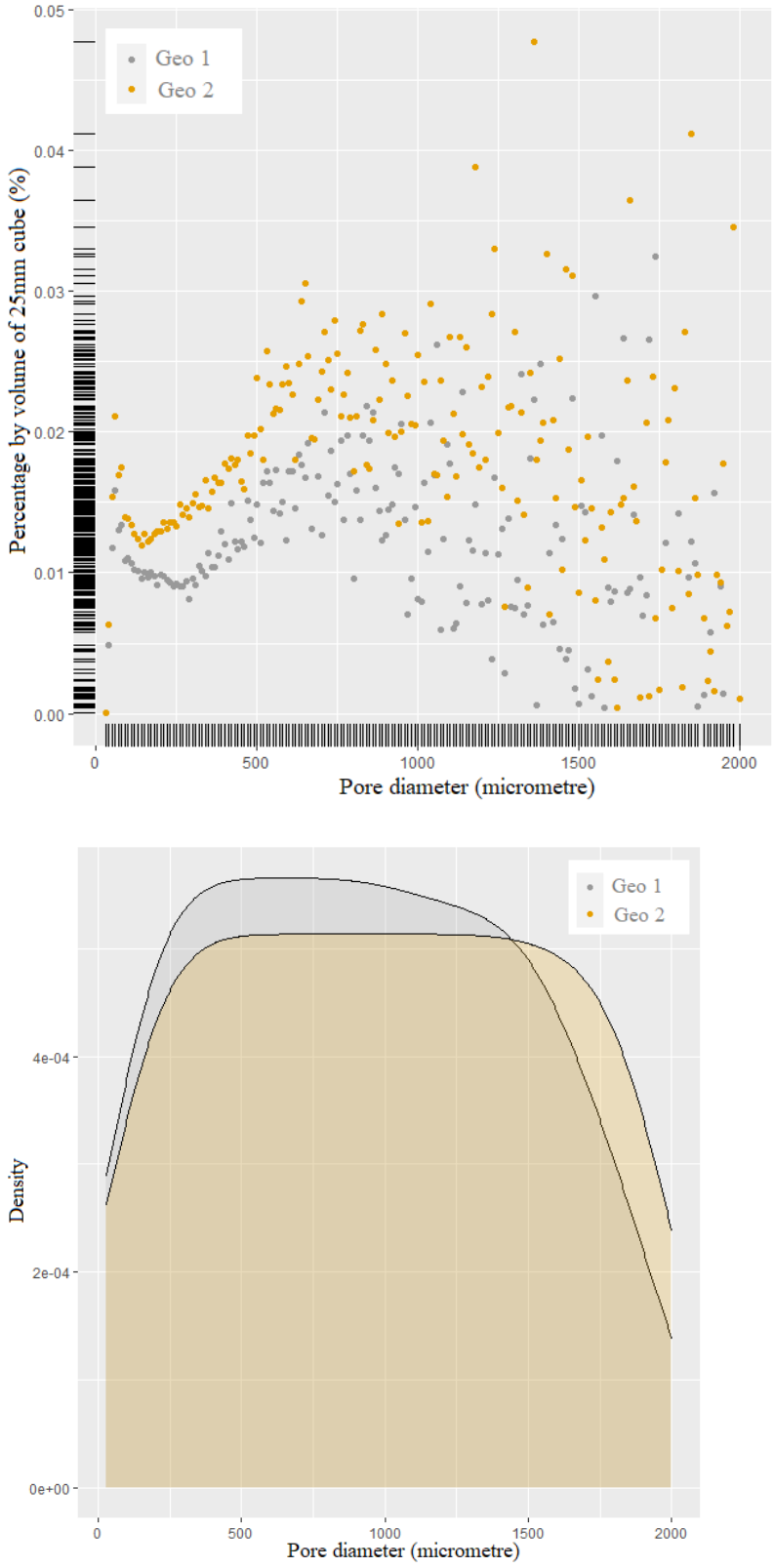

Figure 4.14 Pore size distribution of carbonated Geo 1 and Geo 2 mortars (accelerated carbonation)

b. Pore analysis of different portions inside the specimen using neutron tomography

Because the carbonation depth of Geo 1 and Geo 2 mortar was about 9 mm and 6 mm, the central 5 mm x 5 mm x 5 mm and 7 mm x 7 mm x 7 mm in volumes were deemed as noncarbonated parts and the central 15 mm x 15 mm x 15 mm in volume contained both noncarbonated and carbonated parts. The porosity analysis for different central portions of the 25 mm cube (see Figure 4.15a), therefore, started with a volume of 5x5x5 mm^3 (Figure 4.16a). The next analyses were carried out on the other central portions with increasing volumes of 7x7x7 mm^3 (Figure 4.16b), then 10x10x10 mm^3 (Figure 4.16c), followed by 15x15x15 mm^3 (Figure 4.16d), and finally the whole cube 25x25x25 mm^3.

The porosity results of those portions were presented in Figure 4.15b and Figure 4.15c. As can be seen in Figure 4.15b and Figure 4.15c, the inner 5mm x 5 mm x 5mm portion had the highest porosity (11.57% and 11% for Geo 1 and Geo 2, respectively) while the whole cube has the lowest porosity (3.27% and 5.51%). The greater volume was analysed, the lower porosity it was to be found. These findings implied that the porosity of one-part fly ash/slag geopolymer mortars dwindled owing to carbonation. It was probably because products, formed by the reactions of CO_2 and alkaline hydroxides in geopolymeric matrices(Bernal et al. 2012; Davidovits 2005), filled the empty spaces on pores. The elemental mapping (Figure 4.17), obtained by scanning electron microscopy (SEM) combined with energy dispersive X-ray spectrometry (EDS), depicted the presence of these carbonation products in the microstructure of carbonated geopolymer mortars. Elemental maps were in different colours, with Ca in yellow, Na in red and C in green. In Figure 4.17, C-containing regions were coincident with Ca-rich regions and Na-containing areas, which

suggested that calcium carbonate and sodium carbonated were likely to be present. Such effect of carbonation on geopolymers is akin to that on Portland cement-based materials.

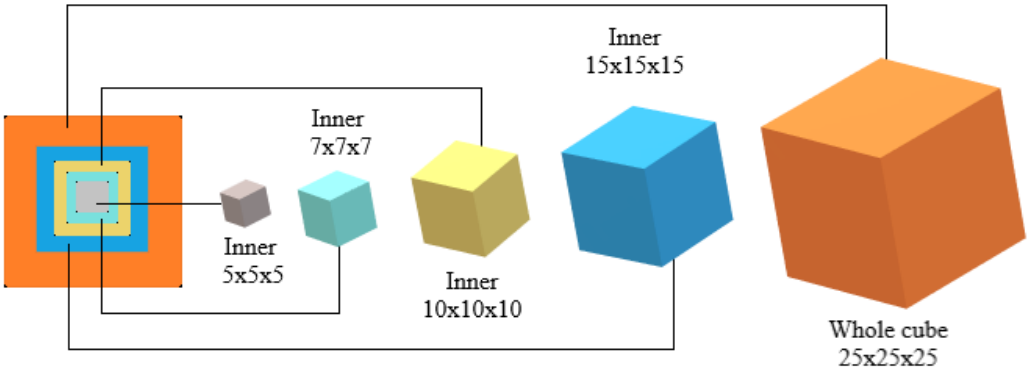

(a)

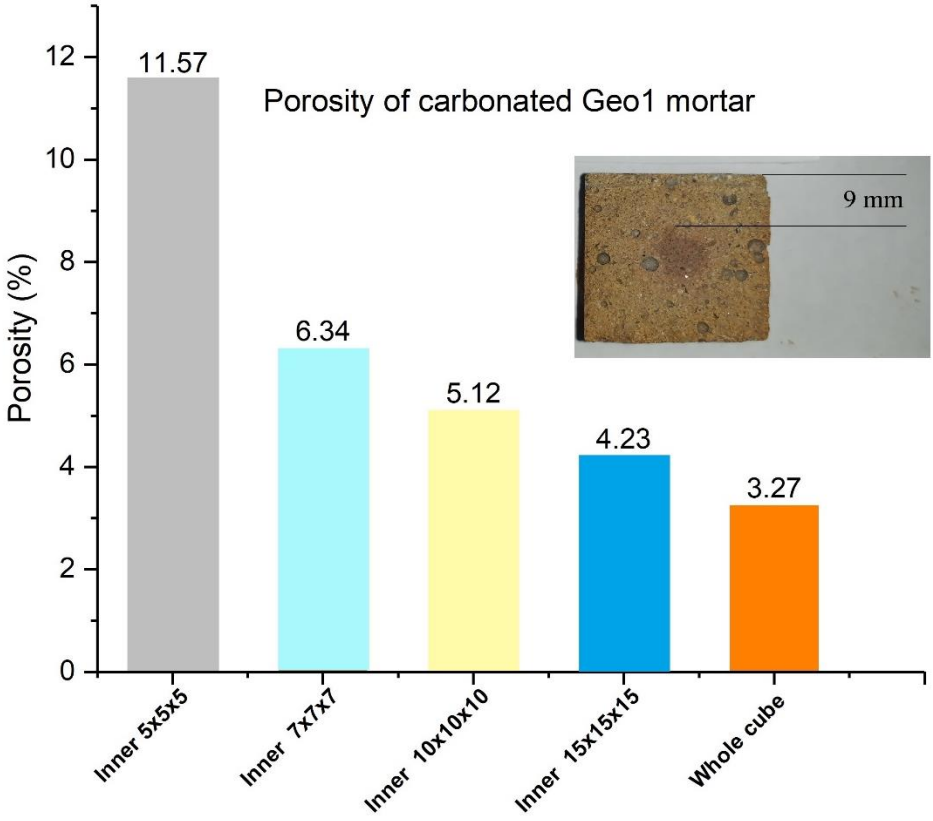

(b)

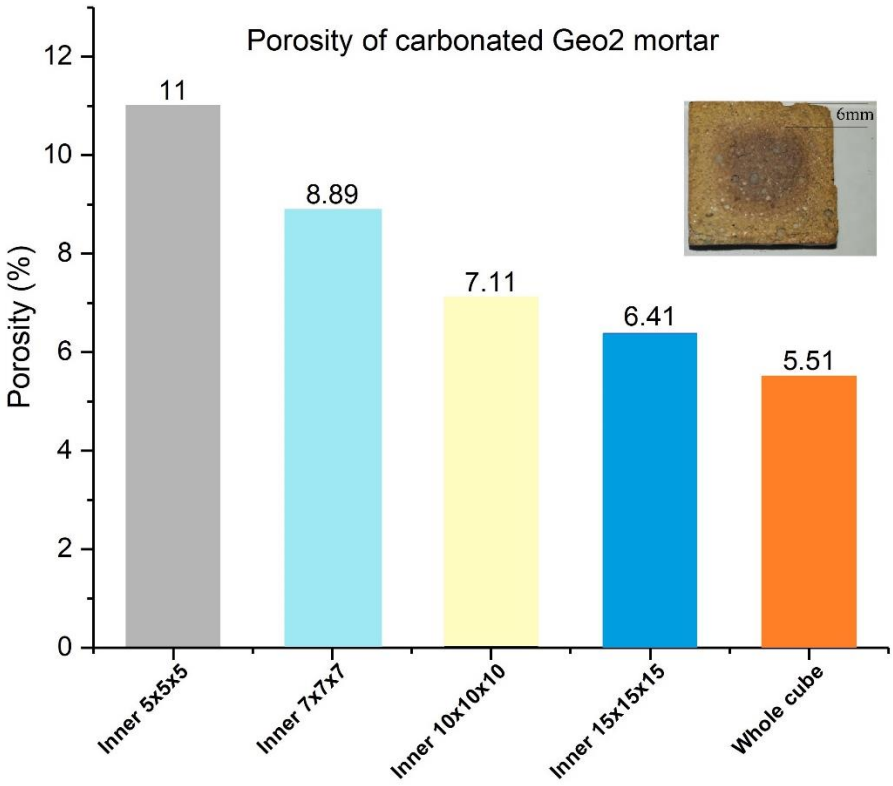

(c)

Figure 4.15 Porosity analysis of different portions in 25 mm cubes of Geo 1 mortar (a) and Geo 2 mortar (b)

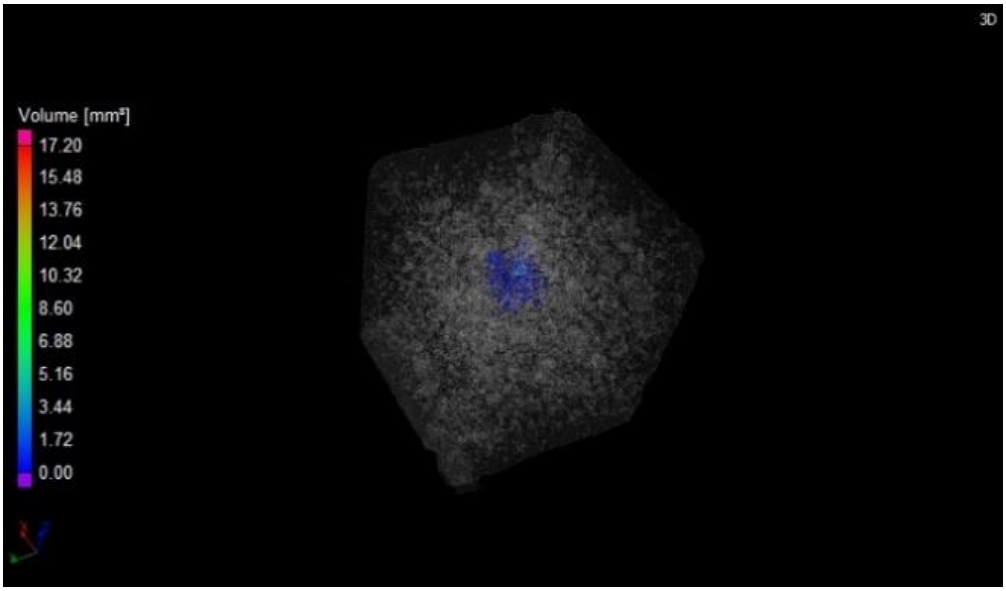

(a)

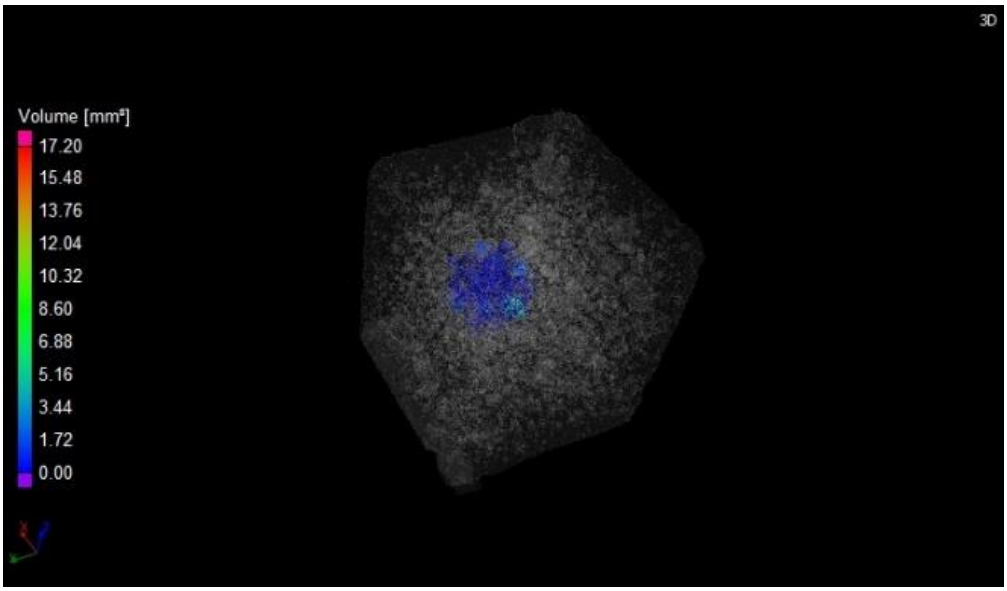
3D
Volume [mm³]
17.20
15.48
13.76
12.04
10.32
8.60
6.88
5.16
3.44
1.72
0.00

(b)

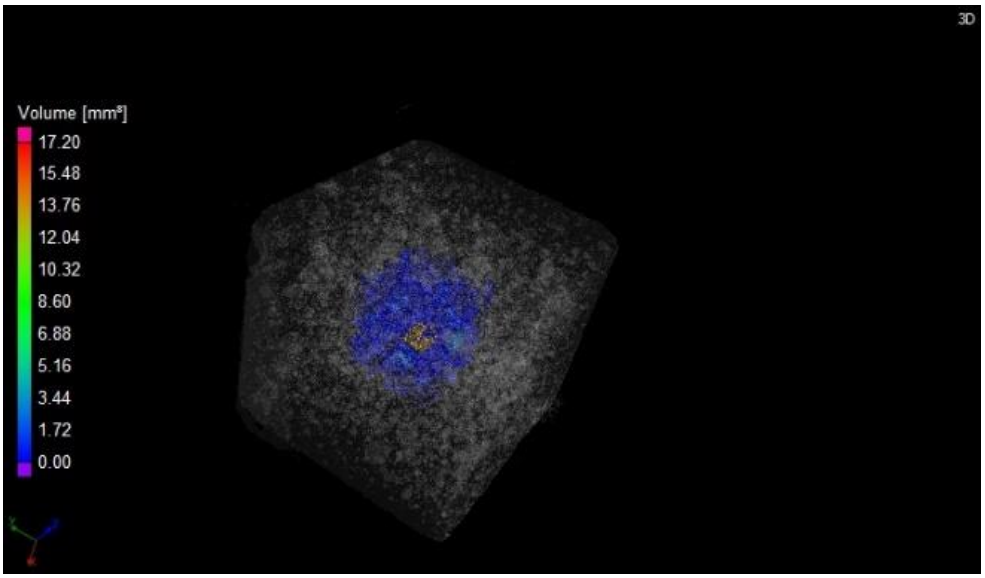
3D
Volume [mm³]
17.20
15.48
13.76
12.04
10.32
8.60
6.88
5.16
3.44
1.72
0.00

(c)

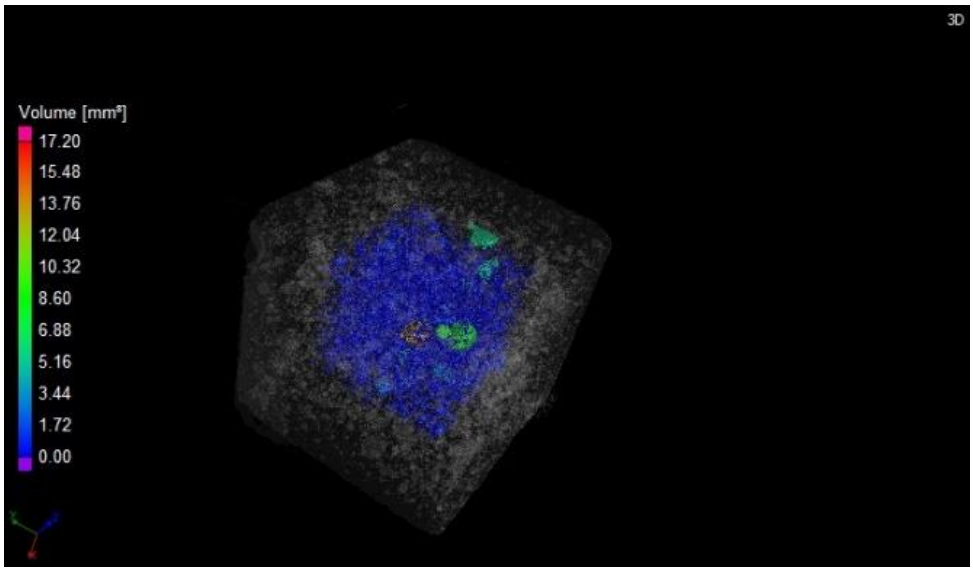

(d)

Figure 4.16 Tomographic reconstructions of 5 x 5 x 5mm (a), 7 x 7 x 7mm (b), 10 x 10 x 10mm (c) and 15 x 15 x 15mm (d) in volumes

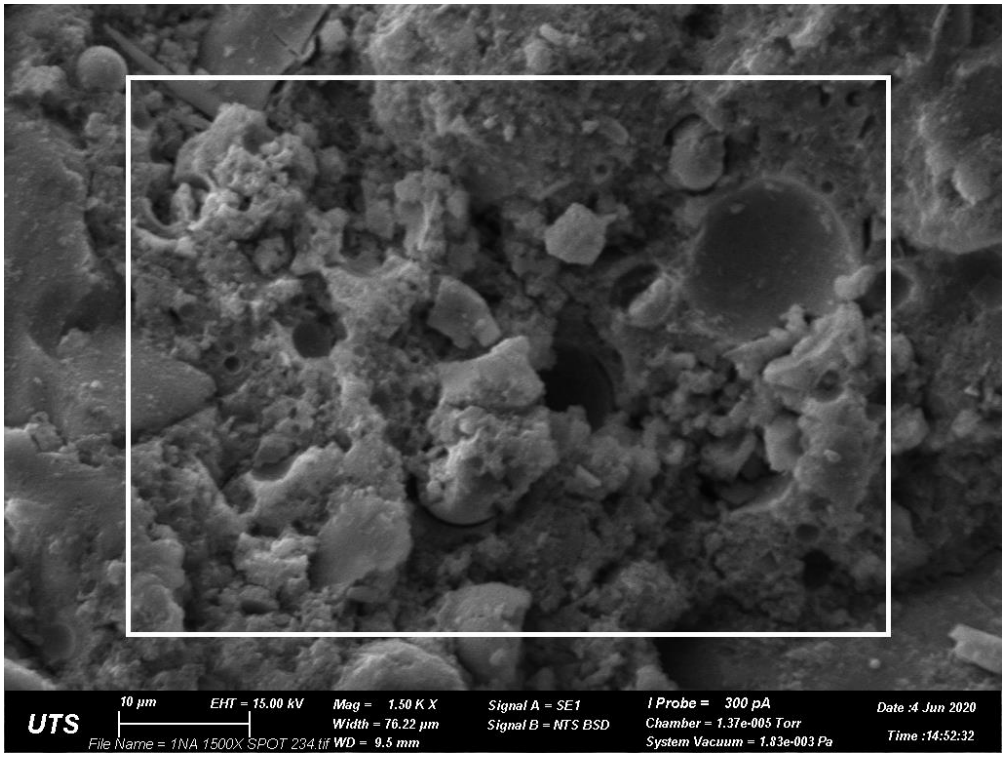

(a)

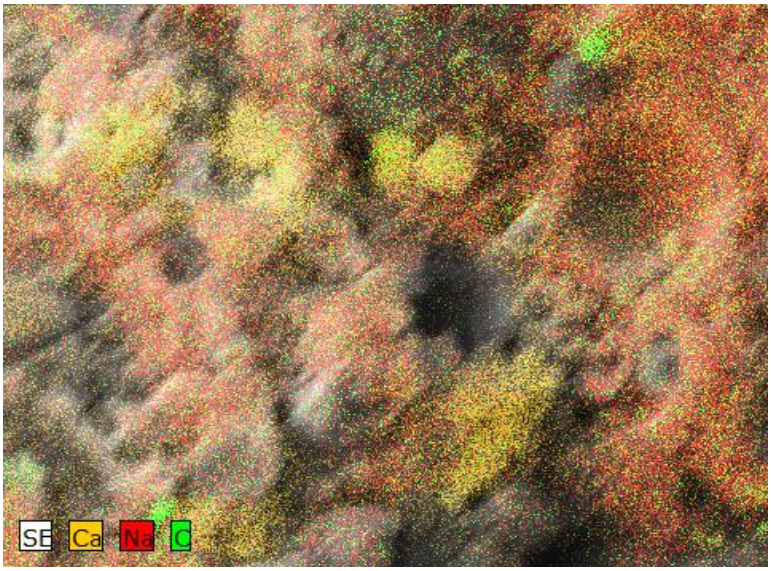

(b)

Figure 4.17. Selected mapping area of a region on the surface of a carbonated Geo 2 mortar (a) and compositional maps for Na, Ca and C (b)

c. Pore analysis of noncarbonated and carbonated portions using neutron tomography and Mercury intrusion capillary pressure measurements

To confirm the conclusion obtained in section 3.2.2, the pore characteristics analysis of a noncarbonated portion and a carbonated portion in the same specimen were carefully inspected. The noncarbonated portion was a volume of 7mm x 7mm x 7mm in the centre of the specimen (Figure 4.18), while the carbonated portion was a volume of 20mm x 20mm x 5mm at the surface of the specimen (Figure 4.19). The porosity of noncarbonated portions was about 6.3% and 8.9% for Geo 1 and Geo 2 mortars, respectively. In the meantime, carbonated portions showed considerably lower porosities with 4.0% for Geo 1 and 6.0% for Geo 2, two-thirds of those of noncarbonated portions. Further, the differences in pore size regions of noncarbonated and carbonated portions were clearly seen in Figure 4.20a and Figure 4.21a with the

pore size in the range of 15 µm to 2000 µm, in which greater pores were found in noncarbonated parts. Figure 4.20b and Figure 4.21b were the extensions of Figure 4.20a and Figure 4.21a which depicted the pore size in the range of 15 µm to 500 µm. These results fully endorsed the conclusion that carbonation led to a pore refinement in one-part fly ash/slag geopolymer mortars investigated.

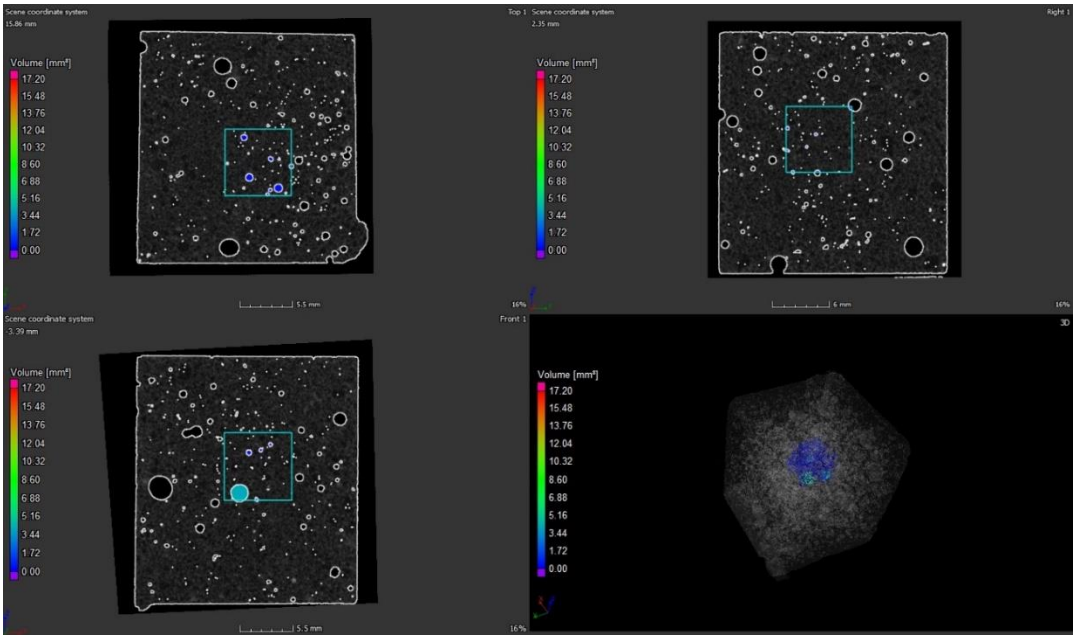

Figure 4.18 Tomographic reconstruction of a noncarbonated portion (7mm x 7mm x 7mm) in the centre of a specimen

Generally, the pore sizes are classified as gel pores and capillary pores, in which pores above 10nm are considered as capillary pores and these are mainly responsible for transport of harmful species such as chloride and other ions. Changes in pore sizes less than about 140um is not easily discernible from this technique whereas Mercury Intrusion Porosity (MIP) measurements can easily distinguish changes in pores in this smaller size region. Also, neutron tomography can handle large specimens (50x50x50mm), whereas MIP can handle only small specimens (about 15mm diameter

by 10mm height). In the experiments performed, 25x25x25mm cubes were used for neutron tomography and 8x8x15mm specimens were used for MIP. Neutron tomography is capable of analysing a board range of pore sizes from 15 µm to 4000 µm, while MIP is able to measure pore sizes from 7nm up to 140 µm.

Due to carbonation, a reduction of 30% in porosity in the range of 15 µm to 2000 µm in geopolymer mortars was clearly observed using neutron tomography. To support the findings by neutron tomography and also to investigate pores with diameter smaller than 140 µm, MIP results were analysed. As depicted in Figures 4.22a, 4.22b, 4.23a and 4.23b, a reduction in porosity (due to carbonation) in range from 7nm up to 140 µm was clearly observed. The porosity in non-carbonated portions of Geo 1 and Geo 2 mortars were 13.4% and 16.9%, respectively. In contrast, the porosities in carbonated portions of Geo 1 and Geo 2 mortars were 9.9% and 10.2%, respectively. This corresponds to a decrease of 30% and 40%, for Geo1 and Geo2, respectively. This finding is similar to the reduction in porosity obtained by neutron tomography in the range of 15µm to 2000µm.

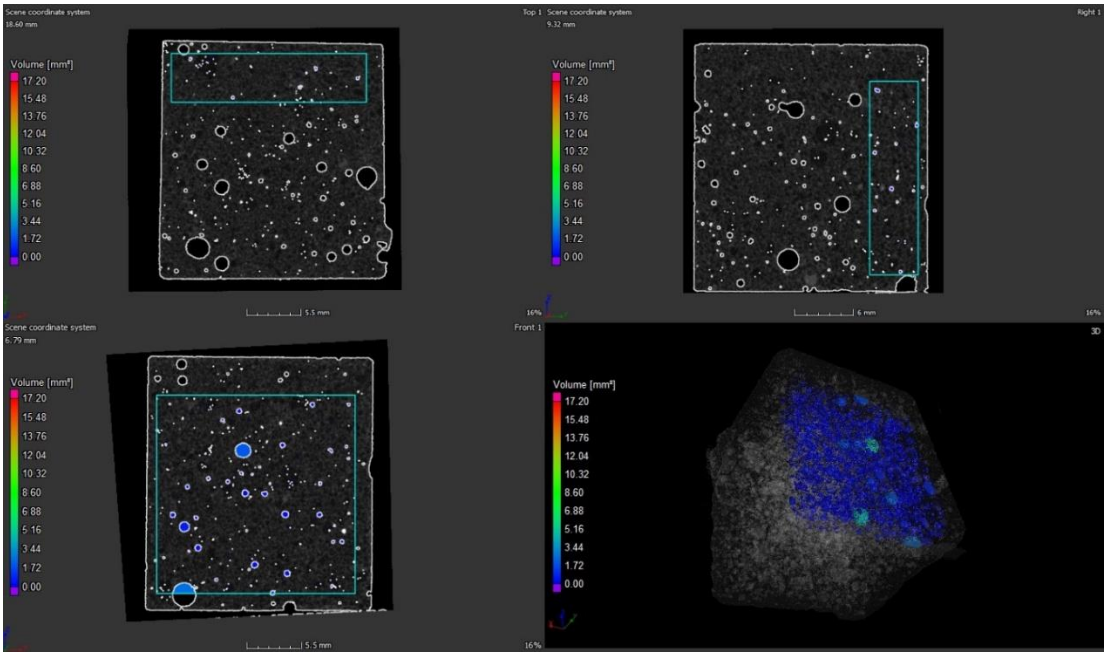

Figure 4.19 Tomographic reconstruction of carbonated portion (20 x 20 x 5mm) at the surface of a specimen

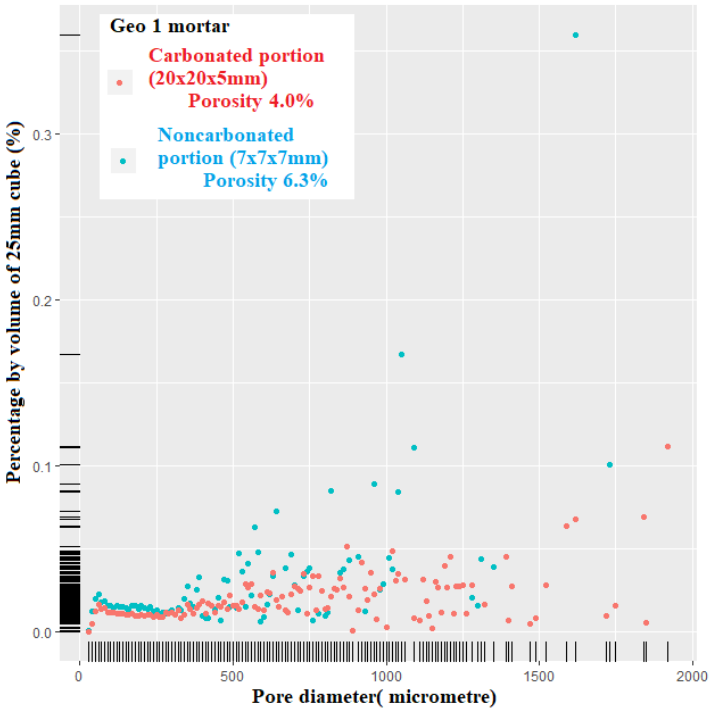

(a)

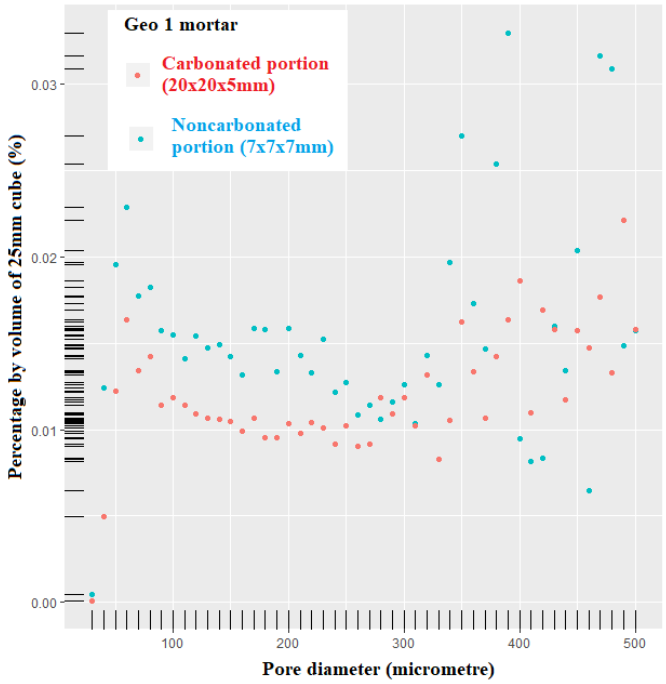

(b)

Figure 4.20 Pore size distribution of noncarbonated and carbonated portions of Geo 1 mortar in the ranged 15-2000µm (a) and in the range 15-500µm (b)

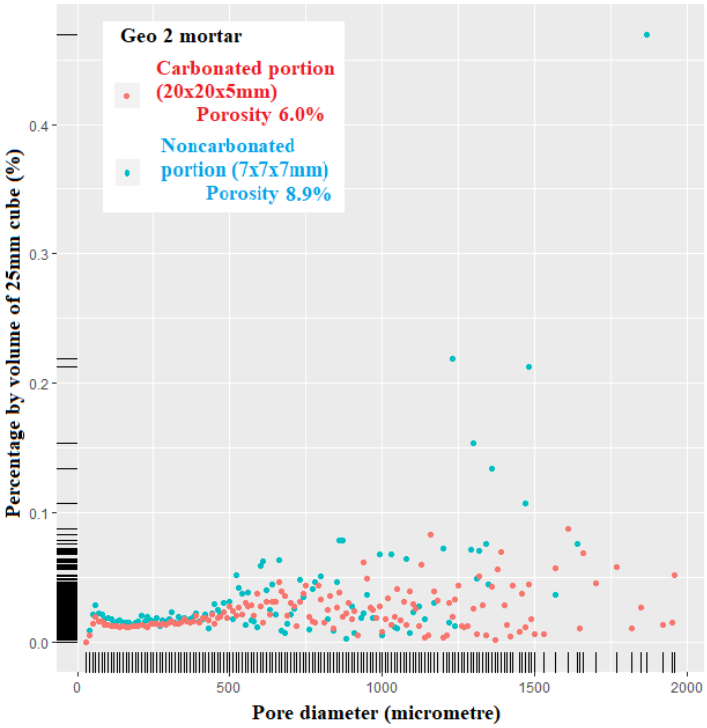

(a)

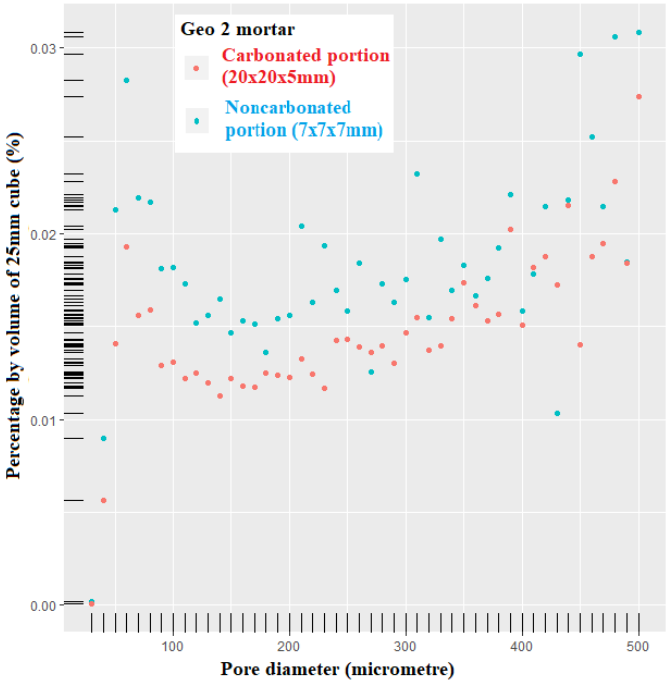

(b)

Figure 4.21 Pore size distribution of noncarbonated and carbonated portions of Geo 2 mortar in the ranged 15-2000µm (a) and in the range 15-500µm (b)

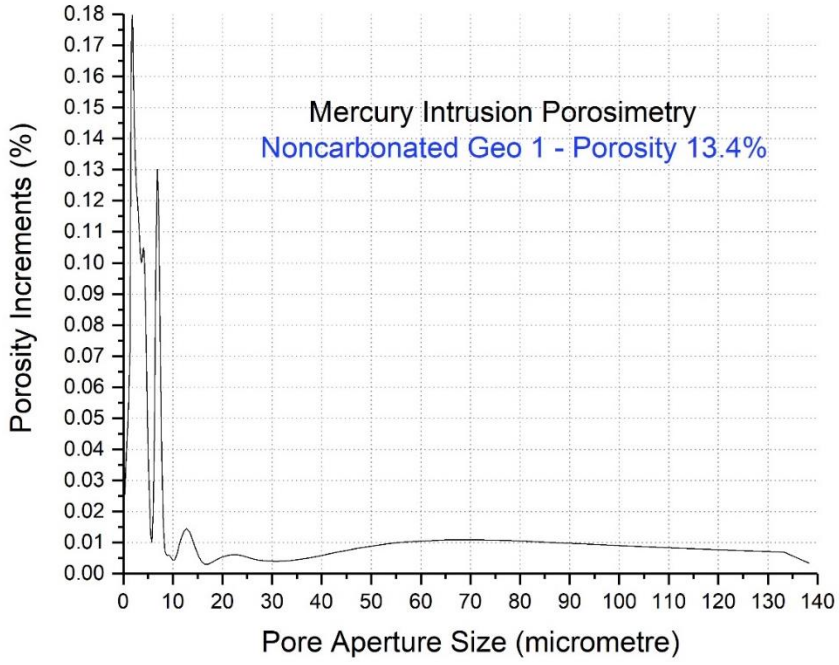

(a)

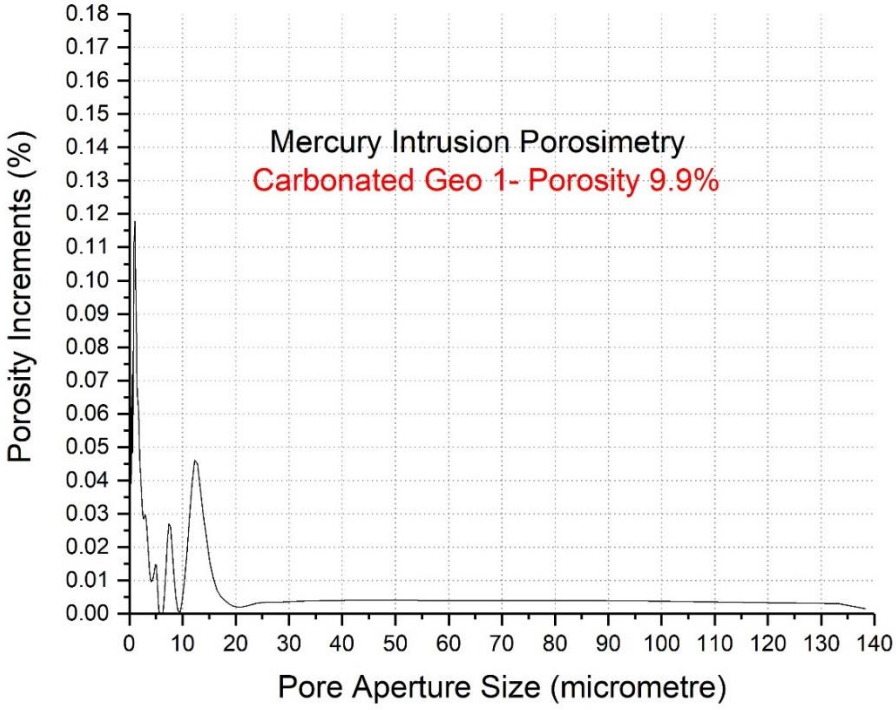

(b)

Figure 4.22 Pore size distribution of non-carbonated (a) and carbonated (b) portions of Geo 1 mortar using MIP

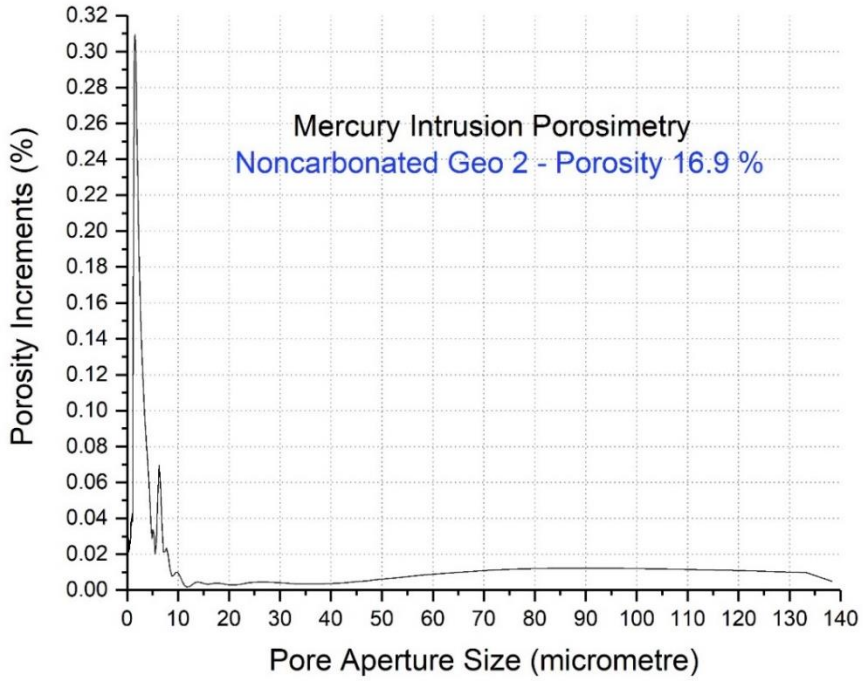

(a)

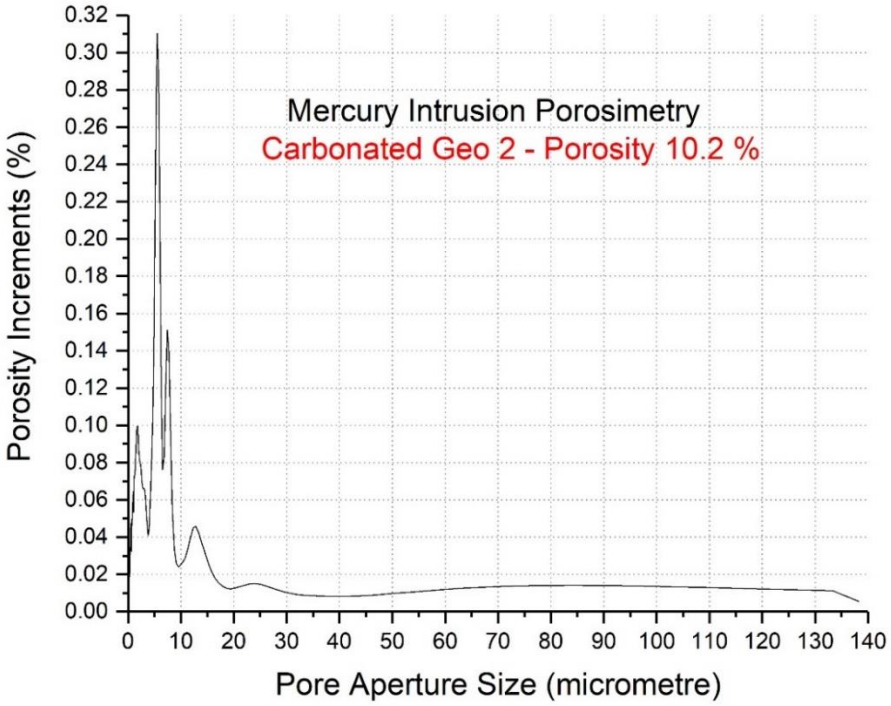

(b)

Figure 4.23 Pore size distribution of non-carbonated (a) and carbonated (b) portions of Geo 2 mortar using MIP

4. 4 Conclusions

This study revealed that alizarin yellow R correlated well with the pH changes in assessing carbonation depth in geopolymer based materials. These findings may be applicable to other novel mortar and concrete applications that do not incorporate ordinary Portland cement; especially those applications that invariably maintain a pH >10.

The employment of a high intensity neutron equipment at ANSTO successfully identified the changes in the pore characteristics of one-part fly ash/slag geopolymer mortars in the carbonation process. The findings revealed that carbonation lowered the porosity in one-part fly ash/slag geopolymer mortars investigated by about 30% in the pore size range of 15 μm to 2000 μm. A similar decrease (due to carbonation) of 30-40% in the range of 7nm to 140μm was obtained using MIP. These two methods of measurements are complementary and hence by performing both neutron tomography and MIP, a full range of pore sizes from 7nm to 4000μm can be studied.

Geopolymer mortars produced with 60% of slag in source materials (Geo 2) displayed a lower carbonation level, compared with geopolymer mortars containing 40% slag (Geo1) under either natural or accelerated CO_2 exposure. After being carbonated, therefore, Geo 2 mortars possessed higher porosity than Geo 1 mortars.
The pH reduction in geopolymer concrete due to carbonation does not fall below 11 and hence steel corrosion may not be affected by carbonation alone.

However, change in porosity due to carbonation can have an effect on subsequent movement of ions such as chlorides and this combined effect needs further investigation.

CHAPTER 5: Chloride Penetration in One-part Fly Ash/Slag Geopolymer Concrete

5.1 Introduction

The penetration of chloride ions in concrete is generally deemed as an important parameter in evaluating the service life of many reinforced concrete structures, because it leads to the damages of the passive layers on the surface of steel reinforcement. Many methods have been developed for appraising the chloride resistance of concrete (Stanish, Hooton & Thomas 1997). Rapid chloride permeability test (RCPT) as per ASTM C1202 (American Society for Testing and Materials 2018) has been adopted widely as a standard test to evaluate the penetration of chloride ions into OPC and blended OPC concretes. RCPT provides several practical advantages such as the simple procedure, short test duration and correlation with compressive strength of concrete (VicRoad 2007; Whiting & Mitchell 1992). At the same time, RCPT has been strongly criticised that it does not well simulate the transport of chloride ions in the concrete structures in the field (Neville 1995; Shi 2003), mainly because the total current passed is a function of the movement of all ions in the pore solution, under the electrical field applied, not only of the chloride ion flux . However, such judgment was deemed as “harsh judgement” because replicating the real situations was “not primary objective of any accelerated test methods” (Cao, Bucea & Meck 1997). Efforts have been made to modify the RCPT test (Cao, Bucea & Meck 1997; Yang, Cho & Huang 2002). The comparison between RCPT with concrete bulk resistivity (Konečný et al. 2017); accelerated chloride migration test (ACMT) (Yang 2004); rapid chloride migration test (RCMT) and electrical resistance test (Bagheri & Zanganeh 2012) were

made. However, the ability of RCPT to predict concrete resistance to chloride penetration is still a controversial issue. Another commonly used method of determining chloride penetration in OPC and blended OPC concretes was ASTM C1556 (???Materials 2016) or NT Build 443 (NORDTEST 1995), which was considered a reference test method for determining chloride penetration into concrete with a satisfactory precision (Tang & Sørensen 2001). The method in accordance with ASTM C1556 or NT Build 443 is an accelerated diffusion test where specimens are exposed to a 16.5% NaCl solution for at least 35 days with the outcome of chloride diffusion coefficient. The correlation of this accelerated diffusion test (16.5% NaCl) with the natural diffusion test, however, has hardly been mentioned in any previous literature. Therefore, the suitability of such intensely accelerated diffusion test needs further investigation.

For studying chloride penetration in geopolymer or alkali activated concretes, many tests were adopted such as RCPT, NT Build 492, ponding test ASTM C1543 and diffusion test ASTM C1556 (Bernal & Provis 2014). An appropriate method for this purpose, however, is still not clear and as a result 3 different tests were adopted in the present investigation. This study aims to investigate the chloride resistance of one-part fly ash/slag geopolymer concretes, using accelerated tests including RCPT as per ASTM C1202 and diffusion test as per ASTM C1556. The correlation between the charge passed obtained in RCPT and apparent chloride diffusion coefficient of such geopolymer concrete was also analysed, to determine the suitability of RCPT in evaluating chloride resistance in one-part geopolymer concrete. More to this point, RCPT was modified and performed at 30V and 10V in order to enhance the accuracy of such test in assessing chloride resistance of geopolymer concrete. A short

investigation of comparison of chloride penetration in reinforced geopolymer concretes and OPC concrete, in a 3.5% NaCl environment was also performed.

5.2 Methodology

5.2.1 Materials and concrete mix proportions

The investigation on chloride resistance of one-part geopolymer concretes was carried out and compared with OPC concrete and OPC+25% fly ash concrete. The mix proportion of concrete is shown in Table 1. All concrete mixes have the same amount of binder, sand and aggregate, but different water to binder ratios. The compressive strength od all mixes is about 50 MPa at 28 days in accordance with ASTM C39/C39M-18 (Materials 2018a). Volume of permeable voids (VPV) was determined as per ASTM C642-06 (Materials 2006), as follows:

$$VPV, \% = \frac{(C-A).100}{(C-D)} \qquad (1)$$

In equation (1), C is mass of surface-dry sample in air after immersion and boiling (g); A is mass of oven-dried sample in air (g) and D is apparent mass of sample in water after immersion and boiling (g).

Table 1. Mix proportion of concretes and geopolymer binders (Geo 1 and Geo 2)

Mix proportion of concretes						
Binder type	Binder (kg/m^3)	Sand (kg/m^3)	10 mm aggregate (kg/m^3)	20 mm aggregate (kg/m^3)	W/B	Compressive strength at 28 days (MPa)
Geo1	410	835	525	790	0.33	53.0
Geo 2	410	835	525	790	0.35	52.0
OPC	410	835	525	790	0.50	53.5
OPC+25% Fly ash	410	835	525	790	0.47	47.0
Mix proportion of geopolymer binders						
	Slag/(Fly ash + Slag)		SiO_2/Al_2O_3		Sodium activator powder	

			(%)
Geo 1	0.4	2.6	16%
Geo 2	0.6	2.4	16%

5.2.2 Preparation of specimens

The procedure of mixing concrete was described in chapter 4 (section 4.2.2). After the completion of mixing concrete, 100 mm cube concrete specimens were cast and removed from the mould after 1 day. Geo 1 and Geo 2 specimens were then wrapped in plastic films and placed in the oven at 60^{o}C for 6 hours. Following that, plastic films were removed, and concrete specimens were placed in air in the laboratory. For OPC and OPC+25% Fly ash concretes, specimens were placed in a lime water tank until 28 days. At the age of 28 days, each specimen was cut into three portions with the lengths of 75mm, 50mm and 50mm (see Figure 5.1a). Except the bottom cast surface, all surfaces of the 75mm portions were then covered by a silicone sealant that has high resistance to water, chlorine, fungus and weathering. Only one surface (bottom cast surface) was not covered so that chloride ions could penetrate in concrete (see Figure 5.2b). The two portions of 50mm in length were then used for RCPT.

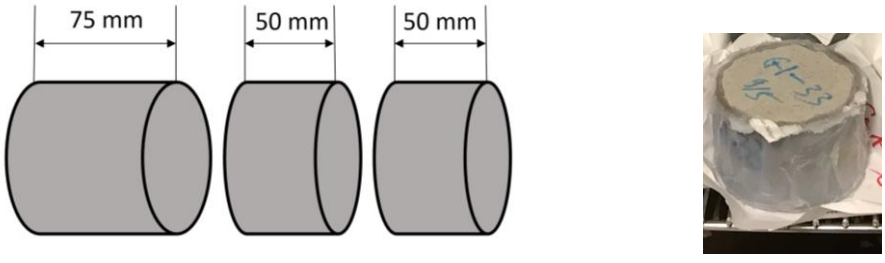

(a) (b)

Figure 5.1 Three portions sliced from one concrete specimen

The preparation of test specimens for testing chloride penetration in one-part fly ash/slag concrete was describe in Figure 5.2. In each concrete cylindrical specimen of 200mm long, a 75mm portion was used for diffusion test as per ASTM C1556, a 50mm portion was used for RCPT and another 50 mm portion was used for modified RCPT. At least three identical specimens were tested according to the relevant standards.

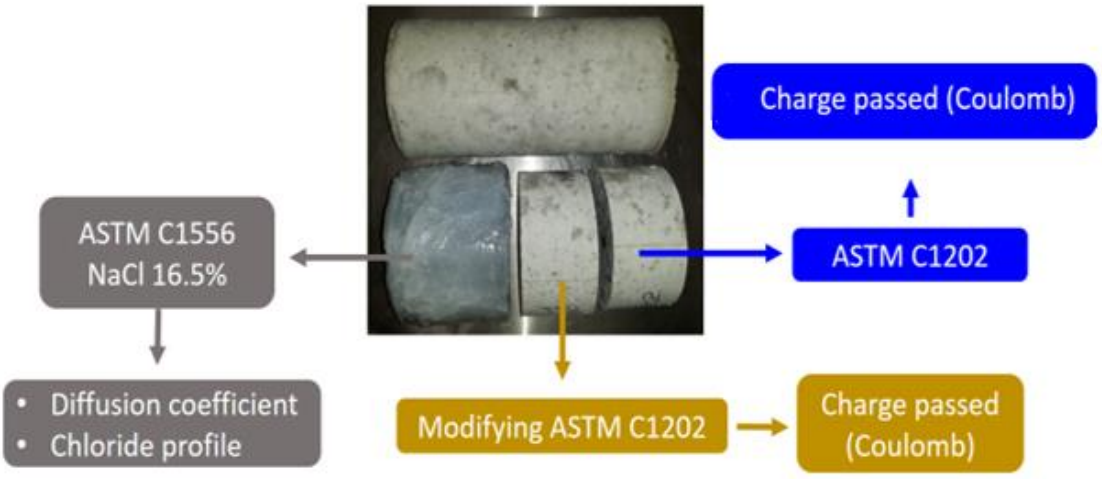

Figure 5.2 Preparation of test specimens for chloride penetration in concrete by rapid chloride permeability and chloride diffusion

5.2.3 Rapid chloride permeability test as per ASTM C1202 and modified rapid chloride permeability tests

The 50mm thick and 100mm diameter concrete samples, mentioned in section 5.2.2, were fully water saturated. Firstly, six 50mm thick concrete specimens were placed in the vacuum pump for 3 hours at a pressure of 50 mm Hg. Then distilled water was filled in the container and specimens were soaked for 18hours ± 2 hours. After being removed from water, concrete specimens were kept at higher relative humidity and then placed between two reservoirs that contains solutions of 3.0% NaCl and 0.3N NaOH, as shown in Figure 5.3. An electrical source of 60 V was applied

across the cell. Apart from 60V, 30V and 10V were also applied in the test. The negative terminal was connected to the electrode in the NaCl solution and the positive terminal was connected to the electrode in the NaOH solution for 6 hours. The total charge passed was then determined. The correlation of the total charge passed with apparent chloride coefficient (D_a), measured in section 5.2.3, was carefully investigated. Regarding modified RCPT, power sources of 30V and 10V were connected to two reservoirs and then the total charge passed was measured in the same way as in the test at 60V.

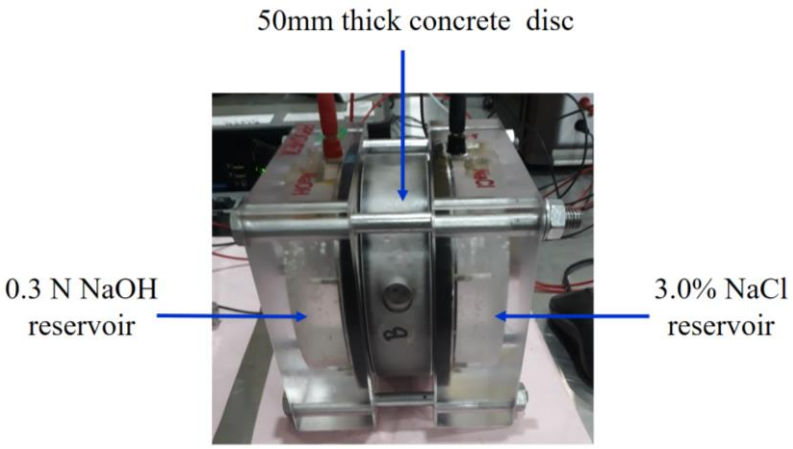

Figure 5.3 A test cell in RCPT test

5.2.5 Investigation of ion movements in rapid chloride permeability test

To understand the movement of ions and cations in rapid chloride permeability test, solutions in two reservoirs before and after the completion of a test at 60V were collected. The concentration of cations in such two solutions were then analysed by an inductively coupled plasma mass spectrometry (ICP-MS), while the concentration of ions were carried out using an ion chromatography (IC).

5.2.6 Chloride bulk diffusion test as per ASTM C1556 and determination of acid soluble chloride as per ASTM C1152

Chloride bulk diffusion test as per ASTM C1556

The 75mm portions were immersed in a water bath at least for 48 hours so that the mass did not change by more than 0.1% . The fully saturated specimens were then placed in the small tank containing 16.5% NaCl solution. These small tanks were sealed and placed in the laboratory for 3 months.

Determination of acid soluble chloride as per ASTM C1152

After being removed from the sodium chloride solution, specimens were ground every 1mm against 25 mm depth of concrete specimens using Germann Instruments‟ Profile Grinder. The sample powders were obtained in layers parallel to the exposed surface. The procedure of calculating apparent chloride diffusion coefficient was described in detail in a study of Noushini et al. (Noushini et al. 2019). In which the acid soluble chloride (total chloride) was measured in accordance with ASTM C1152 (American Society for Testing and Materials 2012). A 20 ml of 20% acid nitric was used to disperse with 3.5 g of sample powder in a beaker. The beaker was covered by a watch glass and allowed to stand for 1 to 2 minutes. The covered beaker was rapidly heated to boiling for several seconds and removed from hot plate. The solution in the beaker was filtered using filter papers with a pore size of 5–10 μm in a Buchner funnel and suctioned filtration flask. The beaker and the filter paper were rinsed twice with small portions of water. The solution obtained was about 50 ml. The chloride content of in the solution was determined by A Metrohm 855 Robatic Titrosampler with $AgNO_3$ solution in accordance with ASTM C114 (Materials 2018b), as follows:

$$Cl, \% = \frac{3.545(V_1 - V_2)N}{W} \quad (1)$$

In the Equation 1, V_1 is millilitres of 0.05N $AgNO_3$ solution used for sample titration, V_2 is millilitres of 0.05N $AgNO_3$ solution used for blank titration, N is exact normality of 0.05N $AgNO_3$ solution and W is weight of sample (g).

Determination of apparent chloride coefficient (D_a)

Acid soluble chloride profile was plotted by means of a non-linear regression analysis. Chloride ion content was determined from the exposure surface layer in the regression analysis. All other chloride ion content measurements are included in the regression analysis

$$C(x,t) = C_s - (C_s - C_i).\,\mathrm{erf}\left(\frac{x}{\sqrt{4.D_a.t}}\right) \quad (2)$$

In Equation 2, C(x, t) is chloride concentration measured at depth x and exposure time t, mass %; C_s is projected chloride concentration at the interface between the exposure liquid and test specimen that is determined by the regression analysis in mass %; C_i is initial chloride concentration of the binder prior to submersion in the exposure solution, mass %; x is the depth below the exposed surface in m; t is the exposure time, seconds; Da is the apparent diffusion coefficient in m^2/s; and erf is the error function described in Equation 3.

$$\mathrm{erf}(z) = \frac{2}{\sqrt{\pi}} \int_0^z \exp(-u^2)\, du \quad (3)$$

5.3 Results and discussions

5.3.1 Charge passed in rapid chloride permeability test

For safety reason, most RCPT instruments limit current to 500 mA. When the current is over 500 mA, overheating happens, and the test will be terminated. When 60 V was applied, 25.0% of RCPT tests of Geo 1 concrete were stopped before 6 hours due to overheating. For Geo 2 concrete the overheating was more severe with 42.8% of specimens had to be stopped before 6 hour duration. In contrast, the test ran well at

60V for OPC and OPC+25% fly ash concretes. Thus, RCPT performed at 60V was not appropriate for testing chloride resistance for these one part geopolymer concretes. Meanwhile, the tests carried out at 30V and 10V were successfully completed in all type of concretes investigated.

The results of RCPT at 30 V was applied in the test, Geo 1 concrete showed highest value for average charge passed with 2027 coulombs (see Figure 5.4 or Table 5.2). Geo2 with the average chage passed at 1782 coulombs ranked next followed by OPC concrete with average charge passed at 1246 coulombs.

When RCPT was run at 10V (shown in Figure 5.5 or Table 5.2), concrete produced from OPC with 25% fly ash still showed the lowest value for average charge passed (157coulombs). By contrast, the highest value for average charge passed was observed in Geo 2 concrete with 497 coulombs, then Geo 1 concrete with 366 and OPC concrete with 233 coulombs.

Although Geo1 and Geo2 concretes apparently give higher coulomb values than OPC or OPC with fly ash concretes, this does not imply that geopolymer concretes are more vulnerable for chloride ion penetration, due to different ions present in both systems. This is demonstrated clearly from chloride profiles in diffusion tests discussed in section 5.3.2 below.

Table 5.2. Charge passed in RCPT at 30V and 10 V

Concrete type	Mean (Standard Deviation)	Median [Min, Max]
Charge passed at 30 V (coulomb)		
Geo 1	2027 (182)	2051 [1760, 2342]
Geo 2	1782 (218)	1670 [1643, 2033]
OPC	1246 (229)	1176 [1060, 1502]

Charge passed at 10 V (coulomb)		
Geo 1	366 (70)	389 [267, 450]
Geo 2	497 (36)	497 [445, 553]
OPC	233 (55)	203 [200, 296]
OPC+25% Fly ash	157 (28)	156 [123, 192]

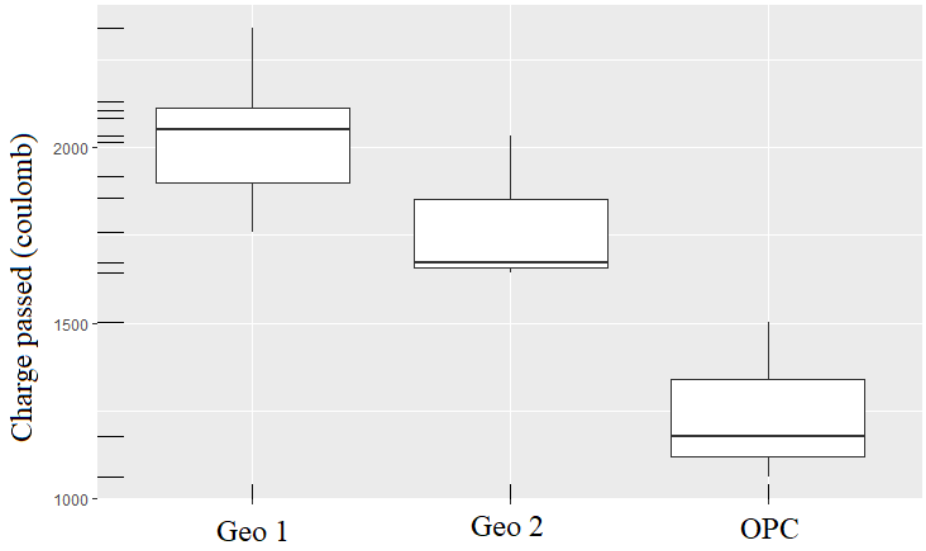

Figure 5.4 Charge passed in RCPT at 30V

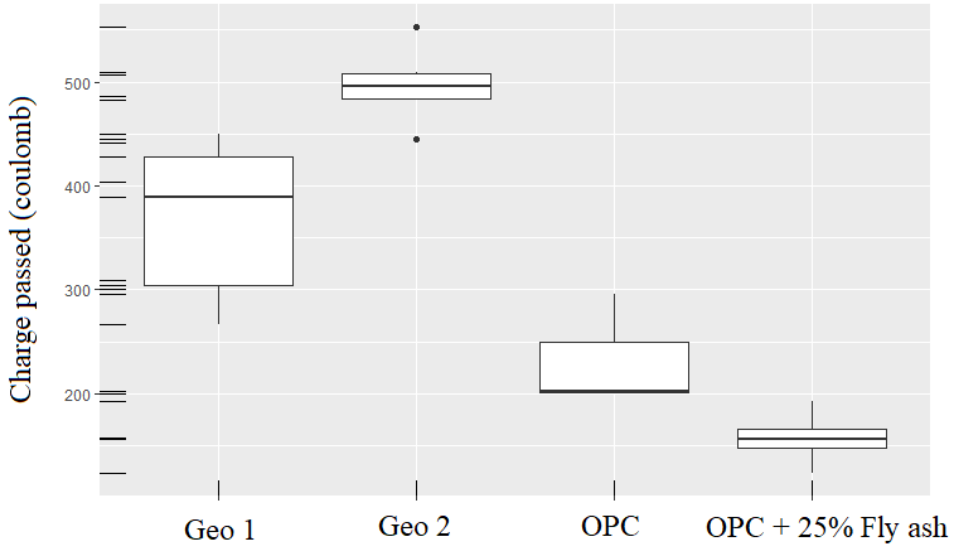

Figure 5.5 Charge passed in RCPT at 10V

5.3.2 Chloride profiles and apparent chloride diffusion coefficient in one-part fly ash/slag geopolymer concrete as per ASTM C1556

Total chloride profiles obtained from Geo 1, Geo 2, OPC and OPC+25% Fly ash concretes which were immersed to 16.5% NaCl solutions were presented in Figure 5.6.

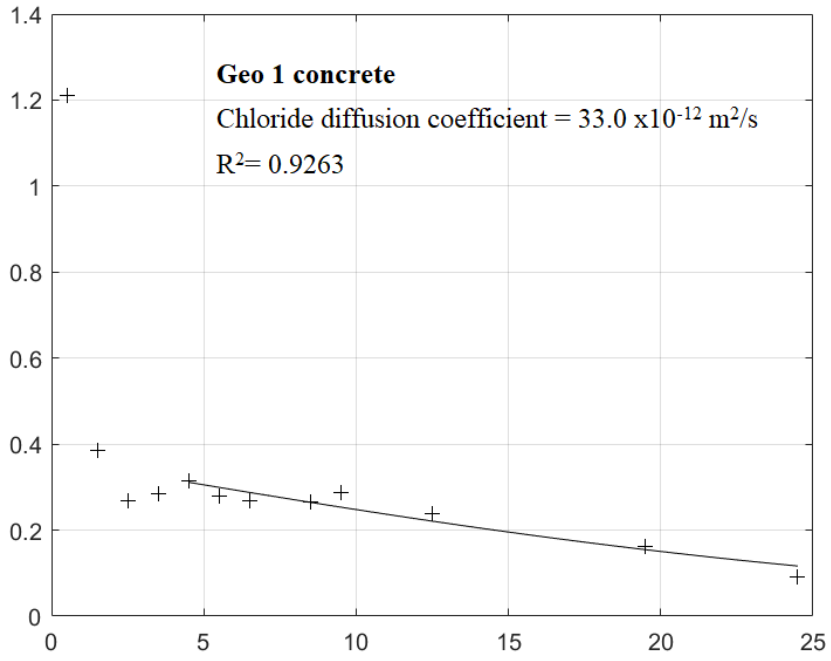

(a)

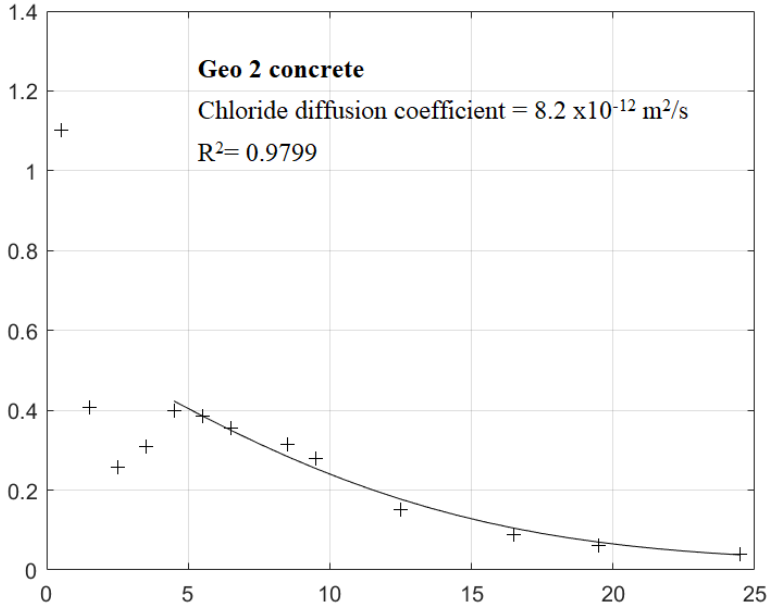
Geo 2 concrete
Chloride diffusion coefficient = 8.2 x10-12 m2/s
R2= 0.9799
1.4
1.2
1
0.8
0.6
0.4
0.2
0
0
5
10
15
20
25

(b)

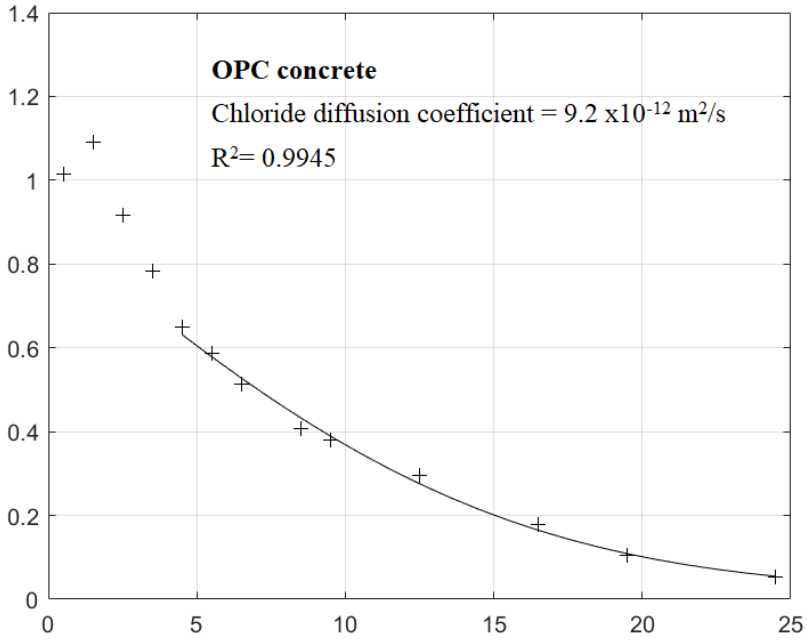
OPC concrete
Chloride diffusion coefficient = 9.2 x10-12 m2/s
R2= 0.9945
1.4
1.2
1
0.8
0.6
0.4
0.2
0
0
5
10
15
20
25

(c)

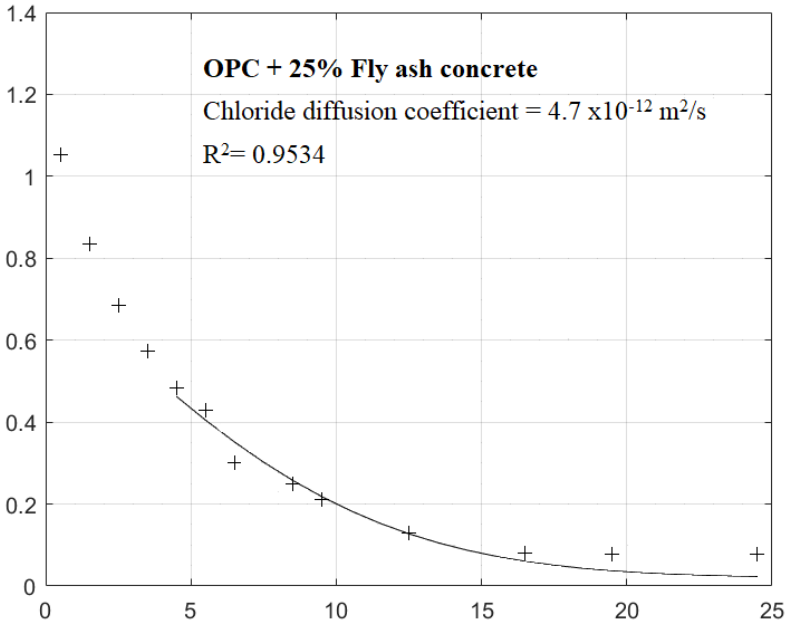

(d)

Figure 5.6 Total chloride profile in (a) Geo 1, (b) Geo 2, (c) OPC and (d) OPC +25% Fly ash concretes.

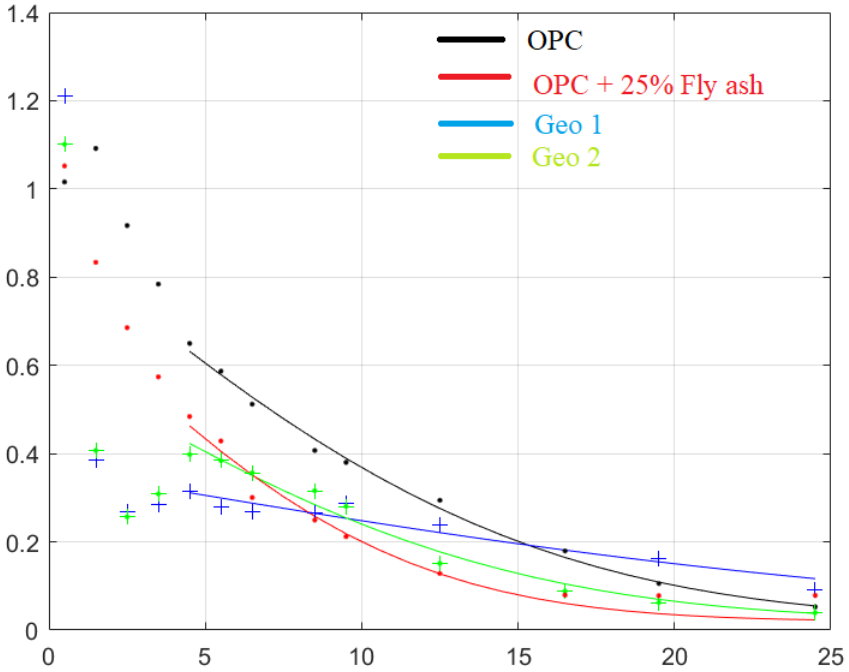

Figure 5.7 Chloride profile of four types of concrete

Based on these total chloride concentrations, apparent chloride diffusion coefficient was calculated and shown in Table 5.3.

Table 5.3 Chloride penetration related properties of geopolymer and OPC concretes investigated

Concrete type	Apparent chloride coefficient (10^{-12} m^2/s)	VPV (%)	Compressive strength (MPa)	Charge passed (coulomb) at 30V	Charge passed (coulomb) at 10V
Geo 1	33.0	11.0	52.9	2027	389
Geo 2	8.3	12.0	52.1	1782	497
OPC	9.2	13.3	52.5	1246	203
OPC+25% fly ash	4.8	13.1	46.5	-	157

Geo 1 concrete showed the highest chloride diffusion coefficient of 33.0 $x10^{-12}$ m^2/s, much higher than that in OPC concrete which was 9.2 $x10^{-12}$ m^2/s. Meanwhile, chloride diffusion coefficients of Geo 2 and OPC+25% fly ash were 8.2 and 4.7 $x10^{-12}$ m^2/s, respectively. This implied that OPC+25% fly ash had highest resistance to chloride penetration, followed by Geo 2 concrete. Hence with the right precursor materials (in this case fly ash/slag combination) it is possible to produce geopolymers which will be as effective as blended cement systems in terms of chloride ion diffusion. Also it should be noted that with a poor selection of precursor materials, the geopolymer produced can become least effective in chloride diffusion.

As shown in Figure 5.7, the chloride contents of OPC and OPC+25% fly ash concretes in layers from 0 - 6 mm, however, were higher than those of Geo 1 and Geo 2 concretes. This happened probably because of differences in curing conditions

applied for producing concretes specimens. As mentioned in section 5.2.2, the curing conditions applied for producing Geo 1 and Geo 2 concretes were sealed and heat curing, while OPC and OPC+25% Fly ash concretes were cured in a lime water tank. The chloride ion concentrations near the surface of heat-cured specimens were found to be considerably lower than those of water cured specimens (Sherman, McDonald & Pfeifer 1996), which explains why OPC and OPC+25% fly ash concretes had higher surface chloride contents than Geo 1 and Geo 2 concretes. Hence for calculation of diffusion co-efficients, chloride ion concentrations for depths below 5mm from the surface were used.

The VPV results showed that all four types of concrete investigated had good quality in accordance with VicRoads Classification for Concrete Durability (VicRoad 2007). However, VPV results did not seem to correlate well with accelerated chloride diffusion coefficients and the correlation coefficient between these two parameters was -0.85 (calculated by using R software) indicating no correlation. Volume of permeable voids (VPVs) of Geo 1 and Geo 2 were 11.0% and 12.0% and their total porosities were almost the same (Vu et al. 2020). However, the chloride diffusion coefficient of Geo 1 concrete was four times higher than that of Geo 2 concrete. It was probably because Geo 2 concrete contained a higher percentage of slag (60% slag by weigh of total precursor) than Geo 1 concrete (only 40% slag). Increasing the slag content (more than 50%) resulted in an increase in pore tortuosity in the alkali activated system (Balcikanli & Ozbay 2016; Lee & Lee 2016; Provis et al. 2012), thus, slowed down the ingress of chloride ions into the alkali activated material. The dominant reaction product in the system, in this case, was C-(N)-A-S-H gel which could chemically and physically bind chloride ions (Susan A. Bernal et al. 2013; Ben Haha et al. 2011; Yuan et al. 2009). On the otherhand, in the alkali activated system with high percentage of

fly ash, the main reaction product was N-A-S-H which was merely able to physically bind chloride ions (Ismail et al. 2013; Zhang, Shi & Zhang 2019). The difference of chloride diffusion coefficients of Geo 1 and Geo 2 concretes, thus, can be explained by the difference in the gels formed in Geo 1 and Geo 2 systems. This also proved that the ratio of fly ash to slag in the precursors plays a significant role in tailoring fly ash/slag geopolymer concretes with high resistance to chloride attack.

The coefficient of correlation between chloride diffusion coefficient and charge passed in RCPT at 10 V, in the current series of tests (with 22 specimens), was 0.38 which was very low. The correlation coefficient between chloride diffusion coefficient and charge passed in RCPT at 30V, in contrast, was 0.72, indicating a good correlation. Thus, rapid chloride permeability tests conducted at 30V was strongly recommended because the issues related to overheating could be avoided, and the charge passed at 30V also showed a good correlation with chloride coefficient measured in the highly accelerated test as per ASTM C1556.

5.3.3 Chloride diffusion test in 3.5% NaCl

As shown in Figures 5.8a, 5.9a and 5.10a, there was no sign of corrosion in Geo 1, Geo 2 and OPC concretes after being immersed in a 3.5% NaCl solution in 6 months.

However, chloride depths, indicated by spraying $AgNO_3$ solution, in Geo1 (Figure 5.8b) was lower than that in OPC (Figure 5.10b). Meanwhile, chloride depth Geo 2 concrete (average depth 7 mm) was about half of that in Geo 1 and OPC concretes (average depth 15 mm) (Figure 5.9b). These findings suggested that chloride diffusion coefficient of concretes exposed to 16.5% NaCl solution for 3 months and charge passed in RCPT at 30V in 6 hours, both, did not correlate well with the chloride

depths in concrete which were immersed in a 3.5% NaCl solution in 6 months. This is probably because of the leaching of anions and cations out of the pore solution, over a long period of time in a long- term test (Tang & Sorensen 2001). Consequently, different chloride ion movement and flow characteristics could have occurred in tests of different durations. More to this point, as suggested by previous researchers, "short-term diffusion coefficients are not necessarily the best indicators of longer-term chloride resistance" (Sirivivatnanon & Khatri 2011). For blended cement based concretes, the chloride diffusion coefficient also reduced with time when the exposure period increased (Sirivivatnanon & Khatri 2011). The same phenomenon of decreasing chloride diffusion coefficient may occur with geopolymer concretes too, but this needs further investigation. Different results for diffusion coefficient were obtained in the two tests mentioned above, performed for 3 months in 16.5% solution in an accelerated test and for 6 months in 3.5% NaCl solution in natural diffusion test.

(a)

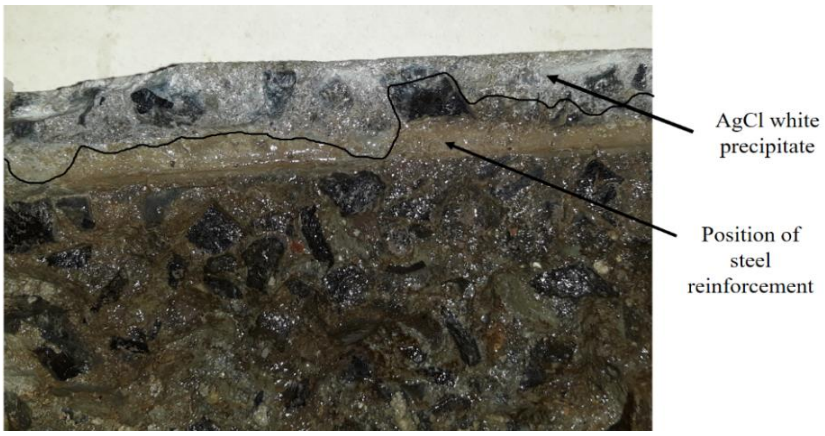

(b)

Figure 5.8 (a) Steel reinforcement and (b) chloride depth in Geo 1 concrete after 6 months exposure in a 3.5% NaCl solution

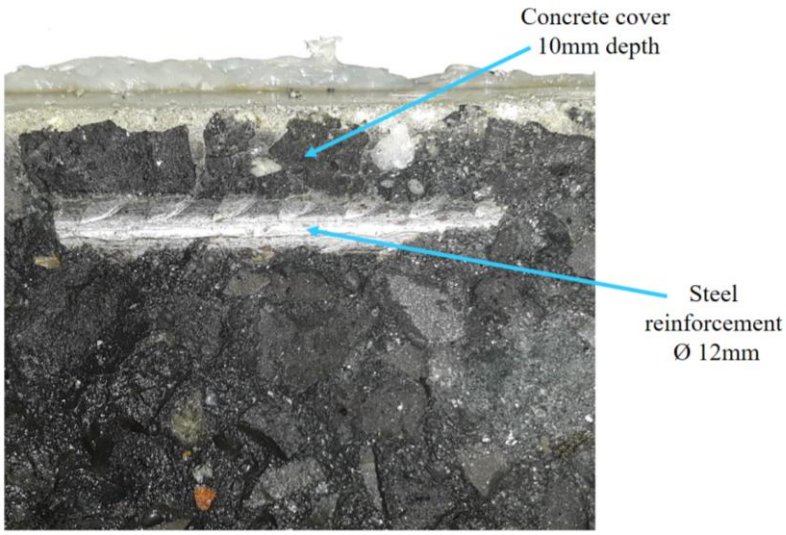

(a)

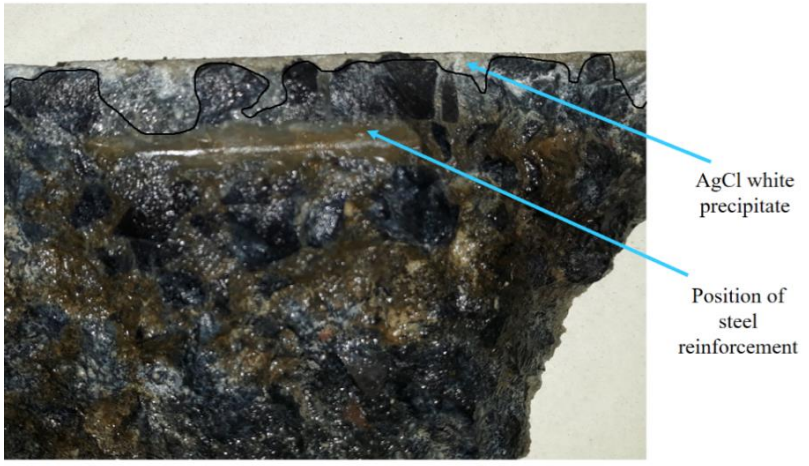

(b)

Figure 5.9 (a) Steel reinforcement and (b) chloride depth in Geo 2 concrete after 6 months exposure in a 3.5% NaCl solution

(a)

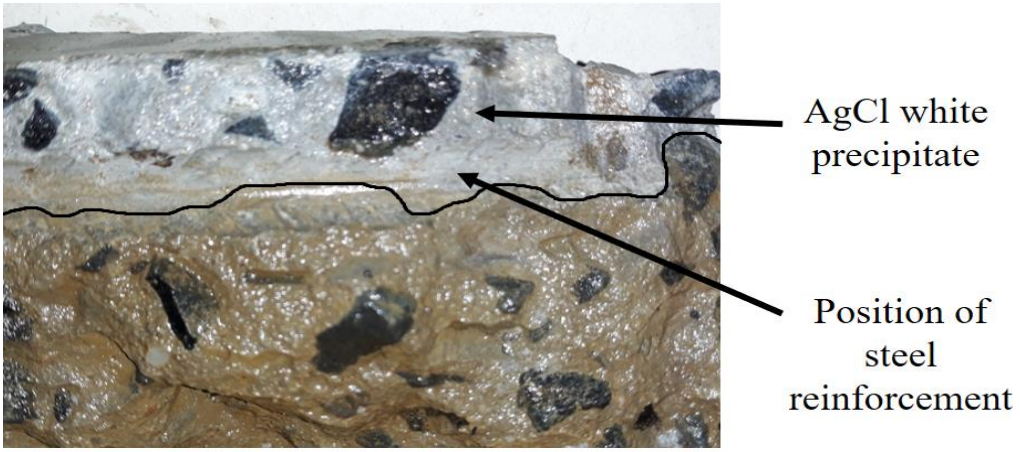

(b)

Figure 5.10 (a) Steel reinforcement and (b) chloride depth in Geo 2 concrete after 6 months exposure in a 3.5% NaCl solution

5.3.4 Movement of ions in one-part fly ash/slag geopolymer concrete under the electrical field applied in rapid chloride permeability test (RCPT)

The movement of ions in OPC based concrete in a RCPT at 60V was elaborately studied by Andrade (Andrade 1993). Before the electrical field was applied, movement of ions was mainly due to diffusion process because of the differences in the ion concentrations. When the electrical field was employed, the ion migration occurred, driven by the potential difference. Thus, the principal transport of ions in the test was a combination of diffusion and migration. Although the type and concentration of ions in the pore solution of OPC based concretes and geopolymer based concretes are different, the outcomes of the study above (Andrade 1993) can be applied to explain the movement of ions in geopolymer based concretes.

The concentration of anions and cations in solutions in two reservoirs before and after a completion of an initial test at 60V was measured to investigate their movements. Table 5.4 and Figure 5.11 show the changes in anion and cation concentrations in Geo1 concrete and the total charge passed in 6 hours was of 3723

coulombs. In NaCl reservoir, the concentration of chloride ion was reduced by about 10.0% while the concentrations of sodium cation increased by about 13.9%. In NaOH reservoir, the sodium concentrations decreased by 48.6%. An increase of pH by 84.1% in NaCl reservoir and a pH reduction of about 1.5% in NaOH reservoir were recorded. The pH changes in both NaCl and NaOH reservoirs after testing were probably caused by the electrolysis of water (Andrade 1993). At the NaCl reservoir, a reduction reaction in H_2O happened to produce OH^- ions to balance the lack of electric charge due to the movement of Cl^- ions in the 50mm thick concrete specimen, as shown in Figure 5.11. The OH^- ions, which were just produced, also moved in the 50mm concrete specimen under electrical field. The OH^- movement happened more easily and contributed more towards charge passed than that of Cl^- (Cao, Bucea & Meck 1997). As a result, an increase in pH from 6.9 to 12.5, took place in NaCl reservoir. In NaOH reservoir, an oxidation process in H_2O to produce H^+ ions to balance the electric charge because Na^+ cations moved out of NaOH solution to come into geopolymer concrete. This would lead to a considerable reduction in pH. However, OH^- ions from concrete also moved to NaOH reservoir due to the force of the electrical field. Thus, only a pH reduction of 1.5% was observed in NaOH reservoir. In NaCl reservoir, the concentration of chloride ion reduced about 10.0% for Geo1 concrete and 6.3% for OPC concrete (see Tables 5.4 and 5.6), while the concentration of sodium cation increased by 13.9% for Geo1 and by 4% for OPC concrete. In NaOH reservoir, the sodium concentration decreased by 48.6% for Geo 1 concrete and by 14.7% for OPC concrete. Changes in anion and cation concentrations in Geo 1 concrete was much more than that in OPC concrete, which explained well why the charge passed in Geo 1 concrete (3723 coulomb) was higher than that in OPC concrete (2863 coulomb). These changes in the ion concentrations implied that the

charge passed really meant in terms of total ionic migration which did not equal to chloride ion migration only. In other words, the charge passed was generally contributed by the movement of all ions present in the system such as Na^+ and OH^-, not attributed by only Cl^-.

This clearly shows that most geopolymer concretes will register a higher chage passed in a RCPT when compared with OPC concretes. However, the chloride ion movement in geopolymer concretes can be slower than OPC concretes depending on the composition of the geopolymer.

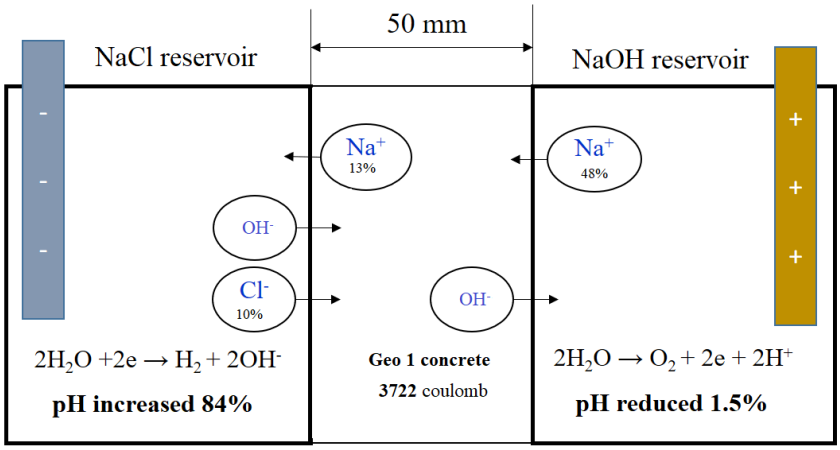

Figure 5.11 Movement of ions in rapid chloride permeability test (RCPT) for Geo 1 concrete

Table 5.4 Changes in concentrations of anion and cation in Geo 1 concrete in rapid chloride permeability test

Geo 1 concrete with charge passed **3723** (coulomb)				
Ion concentration (mg/l)	NaCl reservoir		NaOH reservoir	
	Before test	After test	Before test	After test
Cl^-	22490	20280	210	240

Na^+	15637	17817	8798	4519
pH	6.9	12.7	13.0	12.8

As can be seen in Table 5.4, 5.5 and 5.6, a reduction in Cl^- concentrations in NaOH reservoir of Geo 2 and OPC occurred while an increase in Cl^- concentrations was observed in NaOH reservoir of Geo 1 concrete. It implied that Cl^- ions in NaCl reservoir in RCPT for Geo 1 were moved through the concrete disc and transferred to NaOH reservoir, which explains well why the high charge passed was recorded. On the otherhand, much lower charge passed was observed in RCPT of Geo 2 and OPC concretes.

Table 5.5 Changes in concentrations of anion and cation in OPC concrete in rapid chloride permeability test

OPC concrete with charge passed **2863** (coulomb)				
Ion concentration (mg/l)	NaCl reservoir		NaOH reservoir	
	Before test	After test	Before test	After test
Cl^-	22490	21070	210	205
Na^+	15637	16303	8798	7509
pH	6.9	12.5	13.0	12.9

Table 5.6 Changes in concentrations of anion and cation in Geo 2 concrete in rapid chloride permeability test

Geo 2 concrete with charge passed **2119** (coulomb)				
Ion concentration (mg/l)	NaCl reservoir		NaOH reservoir	
	Before test	After test	Before test	After test
Cl^-	22490	20655	550	523
Na^+	-	14151	6514	5026
pH	6.9	12.6	13.0	12.9

5.4 Conclusions

The results of apparent chloride diffusion coefficient obtained in an accelerated diffusion test as per ASTM C1556 showed that OPC+25% Fly ash had the highest resistance to chloride penetration, followed by Geo 2 concrete, then OPC concrete and finally Geo 1 concrete. The chloride diffusion coefficient results correlated well with the results of charge passed in rapid chloride permeability test at 30V with a correlation coefficient of 0.72. From the current series of tests, the charge passed at 10V gave a correlation coefficient of only 0.38.

For evaluating chloride resistance using rapid chloride permeability test, therefore, RCPT at 30V was recommended because of the issue of over-heating in RCPT at 60V.

The discussion based on VPV and chloride diffusion coefficient implied that increasing slag content improved the chloride resistance of geopolymer concrete. Also, the main mechanisms of chloride binding in one-part fly ash/slag geopolymer investigated were either physical or chemical due to presence of both fly ash and slag. It is recommended to investigate further the chloride binding mechanism of one-part fly ash/slag geopolymer.

A brief investigation, on one-part fly ash/slag geopolymer, on changes of ion concentrations and pH in the NaOH and NaCl reservoirs, before and after performing RCPT, implied that the charge passed really meant in terms of total ionic migration which does not equal to chloride ion migration only.

The evaluation of chloride resistance by chloride depth after 6 months duration, obtained in a 3.5% NaCl solution, replicating natural chloride conditions, showed Geo 2 have better resistance to chlorides than Geo 1 and OPC concretes. It is difficult to

differentiate the performance of different geopolymer concretes for chloride resistance, using charge passed as shown by the results at RCPT at 30V and 10V. More work is needed in the future to study the change in chloride diffusion characteristics with age of geopolymer concrete.

CHAPTER 6: Conclusions and Recommendations

6.1 Conclusions

1. This study investigated two important corrosion related aspects including carbonation and chloride penetration resistance of one-part fly ash/slag geopolymer mortars and concretes, which was shown in Chapter 4 and Chapter 5. The use of a set retarder to improve setting time of one-part fly ash/slag geopolymer mortars, which was a serious issue for producing mortars and concretes, was studied in Chapter 3. Chapter 2 provided a profound overview based on available information on carbonation and chloride resistance on different geopolymeric systems.

2. As presented in chapter 3, using set retarder investigated can improve the setting time of one-part fly ash/ slag geopolymer mortars to obtain sufficient setting time for mixing and casting mortars and concretes. This retarder also reduced the heat released by the dissolution and geopolymerisation reactions, which is good for producing mass concrete structure components. Using this retarder, however, can reduce the compressive strength of geopolymer mortars if the retarder content is over 8%. However, it can be avoidable by using an amount of less than 8% retarder. An appropriate amount of retarder is 2-6 % was found to be suitable for obtaining appropriate setting time, workability and compressive strength. Regarding curing conditions, both seal curing (where specimens were wrapped in plastic films and placed in the ambient temperature) and sealed and heat curing (where specimens were wrapped in plastic films, put in the oven at 60^{o}C for 6 hours, then exposed to the air) can be applied for in-situ and precast concrete productions.

3. Chapter 4 showed interesting results in term of carbonation and its effects on properties of one-part geopolymer mortars and concretes investigated. Two pH indicators including alizarin yellow R and phenolphthalein, was used to access carbonation front depth. Alizarin yellow R was found to correlate well with the pH changes due to carbonation because pH level in carbonated parts was always higher than 10. Further, the porosities in carbonated parts were decreased about 30 - 40%, compared to noncarbonated parts, obtained by both neutron tomography and MIP. The results implied that steel corrosion may not merely happen by carbonation because the pH value at the surface was higher than 10.

4. Chapter 5 discussed the appropriateness of rapid chloride permeability test (RCPT) in assessing chloride resistance of one-part geopolymer concrete. RCPT performed at 30V showed a good correlation with results of apparent chloride diffusion coefficient obtained in an accelerated test in 16.5% NaCl as per ASTM C1556, while RCPT carried out at 10V did not. However, it was difficult to differentiate the performance of different geopolymer concretes for chloride resistance, using charge passed as shown by the results of RCPT at 30V and 10V. Among four different types of concrete, in an accelerated test in 16.5% NaCl, OPC+25% Fly ash had the highest resistance to chloride penetration, followed by Geo 2 concrete, then OPC concrete and finally Geo 1 concrete. Evaluating chloride resistance by chloride depth obtained in a 3.5% NaCl solution, however, showed a different trend. In which Geo 2 and Geo1 shower better resistance to chloride than OPC. The discussion based on VPV and chloride diffusion coefficient in accelerated chloride diffusion test implied that increasing slag content improved the chloride resistance of geopolymer concrete. The main mechanisms of chloride binding in one-part fly ash/slag geopolymer investigated were both physical or chemical due to the presence of both

fly ash and slag. A brief investigation, in one-part geopolymer fly ash/slag geopolymer, on changes of ion concentrations and pH in the NaOH and NaCl reservoirs, before and after performing RCPT, implied that the charge passed really meant in terms of total ionic migration which does not equal to chloride ion migration only.

6.2 Recommendations for future research

Based on the findings of the study carefully presented above, several recommendations were made for future research.

1. The tests on carbonation resistance should be done in a longer period of time and under different relative humidity (RH) and varying temperatures because RH and temperature significantly affect the rate of carbonation in concretes. In that case, a more comprehensive results can be obtained.

2. Carbonation caused carbonated concretes to become denser, but how such change affects the overall performance and especially steel corrosion is not clearly explained in this study. Further work on this essential aspect of geopolymer concrete needs to be carefully examined to further understanding and accelerate applications of one-part geopolymer concretes in construction industry.

3. The ratio of fly ash/ slag ratios was proved to have considerable effect on porosity and hence, durability of fly ash/slag geopolymer concrete. The tests of chloride resistance in this study were carried out only on geopolymer matrices produced from two different ratios of fly ash to slag. More ratios of fly ash to slag need to be investigated to yield more profound results. Also, chloride binding mechanism of one-part fly ash/slag geopolymer needs to be further access.

4. In the study, testing chloride resistance in a 3.5% NaCl solution, imitating natural chloride conditions, was done in only 6 months. This test needs to be done in a longer time to be able to produce useful results.

5. The tests on chloride testing in this study did not show a good connection with the natural chloride test. More test methods should be included.

References

Abdel-Gawwad, H.A., Mohamed, S.A. & Mohammed, M.S. 2019, „Recycling of slag and lead-bearing sludge in the cleaner production of alkali activated cement with high performance and microbial resistivity", *Journal of Cleaner Production*, vol. 220, pp. 568–80.

Ahmad, S. 2003, „Reinforcement corrosion in concrete structures, its monitoring and service life prediction - A review", *Cement and Concrete Composites*, vol. 25, pp. 459–71.

American Society for Testing and Materials 2012, *Acid-Soluble Chloride in Mortar and Concrete- ASTM C 1152*.

American Society for Testing and Materials 2014, *Standard Practice for Mechanical Mixing of Hydraulic Cement Pastes and Mortars*, ASTM International, United States.

American Society for Testing and Materials 2015, *Standard Test Method for Flow of Hydraulic Cement Mortar ASTM C1437 − 15*, ASTM International, United States.

American Society for Testing and Materials 2016, *Standard Test Method for Compressive Strength of Hydraulic Cement Mortars ASTM C109/C109M − 16a*, United States.

American Society for Testing and Materials 2018, *Standard Test Method for Electrical Indication of Concrete's Ability to Resist Chloride (ASTM C1202-18)*.

American Society for Testing and Materials 2019, *Standard Test Methods for Time of Setting of Hydraulic Cement by Vicat Needle*, ASTM International, United States, pp. 1–8.

Andrade, C. 1993, „Calculation of chloride diffusion coefficients in concrete from ionic migration measurements“, *Cement and Concrete Research*, vol. 23, no. 3, pp. 724–42.

Angst, U., Elsener, B., Larsen, C.K. & Vennesland, Ø. 2011, „Chloride induced reinforcement corrosion: Rate limiting step of early pitting corrosion“, *Electrochimica Acta*, vol. 56, pp. 5877–89.

Australia Cement Industry Federation 2017, *Industry Report 2017*, Australia.

Babaee, M., Khan, M.S.H. & Castel, A. 2018, „Passivity of embedded reinforcement in carbonated low-calcium fly ash-based geopolymer concrete“, *Cement and Concrete Composites*, vol. 85, pp. 32–43.

Badar, M.S., Kupwade-patil, K., Bernal, S.A., Provis, J.L. & Allouche, E.N. 2014, „Corrosion of steel bars induced by accelerated carbonation in low and high calcium fly ash geopolymer concretes“, *Construction and Building Materials*, vol. 61, pp. 79–89.

Bagheri, A.R. & Zanganeh, H. 2012, „Comparison of Rapid Tests for Evaluation of Chloride Resistance of Concretes with Supplementary Cementitious Materials“, *Journal of Materials in Civil Engineering*, vol. 24, no. 9, pp. 1175–82.

Balcikanli, M. & Ozbay, E. 2016, „Optimum design of alkali activated slag concretes for the low oxygen/chloride ion permeability and thermal conductivity“, *Composites Part B: Engineering*, vol. 91, pp. 243–56.

Beaudoin, J.J., Ramachandran, V.S. & Feldman, R.F. 1990, „Interaction of chloride and C-S-H“, *Cement and Concrete Research*, vol. 20, pp. 875–83.

Bernal, S.A., Nicolas, R.S., Myers, R.J., Gutiérrez, R.M., Puertas, F., van Deventer, J.S.J. & Provis, J.L. 2014, „MgO content of slag controls phase evolution and

structural changes induced by accelerated carbonation in alkali-activated binders", *Cement and Concrete Research*, vol. 57, pp. 33–43.

Bernal, S.A. & Provis, J.L. 2014, „Durability of alkali-activated materials: Progress and perspectives", *Journal of the American Ceramic Society*, vol. 97, no. 4, pp. 997–1008.

Bernal, S.A., Provis, J.L., Brice, D.G., Kilcullen, A., Duxson, P. & van Deventer, J.S.J.. 2012, „Accelerated carbonation testing of alkali-activated binders significantly underestimates service life : The role of pore solution chemistry", *Cement and Concrete Research*, vol. 42, no. 10, pp. 1317–26.

Bernal, S. A., Provis, J.L., Walkley, B., Nicolas, R.S., Gehman, J.D., Brice, D.G., Kilcullen, A.R., Duxson, P. & van Deventer, J.S.J. 2013, „Gel nanostructure in alkali-activated binders based on slag and fly ash , and effects of accelerated carbonation", *Cement and Concrete Research*, vol. 53, pp. 127–44.

Bernal, Susan A., Provis, J.L., Walkley, B., San Nicolas, R., Gehman, J.D., Brice, D.G., Kilcullen, A.R., Duxson, P. & Van Deventer, J.S.J. 2013, „Gel nanostructure in alkali-activated binders based on slag and fly ash, and effects of accelerated carbonation", *Cement and Concrete Research*, vol. 53, pp. 127–44.

Bertolini, L., Elsener, B., Pedeferri, P. & Polder, R.B. 2013, „Carbonation-induced Corrosion", *Corrosion of Steel in Concrete - Prevention, Diagnosis, Repair*, John Wiley & Sons.

Buchler, M. 2005, „Corrosion inhibitors for reinforced concrete", *Corrosion in reinforced concrete structures*, Woodhead Publishing, pp. 190–214.

Cao, H.T., Bucea, L. & Meck, E. 1997, „Rapid assessment of concrete"s resistance to chloride penetration-modified ASTM C 1202", *Concrete 97 Conference*.

Castel, A., François, R. & Arliguie, G. 1999, „Effect of loading on carbonation penetration in reinforced concrete elements“, *Cement and Concrete Research*, vol. 29, pp. 561–5.

Chess, P.M. 2014, „Corrosion in reinforced concrete structures“, in P.M. Chess & J. Broomfield (eds),*Cathodic Protection of Steel in Concrete and Masonry*, Taylor & Francis Group, pp. 1–16.

Chindaprasirt, P. & Chalee, W. 2014, „Effect of sodium hydroxide concentration on chloride penetration and steel corrosion of fly ash-based geopolymer concrete under marine site“, *Construction and Building Materials*, vol. 63, pp. 303–10.

Collins, F. 2010, „Inclusion of carbonation during the life cycle of built and recycled concrete: Influence on their carbon footprint“, *International Journal of Life Cycle Assessment*, vol. 15, no. 6, pp. 549–56.

Criado, M., Palomo, A. & Fernández-Jiménez, A. 2005, „Alkali activation of fly ashes. Part 1: Effect of curing conditions on the carbonation of the reaction products“, *Fuel*, vol. 84, pp. 2048–54.

Cyr, M. & Pouhet, R. 2016, „Carbonation in the pore solution of metakaolin-based geopolymer“, *Cement and Concrete Research*, vol. 88, pp. 227–35.

Davidovits, J. 1991, „Geopolymers: Inorganic polymeric new materials“, *Journal of Thermal Analysis*, vol. 37, pp. 1633–56.

Davidovits, J. 1994, „Properties of Geopolymer Cements“, *First International Conference on Alkaline Cements and Concretes*, Kiev, pp. 131–49.

Davidovits, J. 2002, „Environmentally Driven Geopolymer Cement Applications“, *Geopolymer 2002 Conference*, Melbourne, Australia, pp. 1–9.

Davidovits, J. 2005, „Geopolymer chemistry and sustainable development. The poly

(sialate) terminology: a very useful and simple model for the promotion and understanding of green-chemistry", *2005 Geopolymer Conference*, pp. 9–15.

Davidovits, J. 2015, „The manufacture of geopolymer cements", *Geopolymer Chemistry and Applications*, Institut Géopolymère, Saint-Quentin France, pp. 537–68.

Delagrave, A., Marchand, J., Ollivier, J., Julien, S. & Hazrati, K. 1997, „Chloride Binding Capacity of Various Hydrated Cement Paste Systems", *Advanced Cement Based Materials*, vol. 6, pp. 28–35.

Duan, P., Yan, C., Luo, W. & Zhou, W. 2016, „Effects of adding nano-TiO2 on compressive strength, drying shrinkage, carbonation and microstructure of fluidized bed fly ash based geopolymer paste", *Construction and Building Materials*, vol. 106, pp. 115–25.

El-Reedy, M. 2008, „Introduction", *Steel-reinforced concretestructures: assessment and repair of corrosion*, Taylor & Francis Group, The United States of America, pp. 1–3.

Fawer, M., Concannon, M. & Rieber, W. 1999, „Life cycle inventories for the production of sodium silicates", *International Journal of Life Cycle Assessment*, vol. 4, no. 4, pp. 207–12.

Fernández-Jiménez, A., Cristelo, N., Miranda, T. & Palomo, Á. 2017, „Sustainable alkali activated materials: Precursor and activator derived from industrial wastes", *Journal of Cleaner Production*, vol. 162, pp. 1200–9.

Fernández-Jiménez, A., Palomo, A. & Criado, M. 2005, „Microstructure development of alkali-activated fly ash cement: A descriptive model", *Cement and Concrete Research*, vol. 35, pp. 1204–9.

Fernández-Jiménez, A., Palomo, A., Sobrados, I. & Sanz, J. 2006, „The role played by the reactive alumina content in the alkaline activation of fly ashes“, *Microporous and Mesoporous Materials*, vol. 91, pp. 111–9.

Fernández-Jiménez, A., Puertas, F., Sobrados, I. & Sanz, J. 2003, „Structure of Calcium Silicate Hydrates Formed in Alkaline-Activated Slag : Influence of the Type of Alkaline Activator“, *Journal of the American Ceramic Society*, vol. 86, no. 8, pp. 1389–94.

Garbe, U., Randall, T., Hughes, C., Davidson, G., Pangelis, S. & Kennedy, S.J. 2015, „A New Neutron Radiography / Tomography / Imaging Station DINGO at OPAL“, *Physics Procedia*, vol. 69, no. October 2014, pp. 27–32.

García-González, C.A., Hidalgo, A., Andrade, C., Alonso, M.C., Fraile, J., López-Periago, A.M. & Domingo, C. 2006, „Modification of composition and microstructure of Portland cement pastes as a result of natural and supercritical carbonation procedures“, *Industrial and Engineering Chemistry Research*, vol. 45, no. 14, pp. 4985–92.

Gluth, G.J.G., Arbi, K., Bernal, S.A., Bondar, D., Ashish, K.D., Vilma, D., Karl, D., Pipilikaki, P., Valcke, S.L.A., Ye, G., Zuo, Y. & Provis, J.L. 2020, „RILEM TC 247-DTA round robin test : carbonation and chloride penetration testing of alkali-activated concretes“, *Materials and Structures*, vol. 53, no. 21.

Ben Haha, M., Le Saout, G., Winnefeld, F. & Lothenbach, B. 2011, „Influence of activator type on hydration kinetics, hydrate assemblage and microstructural development of alkali activated blast-furnace slags“, *Cement and Concrete Research*, vol. 41, no. 3, pp. 301–10.

Hansson, C.M. 2016, „An introduction to corrosion of engineering materials“,

Corrosion of Steel in Concrete Structures, Woodhead Publishing, Oxford, pp. 3–18.

Huanhai, Z., Xuequan, W., Zhongzi, X. & Mingshu, T. 1993, „Kinetic study on hydration of alkali-activated slag“, *Cement and Concrete Research*, vol. 23, pp. 1253–8.

Hunkele, F. 2005, „Corrosion in reinforced concrete: processes and mechanisms“, *Corrosion in Reinforced Concrete Structures*, Woodhead Publishing, pp. 1–45.

IPCC Guidelines for National Greenhouse Gas Inventories 1996, *Chapter 2. Industrial processes*.

Ismail, I., Bernal, S.A., Provis, J.L., San Nicolas, R., Brice, D.G., Kilcullen, A.R., Hamdan, S. & Van Deventer, J.S.J. 2013, „Influence of fly ash on the water and chloride permeability of alkali-activated slag mortars and concretes“, *Construction and Building Materials*, vol. 48, pp. 1187–201.

Khan, M.S.H., Castel, A. & Noushini, A. 2016, „Carbonation of a low-calcium fly ash geopolymer concrete“, *Magazine of Concrete Research*, vol. 69, no. 1, pp. 24–43.

Konečný, P., Lehner, P., Ponikiewski, T. & Miera, P. 2017, „Comparison of Chloride Diffusion Coefficient Evaluation Based on Electrochemical Methods“, *Procedia Engineering*, vol. 190, pp. 193–8.

Kupwade-Patil, K. & Allouche, E.N. 2013, „Examination of Chloride-Induced Corrosion in Reinforced Geopolymer Concretes“, *Journal of Materials in Civil Engineering*, vol. 25, no. 10, pp. 1465–76.

Law, D.W., Arham, A.A., Molyneaux, T.K., Patnaikuni, I. & Wardhono, A. 2015, „Long term durability properties of class F fly ash geopolymer concrete“, *Materials and Structures*, vol. 48, no. 3, pp. 721–31.

Lee, N.K. & Lee, H.K. 2016, „Influence of the slag content on the chloride and sulfuric acid resistances of alkali-activated fly ash/slag paste“, *Cement and Concrete Composites*, vol. 72, pp. 168–79.

Lloyd, N. & Rangan, V. 2009, „Geopolymer concrete - Sustainable cementless concrete“, *Tenth ACI International Conference*, pp. 33–53.

Lloyd, R.R., Provis, J.L. & Van Deventer, J.S.J. 2010, „Pore solution composition and alkali diffusion in inorganic polymer cement“, *Cement and Concrete Research*, vol. 40, no. 9, pp. 1386–92.

Martín-Del-Río, J.J., Alejandre, F.J., Márquez, G. & Blasco, F.J. 2013, „An argument for using alizarine yellow R and indigo carmine to determine in situ the degree of alkalinity in reinforced concrete“, *Construction and Building Materials*, vol. 40, pp. 426–9.

Materials, A.S. for T. and 2006, *Standard Test Method for Density , Absorption , and Voids in Hardened Concrete - ASTM C642-06*.

Materials, A.S. for T. and 2016, *Determining the Apparent Chloride Diffusion Coefficient of Cementitious Mixtures by Bulk Diffusion- ASTM C 1556-11a*.

Materials, A.S. for T. and 2018a, *Standard Test Method for Compressive Strength of Cylindrical Concrete Specimens - ASTM C39/C39M-18*.

Materials, A.S. for T. and 2018b, *Standard Test Methods for Chemical Analysis of Hydraulic Cement- ASTM C114*.

Miranda, J.M., Ferna´ndez-Jime´nez, A., Gonza´lez, J.A. & Palomo, A. 2005, „Corrosion resistance in activated fly ash mortars“, *Cement and Concrete Research*, vol. 35, pp. 1210–7.

Modena, C., Tecchio, G., Pellegrino, C., da Porto, F., Zanini, M.A. & Donà, M. 2014,

„Retrofitting and Refurbishment of Existing Road Bridges“, *Maintenance and Safety of Aging Infrastructure*, CRC Press - Balkema – Taylor & Francis, Leiden, The Netherlands, pp. 469–533.

Monticelli, C., Natali, M.E., Balbo, A., Chiavari, C., Zanotto, F., Manzi, S. & Bignozzi, M.C. 2016a, „A study on the corrosion of reinforcing bars in alkali-activated fly ash mortars under wet and dry exposures to chloride solutions“, *Cement and Concrete Research*, vol. 87, pp. 53–63.

Monticelli, C., Natali, M.E., Balbo, A., Chiavari, C., Zanotto, F., Manzi, S. & Bignozzi, M.C. 2016b, „Corrosion behavior of steel in alkali-activated fly ash mortars in the light of their microstructural , mechanical and chemical characterization“, *Cement and Concrete Research*, vol. 80, pp. 60–8.

Morandeau, A., Thiéry, M. & Dangla, P. 2014, „Investigation of the carbonation mechanism of CH and C-S-H in terms of kinetics , microstructure changes and moisture properties“, *Cement and Concrete Research*, vol. 56, pp. 153–70.

Muriithi, G.N., Petrik, L.F. & Doucet, F.J. 2020, „Synthesis, characterisation and CO2 adsorption potential of NaA and NaX zeolites and hydrotalcite obtained from the same coal fly ash“, *Journal of CO2 Utilization*, vol. 36, no. August 2019, pp. 220–30.

Nedeljkovic, M., Zuo, Y., Arbi, K. & Ye, G. 2017, „Natural carbonation of alkali-activated fly ash and slag pastes“, *Fib Symposium 2017*, Maastrich, the Netherlands, pp. 2213–23.

Nedeljković, M., Zuo, Y., Arbi, K. & Ye, G. 2018, „Carbonation Resistance of Alkali-Activated Slag Under Natural and Accelerated Conditions“, *Journal of Sustainable Metallurgy*.

Neville, A. 1995, „Chloride attack of reinforced concrete: an overview“, *Materials and Structures*, vol. 28, no. 2, pp. 63–70.

NORDTEST 1995, *Concrete, hardened accelerated chloride penetration - NT Build 443*, Finland.

Noushini, A., Castel, A., Aldred, J. & Rawal, A. 2019, „Chloride diffusion resistance and chloride binding capacity of fly ash-based geopolymer concrete“, *Cement and Concrete Composites*, no. April, p. 103290.

Olivia, M. & Nikraz, H.R. 2011, „Durability of Fly Ash Geopolymer Concrete in a Seawater Environment“, *Proceedings of the Concrete 2011 Conference*, The Concrete Institute of Australia, Perth, Australia.

Pacheco-torgal, F., Abdollahnejad, Z., Camões, A.F., Jamshidi, M. & Ding, Y. 2012, „Durability of alkali-activated binders : A clear advantage over Portland cement or an unproven issue ?“, *Construction and Building Materials*, vol. 30, pp. 400–5.

Page, C.L. & Treadaway, K.W.J. 1982, „Aspects of the electrochemistry of steel in concrete“, *Nature*, vol. 297, pp. 109–15.

Palomo, A., Alonso, S. & Fernandez-jime, A. 2004, „Alkaline Activation of Fly Ashes : NMR Study of the Reaction Products“, *Journal of the American Ceramic Society*, vol. 87, no. 6, pp. 1141–5.

Palomo, A., Krivenko, P., Garcia-Lodeiro, I., Kavalerova, E., Maltseva, O. & Fernández-Jiménez, A. 2014, „A review on alkaline activation : new analytical perspectives“, *Materiales de Construcción*, vol. 64, no. 315, p. e022.

Papadakis, V.G., Vayenas, C.G. & Fardis, M.N. 1989, „A reaction engineering approach to the problem of concrete carbonation“, *AIChE Journal*, vol. 35, no. 10, pp. 1639–50.

Pasupathy, K., Berndt, M., Castel, A., Sanjayan, J. & Pathmanathan, R. 2016, „Carbonation of a blended slag-fly ash geopolymer concrete in field conditions after 8 years“, *Construction and Building Materials*, vol. 125, pp. 661–9.

Pasupathy, K., Berndt, M., Sanjayan, J., Rajeev, P. & Cheema, D.S. 2017, „Durability of low - calcium fly ash based geopolymer concrete culvert in a saline environment“, *Cement and Concrete Research*, vol. 100, pp. 297–310.

Polder, R.B. 2005, „Electrochemical techniques for corrosion protection and maintenance“, *Corrosion in reinforced concrete structures*, Woodhead Publishing, pp. 215–41.

Portland Cement Association 2002, *Types and Causes of Concrete Deterioration*, *PCA R&D Serial No. 2617*.

Pouhet, R. & Cyr, M. 2016, „Carbonation in the pore solution of metakaolin-based geopolymer“, *Cement and Concrete Research*, vol. 88, pp. 227–35.

Provis, J.L. & Bernal, S.A. 2014, „Geopolymers and Related Alkali-Activated Materials“, *Annual Review of Materials Research*, vol. 44, no. 3, pp. 3–29.

Provis, J.L., Duxson, P., Kavalerova, E., Krivenko, P. V, Puertas, F. & van Deventer, J.S.J. 2014, *Historical Aspects and Overview BT - Alkali Activated Materials: State-of-the-Art Report, RILEM TC 224-AAM*, in J.L. Provis & J.S.J. van Deventer (eds), Springer Netherlands, Dordrecht, pp. 11–57.

Provis, J.L., Myers, R.J., White, C.E., Rose, V. & Van Deventer, J.S.J. 2012, „X-ray microtomography shows pore structure and tortuosity in alkali-activated binders“, *Cement and Concrete Research*, vol. 42, no. 6, pp. 855–64.

Pu, Q., Jiang, L., Xu, J., Chu, H., Xu, Y. & Zhang, Y. 2012, „Evolution of pH and chemical composition of pore solution in carbonated concrete“, *Construction and*

Building Materials, vol. 28, pp. 519–24.

Räsänen, V. & Penttala, V. 2004, „The pH measurement of concrete and smoothing mortar using a concrete powder suspension“, *Cement and Concrete Research*, vol. 34, no. 5, pp. 813–20.

Raupach, M. & Robler, G. 2005, „Surface treatments and coatings for corrosion protection“, *Corrosion in reinforced concrete structures*, Woodhead Publishing, pp. 163–89.

Reddy, D. V., Edouard, J.-B., Sobhan, K. & Rajpathak, S.S. 2011, „Durability of reinforced fly ash-based geopolymer concrete in the marine environment“, *36th Conference on Our World in Concrete & Structures*, Singapore, pp. 14–26.

Richardson, I.G., Brough, A.R., Groves, G.W. & Dobson, C.M. 1994, „The characterization of hardened alkali-activated blast-furnace phase“, *Cement and Concrete Research*, vol. 24, no. 5, pp. 813–29.

Roads and Traffic Authority 2010, *Culvert Risk Assessment Guideline V3.02*, NSW, Australia.

Rozière, E., Loukili, A. & Cussigh, F. 2009, „A performance based approach for durability of concrete exposed to carbonation“, *Construction and Building Materials*, vol. 23, pp. 190–9.

Saha, S. & Rajasekaran, C. 2017, „Enhancement of the properties of fly ash based geopolymer paste by incorporating ground granulated blast furnace slag“, *Construction and Building Materials*, vol. 146, pp. 615–20.

Sherman, M.R., McDonald, D.B. & Pfeifer, D.W. 1996, „Durability aspects of precast prestressed concrete part 2: Chloride permeability study“, *PCI Journal*, vol. 41, no. 4, pp. 76–95.

Shi, C. 2003, „Another look at the rapid chloride permeability test (ASTM C1202 or ASSHTO T277)“, *FHWA Resource Center, Baltimore*.

Shikhov, I. & Arns, C.H. 2015, „Evaluation of Capillary Pressure Methods via Digital Rock Simulations“, *Transport in Porous Media*, vol. 107, no. 2, pp. 623–40.

Sirivivatnanon, V. & Khatri, R. 2011, „Testing and Specifying Chloride Resistance of Concrete“, *8th Austroads Bridge Conference*, pp. 472–87.

Škvára, F., Jílek, T. & Kopecký, L. 2005, „Geopolymer materials based on fly ash“, *Ceramics - Silikaty*, vol. 49, no. 3, pp. 195–204.

Stanish, K.D., Hooton, R.D. & Thomas, M.D.A. 1997, *Testing the Chloride Penetration Resistance of Concrete : A Literature Review. No. FHWA Contract DTFH61-97-R-00022*, United States. Federal Highway Administration.

Tang, L. & Sorensen, H.E. 2001, „Precision of the Nordic test methods for measuring the chloride diffusion / migration coefficients of concrete“, *Materials and Structures*, vol. 34, no. October, pp. 479–85.

Tang, L. & Sørensen, H.E. 2001, „Precision of the Nordic test methods for measuring the chloride diffusion/migration coefficients of concrete“, *Materials and Structures/Materiaux et Constructions*, vol. 34, no. 8, pp. 479–85.

Tennakoon, C., Shayan, A., Sanjayan, J.G. & Xu, A. 2017, „Chloride ingress and steel corrosion in geopolymer concrete based on long term tests“, *Materials & Design*, vol. 116, pp. 287–99.

Torres-Carrasco, M. & Puertas, F. 2015, „Waste glass in the geopolymer preparation. Mechanical and microstructural characterisation“, *Journal of Cleaner Production*, vol. 90, pp. 397–408.

Turner, L.K. & Collins, F.G. 2013, „Carbon dioxide equivalent (CO2-e) emissions: A

comparison between geopolymer and OPC cement concrete“, *Construction and Building Materials*, vol. 43, pp. 125–30.

Tuutti, K. 1982, *Corrosion of steel in concrete*, Stockholm.

VicRoad 2007, *Technical Note 89: Test Methods for the Assessment of Durability of Concrete*, pp. 1–4.

Villain, G., Thiery, M. & Platret, G. 2007, „Measurement methods of carbonation profiles in concrete: Thermogravimetry, chemical analysis and gammadensimetry“, *Cement and Concrete Research*, vol. 37, no. 8, pp. 1182–92.

Volume Graphics 2014, *VGStudio MAX. URL: http://www.volumegraphics.com/en/*.

Vu, T.H., Gowripalan, N., Silva, P. De, Kidd, P. & Sirivivatnanon, V. 2019, „Assessing Corrosion Resistance of Powder Form of Geopolymer Concrete“, *Concrete 2019*, Sydney, Australia.

Vu, T.H., Gowripalan, N., De Silva, P., Paradowska, A., Garbe, U., Kidd, P. & Sirivivatnanon, V. 2020, „Assessing carbonation in one-part fly ash/slag geopolymer mortar: Change in pore characteristics using the state-of-the-art technique neutron tomography“, *Cement and Concrete Composites*, vol. 114, no. July, p. 103759.

Wajima, T., Shimizu, T., Yamato, T. & Ikegami, Y. 2010, „Removal of NaCl from seawater using natural zeolite“, *Toxicological & Environmental Chemistry*, vol. 92, no. 1, pp. 21–6.

Whiting, D. & Mitchell, T.M. 1992, „History of the Rapid Chloride Permeability Test“, *Transportation Research Record*, vol. 1335, no. 1, pp. 55–62.

Wibowo, E., Sutisna, Rokhmat, M., Murniati, R., Khairurrijal & Abdullah, M. 2017, „Utilization of Natural Zeolite as Sorbent Material for Seawater Desalination“,

Procedia Engineering, vol. 170, pp. 8–13.

Yang, C.C. 2004, „Relationship between migration coefficient of chloride ions and charge passed in steady state“, *ACI Materials Journal*, vol. 101, no. 2, pp. 124–30.

Yang, C.C., Cho, S.W. & Huang, R. 2002, „The relationship between charge passed and the chloride-ion concentration in concrete using steady-state chloride migration test“, *Cement and Concrete Research*, vol. 32, no. 2, pp. 217–22.

Yip, C.K., Lukey, G.. C. & van Deventer, J.S.J. 2005, „The coexistence of geopolymeric gel and calcium silicate hydrate at the early stage of alkaline activation“, *Cement and Concrete Research*, vol. 35, pp. 1688–97.

Yuan, Q., Shi, C., De Schutter, G., Audenaert, K. & Deng, D. 2009, „Chloride binding of cement-based materials subjected to external chloride environment - A review“, *Construction and Building Materials*, vol. 23, no. 1, pp. 1–13.

Zhang, J., Shi, C. & Zhang, Z. 2019, „Chloride binding of alkali-activated slag/fly ash cements“, *Construction and Building Materials*, vol. 226.

Zhao, Y. & Jin, W. 2016, „Steel Corrosion in Concrete“, *Steel Corrosion-Induced Concrete Cracking*, Elsevier Inc, pp. 19–30.

Zhou, Y., Gencturk, B., Asce, A.M., Willam, K., Asce, F. & Attar, A. 2015, „Carbonation-Induced and Chloride-Induced Corrosion in Reinforced Concrete Structures“, *Journal of Materials in Civil Engineering*, vol. 27, no. 9.

Zhu, H., Zhang, Z., Zhu, Y. & Tian, L. 2014, „Durability of alkali-activated fly ash concrete : Chloride penetration in pastes and mortars“, *Construction and Building Materials*, vol. 65, pp. 51–9.

Zhuang, X.Y., Chen, L., Komarneni, S., Zhou, C.H., Tong, D.S., Yang, H.M., Yu,

W.H. & Wang, H. 2016, „Fly ash-based geopolymer: Clean production, properties and applications“, *Journal of Cleaner Production*, vol. 125, pp. 253–67.

Zhang, J., Shi, C., Zhang, Z. 2019, „Chloride binding of alkali-activated slag/fly ash cements“, *Construction and Building Materials*, vol. 226, pp. 21–31.